5-2017

Characterization of SufS and SufE of Suf Pathway for FE-S Cluster Assembly in Escherichia Coli

Guangchao Dong
University of South Carolina

CHARACTERIZATION OF SUFS AND SUFE OF SUF PATHWAY FOR FE-S CLUSTER ASSEMBLY IN *ESCHERICHIA COLI*

by

Guangchao Dong

Bachelor of Medicine
Shandong University, 2009

Master of Medicine
Shandong University, 2010

Submitted in Partial Fulfillment of the Requirements

For the Degree of Doctor of Philosophy in

Chemistry

College of Arts and Sciences

University of South Carolina

2017

Accepted by:

F. Wayne Outten, Major Professor

Maksymilian Chruszcz, Committee Member

Linda Shimizu, Committee Member

Mike Wyatt, Committee Member

Cheryl L. Addy, Vice Provost and Dean of the Graduate School

DEDICATION

Dedicated to my beloved son, Brayden Dong

ACKNOWLEDGEMENTS

After I graduated from medical school, I practiced in the internal medicine for two years to complete my internship training like most of my peer colleagues. Then I decided to apply a Ph.D. position, which is a bit different. The reason is quite simple that I want to know how to do research because there are so many questions around me that are not solved. And MD plus Ph.D. must be cool. Well, it sounds cool. But the real Ph.D. life is tough, especially when the result of the experiment is not consistent with my hypothesis and it happens all the time. I am so lucky that I can always get help from my professors, colleagues, and my friends, which supports me and encourages me to make me complete the journey as a graduate student.

I would like to express my deepest appreciation to my advisor, Dr. F. Wayne Outten. He is so kind to accept me as a lab member and to give me this project. I love my project because it has so much biomedical relevance, like the research on inhibitor to our target protein that is similar to a drug discovery process. Also, Dr. Outten is a great mentor. He is so sharp in looking for a valuable research topic that experiments can work most of the times. He does not push me but gives me enough freedom to try my own ideas in the research. When I am in trouble, he is always ready to help. The training from Dr. Outten prepares me well for my future career and it is a fortune to my life.

I would like to thank my research committee members Dr. Maksymilian Chruszcz, Dr. Linda Shimizu, and Dr. Mike Wyatt for their time and advice during my graduate study.

Also, I would like to thank Dr. Patricia Dos Santos, Dr. Thomas Makris, and Job Grant for the valuable advice on my stopped-flow experiment. I must acknowledge NIH grant for the financial support.

I would like to thank all my former and present colleagues. Matthew Blahut, Naimah Bolaji, Clorissa Washington, and Savannah Witcher gave me a lot of technical guidance and research advice. In particular, I want to thank Dr. Yuyuan Dai who taught me ABC about experiments and built a solid basis for my current project. Also, I would like to thank the staff members at the Department of Chemistry and Biochemistry at the University of South Carolina for their efficient work and support.

At last but not least, I want to give my tender thanks to my family. My wife, Chunmei Yan, sacrificed a lot to support my Ph.D. career. My parents, Hui Dong and Fenghua Chen, came to America from China to help me. My son, Brayden Dong, his bright smile is always the best cure. They love me so much. Their company and encouragement helped me to go through the hardship of my life.

ABSTRACT

Fe-S clusters are one major type of the sulfur-containing cofactors, which conduct essential functions in organisms. The Suf pathway is one of the three main pathways for the biosynthesis of Fe-S clusters. In *E. coli*, the Suf pathway is utilized under iron limitation and oxidative stress. This ability is important for pathogens to survive. Also, the Suf pathway is found to be exclusive in bacteria, so it is a good target for novel antibiotic design. SufS is a cysteine desulfurase in the Suf pathway to extract sulfur from L-cysteine. It needs the enhancement of SufE. To better understand the catalytic mechanism of the reaction between SufS and L-cysteine in the presence of SufE, we applied ^{31}P NMR, stopped flow spectroscopy, and site directed mutagenesis. The results show that binding of SufE causes a conformational change of the pyridoxal 5'- phosphate (PLP) cofactor in SufS. The reaction of L-cysteine and PLP is a biphasic process including the fast phase (formation of external aldimine) and slow phase (shift to ketimine). The binding of SufE facilitates the formation of the ketimine. We mutated SufS H123A, which removed the enhancement of SufE to the activity of SufS and the formation of Cys ketimine. Finally, binding of SufE increased the formation of the persulfide in SufS. Characterization of the interaction of SufS and SufE may provide insight for the design of protein-protein interaction inhibitor. We made the Y345A/D346A mutation in SufS. We applied PLP quantification, analytical gel filtration, UV-visible absorption spectroscopic analysis and

circular dichroism to confirm this mutant still keeps the structural integrity. The basal activity of SufS Y345A/D346A is similar as that of wild-type SufS. However, SufE cannot enhance the activity of this mutant. The result of the isothermal titration calorimetry (ITC) shows that there is reduced interaction between this mutant and SufE. Based on the research above, a structural modeling of the SufS-SufE interaction was made through protein-protein docking, which clarifies more details in this interaction. SufS has an essential cofactor PLP that can be a target for the PLP-based inhibitor like DCS and LCS. To investigate if DCS/LCS can inhibit the activity of SufS, we checked the activity of SufS in the presence of either D-cycloserine (DCS) or L-cycloserine (LCS). The results show that there is a dose-dependent inhibition of SufS activity by DCS. The 50% inhibitory concentration (IC_{50}) was calculated to be 1.98 mM. A dose-dependent inhibition of SufS by LCS was also observed and the IC_{50} is 306.1 μM Compared with DCS, LCS shows much better inhibitory effects. The small-molecular docking shows that the nitrogen of DCS to start the nucleophilic attack towards the Schiff base of the PLP and Lys226 is far away from its target, which is not a proper orientation for the transimination reaction. The docking of LCS shows that the nitrogen of LCS for the nucleophilic attack is close to the Schiff base of Lys226 and PLP, which is a proper orientation for the following transimination reaction. The UV-visible absorption spectra of SufS and DCS shows the degradation of internal aldimine and a new intermediate at 380 nm is formed. The spectrum of LCS shows the 380 nm peak is reduced but the 320 nm peak keeps growing, which indicates the intermediate at 320 nm is a stable adduct and it is rarely get rescued by excessive L-cysteine. A reaction mechanism is proposed to depict the reaction between SufS and DCS/LCS.

TABLE OF CONTENTS

LIST OF TABLES

LIST OF FIGURES

LIST OF ABBREVIATIONS

β ME..... 2-Mercaptoethanol

CD..... Circular dichroism

DCS..... D-cycloserine

DTNB.....5,5-dithio-bis-2-nitrobenzoic acid (Ellman's reagent)

DTT.....Dithiothreitol

E. coli..... *Escherichia coli*

IAA.....Iodoacetamide

IPTG..... Isopropyl-1-thio-β-D-galactopyranoside

ITC..... Isothermal titration calorimetry

LCS.....L-cycloserine

NNDP.....N,N-dimethyl-p-phenylenediamine sulfate

PDB.....Protein data bank

PLP..... Pyridoxal 5'-phosphate

PMSF.....Phenylmethylsulfonl fluoride

1,5-I-AEDANS ..... N-(Iodoacetaminoethyl)-1-naphthylamine-5-sulfonic acid

CHAPTER 1
INTRODUCTION

Fe-S cluster and suf operon

Iron-sulfur (Fe-S) clusters are essential metal cofactors used in a wide-range of critical biological pathways, including respiration, photosynthesis, nitrogen fixation, and DNA repair. Fe-S clusters consist of iron in the Fe^{2+} or Fe^{3+} oxidation states bound to sulfide (S^{2-}). Different cluster types are referred to base on the ratios of iron and sulfide present in those clusters, for example [2Fe-2S] or [4Fe-4S] clusters (Figure 1.1). Larger, more complex Fe-S clusters can also be found in some metalloproteins.[1] For example the P-cluster of the nitrogenase complex contains a [7Fe-8S] cluster. Fe-S clusters can be combined with other metals and small molecules to form more complex cofactors, such as the FeMo cofactor also found in nitrogenase that contains [Mo-3Fe-3S] cluster, a [4Fe-3S] cluster bridged by 3 additional sulfide ligands, and a central carbon atom as part of a Fe_6-carbide species.[2, 3]

Despite their ubiquity across all domains of life, Fe-S clusters represent a potential Achilles heel for cells, especially those that grow in the presence of oxygen. Solvent exposed [4Fe-4S] cuboidal Fe-S clusters that contain mixed oxidation states of Fe are sensitive to oxidation by oxygen or reactive oxygen species formed in the cell.[4-6]

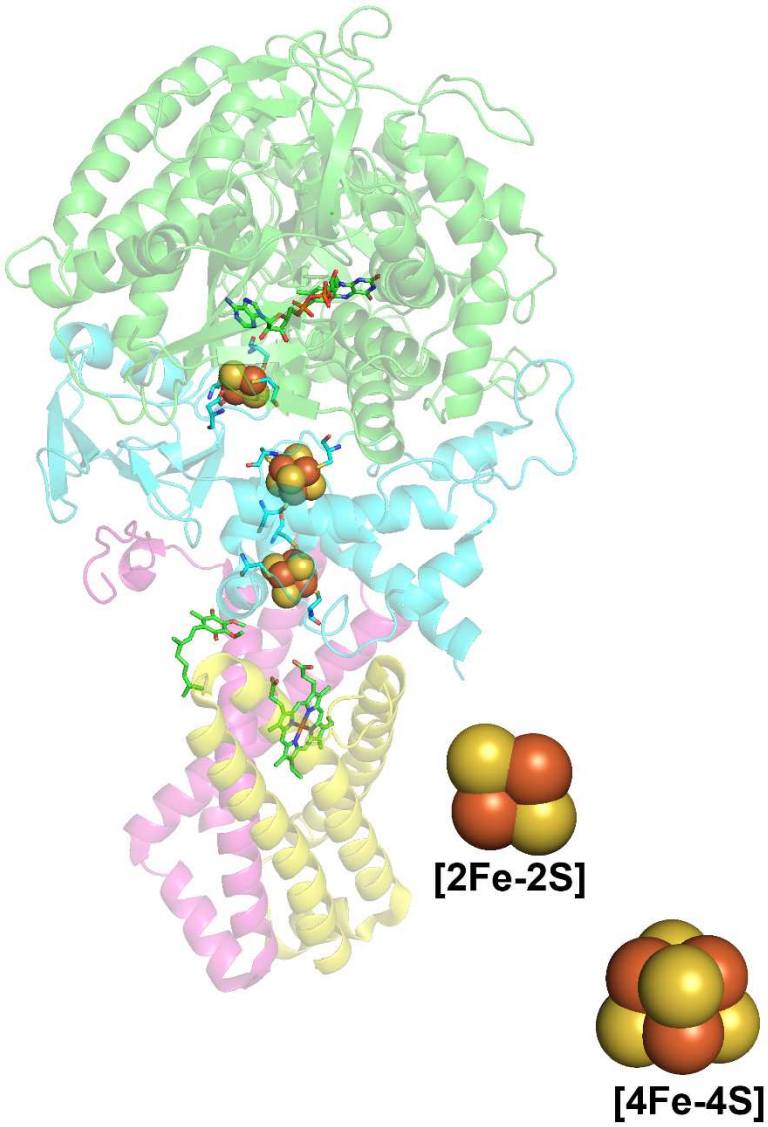

Figure 1.1. Structure of the *E. coli* succinate dehydrogenase complex with Fe-S clusters highlighted as spheres. Ubiquinone, flavin, and heme as well as Fe-S cluster ligands are shown as sticks.

Furthermore, iron availability in the environment greatly decreases in the presence of oxygen due to the oxidation of Fe^{2+} to Fe^{3+} and the formation of insoluble ferric hydroxide compounds. The scarcity of iron can make it difficult for a cell to maintain adequate levels of iron metalloproteins, especially in the case of Fe-S cluster proteins. Finally, Fe-S clusters can be poisoned by other thiophilic metals, such as copper and cobalt, that compete with iron for binding to exposed sulfur ligands.[7-9] Due to the sensitive nature of some types of Fe-S clusters, it is likely that cells growing in the presence of oxygen must constantly repair and/or resynthesize Fe-S cluster cofactors to keep up with the turnover of mature Fe-S metalloproteins.

The selective pressure to maintain adequate levels of essential Fe-S metalloproteins has led to the evolution of so-called Fe-S cluster biogenesis systems. These pathways, often encoded as polycistronic mRNA transcribed from operons in bacteria and Archaea, catalyze the *in vivo* formation of Fe-S clusters from iron and sulfide building blocks. Fe-S cluster biogenesis systems also include Fe-S cluster trafficking proteins that direct the de novo clusters to the appropriate Fe-S metalloprotein in the cell. Multiple Fe-S cluster biogenesis systems have been identified, each with their own peculiar phylogenetic distribution and (in eukarya) sub-cellular location.

Phylogenetic analysis reveals that the most ancient form of the *suf* operon consists of just two genes, *sufB* and *sufC* (Figure 1.2).[10, 11] The *sufBC* locus is primarily found in the earliest rooting lineages of the Archaea and Bacteria. It appears that selection for the addition of other *suf* genes occurred throughout evolution, possibly due to changing environmental pressures resulting from oxygenation of the atmosphere and concomitant alterations in iron and sulfur metabolism.[10] The most complex *suf* operons can contain as

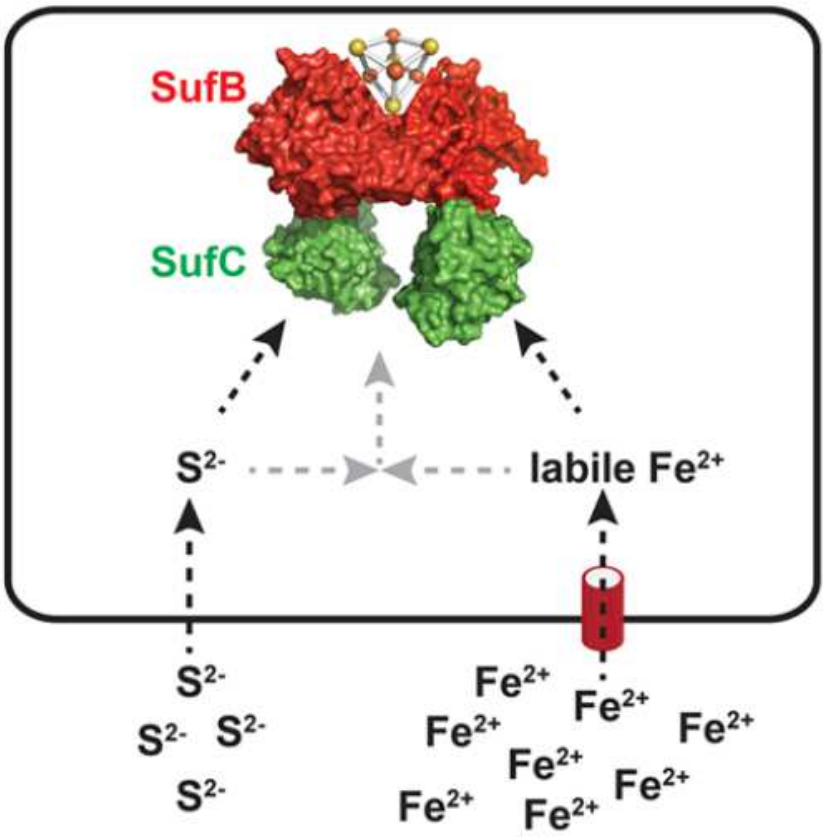

Figure 1.2. Model of the core components of Suf pathway: SufB and SufC.

many as 5-6 genes in addition to *sufB* and *sufC*. The exact roles for some of the Suf proteins are still being elucidated but much progress has been made in characterizing the core process of sulfur donation, *de novo* cluster formation, and downstream Fe-S cluster trafficking. While the simplest and phylogenetically most ancient *suf* operon (*sufBC*) appears in the Archaea, most of the progress in characterizing the Suf system at the genetic and biochemical levels has occurred in organisms with the more complex Suf systems, especially in the gamma proteobacteria.[12]

Regulation and physiological role of Suf in Proteobacteria

The Suf pathway was first identified as part of the Fur and OxyR regulons in the gammaproteobacterium, *Escherichia coli.*[13, 14] Fur is a global transcriptional regulator of iron homeostasis while OxyR controls the transcription of genes used for H_2O_2 stress defense. Since its initial discovery, the *E. coli* Suf pathway has been well characterized at the biochemical, genetic, and regulatory levels. Furthermore, the Suf pathway has been shown to work under oxidative stress and iron starvation conditions in the gammaproteobacteria, although this property may or may not be maintained in other bacteria.[15-20]

The biosynthesis of Fe-S clusters in *E. coli* is somewhat peculiar as the organism uses either the housekeeping Isc system (which does not appear to be particularly stress-resistant) or the stress-responsive Suf pathway[15, 19, 20] The complete absence of both systems is lethal to *E. coli*.[11, 19] The lethality appears to stem from loss of Fe-S clusters in specific metalloenzymes of the isoprenoid biosynthesis pathway as lethality can be bypassed if an alternate pathway is provided that does not rely on Fe-S cluster cofactors.[21]

In *E. coli*, the Suf pathway consists of SufA, SufB, SufC, SufD, SufE, and SufS organized in an operon as *sufABCDSE*. *E. coli* tightly controls transcription of the *suf* operon through the coordinated action of multiple regulatory proteins (Figure 1.3). Under non-stressed conditions, Fur-Fe^{2+} binds to the *suf* promoter to repress the transcription of the *suf* operon.[13, 19, 22] During iron starvation Fur converts to its iron-free (apo) form, which does not efficiently repress target promoters, and releases *suf* repression allowing increased transcription of the *suf* operon. Oxidative stress activates OxyR, which increases *suf* transcription in conjunction with the DNA-bending protein IHF.[14, 16, 19, 22] Later it was also discovered that IscR regulates the *suf* operon. IscR is an Fe-S cluster binding transcription factor which regulates at least 40 genes in *E. coli*, including the *isc* and *suf* operons.[23, 24] Apo-IscR binds the *suf* promoter to activate transcription of the *suf* operon in response to oxidative stress, iron limitation, and other conditions that perturb Fe-S cluster biogenesis by the Isc pathway[22, 25-28] Coordination of *isc* and *suf* expression is also facilitated by the small RNA RyhB. The expression of *ryhB* is repressed by Fur-Fe^{2+} when iron is replete in the cell.[29] Under limited iron, apo-Fur loses the ability to bind DNA, which releases *ryhB* repression. The *isc* mRNA transcript basepairs with RyhB causing it to be degraded when iron is limited.[30, 31] The sum of this complex regulatory network is that Fe-S cluster biogenesis switches from the Isc to the Suf pathway under conditions of iron limitation and oxidative stress in *E. coli*. The switch to the Suf pathway in these organisms is supported by genetic studies demonstrating that most Δ*suf* deletion strains are more sensitive to oxidative stress, iron starvation, and metal poisoning.[7, 11, 17-20, 32] All of these defects are linked to disruption of Fe-S cluster biogenesis by the stress condition if the Suf machinery is missing.

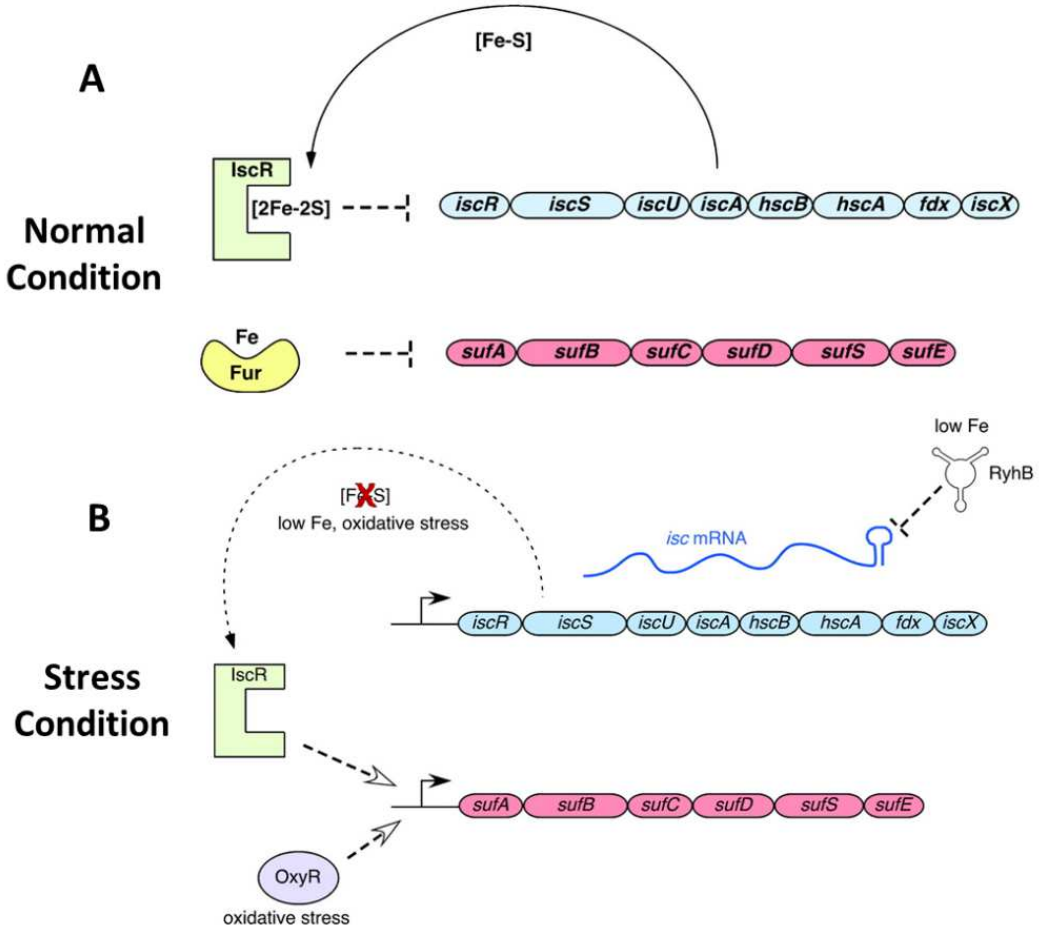

Figure 1.3. Regulation of Fe-S cluster assembly pathways in *E. coli* by IscR and OxyR. (A) Regulation by holo IscR and Fur under normal condition. (B) Regulation by apo IscR and OxyR under stress condition.

Biochemical characterization of the Suf proteins from Proteobacteria

The SufA, SufB, SufC, SufD, SufE, and SufS proteins form the core of the Suf Fe-S cluster biogenesis system in *E. coli* and related bacteria (Figure 1.4). Although sodium sulfide can be used for the Fe-S cluster reconstitution *in vitro*, Fe-S cluster assembly pathways in the Proteobacteria utilize a cysteine desulfurase enzyme to mobilize sulfur from L-cysteine in a reaction that also requires a pyridoxal 5' - phosphate (PLP) cofactor.[19, 33-37] The cysteine desulfurase reaction produces an enzyme bound persulfide that can be transferred to other proteins during cluster assembly.

Cysteine desulfurases can be divided into group I and group II based on sequence analysis.[38] The key difference is the structure of the active site of the desulfurase. In the Suf pathway of *E. coli*, SufS acts as the cysteine desulfurase and is a group II desulfurase enzyme in which its active site residue, Cys364, is located on a rigid loop with a somewhat hydrophobic environment.[39-41] This is in contrast to IscS and other group I enzymes that have a flexible catalytic cysteine loop that is exposed to the environment (Figure 1.5).[42-44] These structural differences may partially explain why the intrinsic activity of SufS is low compared to that of IscS. However, SufS sometimes has a partner protein, SufE, which works to enhance the cysteine desulfurase activity of SufS.[33, 45-47] The *sufE* gene can be found grouped with a group II cysteine desulfurase, like *sufS,* in Bacteriodetes and Gammaproteobacteria but is not wide-spread outside these phyla.[10] Approximately 17% of the currently sequenced bacterial genomes have the *sufE* gene while 89% contain a *sufS* homologue. When SufE interacts with SufS, the cysteine desulfurase activity enhancement can be as high as 50-fold in *Erwinia chrysanthemi* (renamed *Dickeya dadantii*).[33] In *E. coli*, SufE can stimulate SufS activity to 8-fold.[46, 48] X-ray crystallography, enzymology,

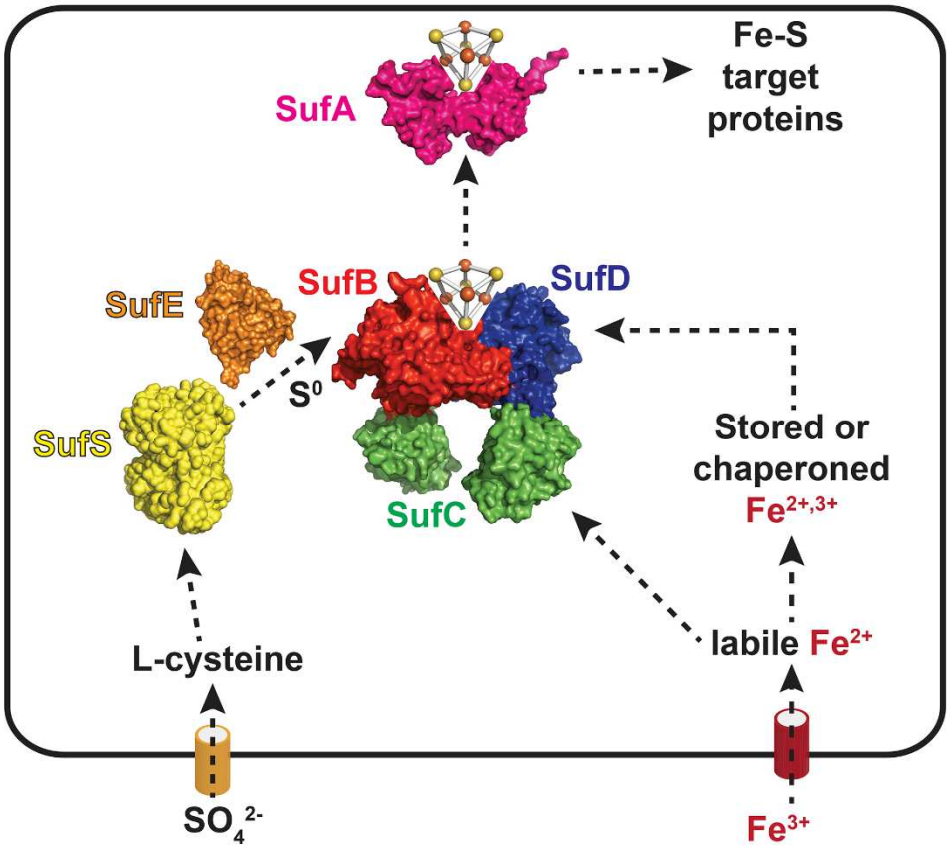

Figure 1.4. Proposed model for Suf function.

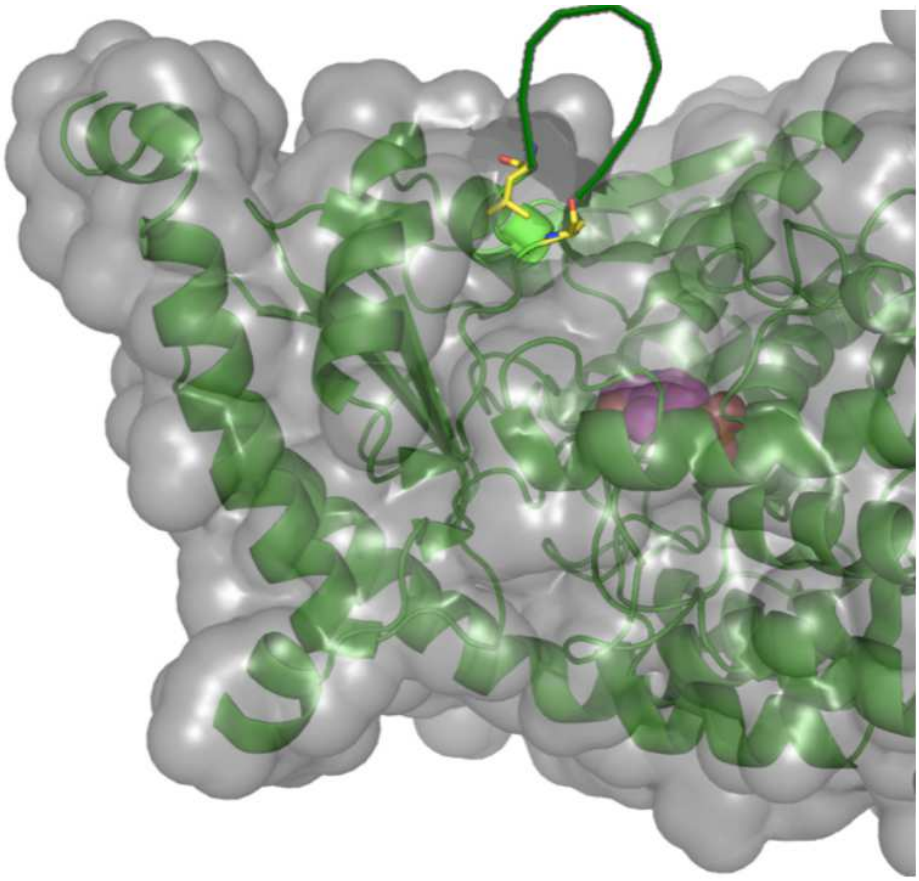

Figure 1.5. Crystal structure of IscS (PDB code: 1P3W). The green loop is a simulated structure containing the active site of IscS.

and site-directed mutagenesis have been used to propose the overall SufS – SufE reaction (Figure 1.6).[33, 45-51] L-cysteine binds to the PLP cofactor, which is in a hydrophobic pocket within the active site and forms an external aldimine. Then Cys364 carries out a nucleophilic attack to extract the sulfur from cysteine, which results in the formation of the persulfide bonded to Cys364 (R-S-SH) and the release of L-alanine. Next the persulfide of SufS is transferred to the SufE cysteine residue, Cys51, via a nucleophilic attack of Cys51 on the R-S-SH species. This resets SufS Cys364 allowing the enzyme to fully turnover, thereby enhancing its activity. In addition to SufE acting as a substrate in the overall ping-pong sulfotransferase reaction, the interaction between SufS and SufE may allosterically stimulate the binding of L-cysteine to PLP, the formation of the external aldimine, and/or the formation of later reaction intermediates in SufS that also provides some enhancement of SufS activity.[48, 51]

A crystal structure of the SufE monomer shows that active site Cys51 is positioned at the end of a loop and oriented so that the side-chain is buried from solvent exposure in a hydrophobic cavity (Figure 1.7).[49] The relative inaccessibility of SufS and SufE active site Cys loops protects the resting proteins from oxidation during exposure to H_2O_2. However, SufS Cys364 and SufE Cys51 must interact to facilitate persulfide transfer. A complex determined for CsdA and CsdE, two homologues of SufS and SufE respectively, indicates that the active site loop of the sulfur acceptor protein (CsdE) is flipped out and interacting with the active site cleft of the cysteine desulfurase (CsdA) when the two proteins bind.[52] A similar conformational change in SufE has been observed by hydrogen – deuterium exchange mass spectrometry (HDX-MS) studies (Figure 1.8).[51] Furthermore, the D74R mutation of SufE that increases the solvent accessibility and

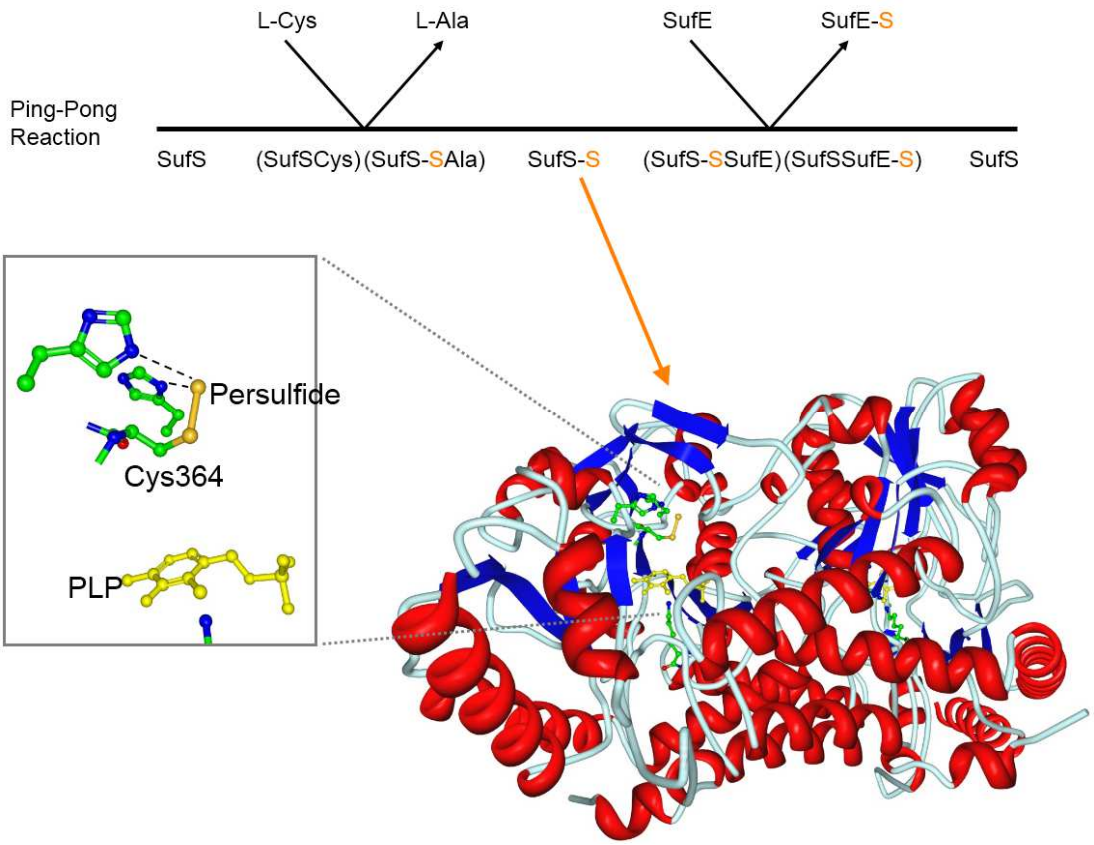

Figure 1.6. Mechanism of the reaction of SufS and L-cysteine in the presence of SufE and the crystal structure of the persulfide form of SufS.

Figure 1.7. Crystal structure of a SufE monomer (PDB code: 1MZG). The grey part is the hydrophobic region. The yellow stick is the active site of SufE (Cys51).

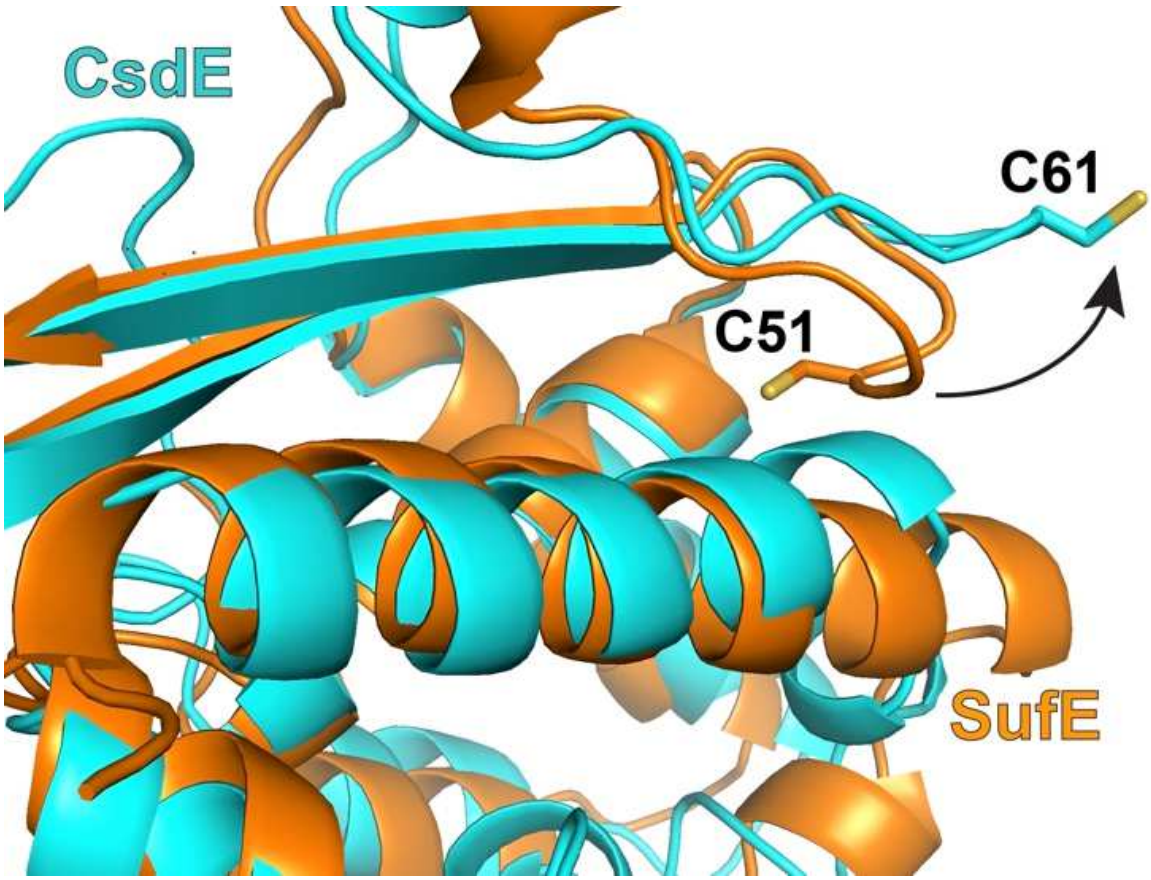

Figure 1.8. Alignment of CsdE (from its complex with CsdA) with resting SufE. Active site Cys residues SufE C51 and CsdE C61 are shown.

dynamics of the loop containing the active site Cys51 also leads to a stronger binding affinity with SufS than that of the wild-type SufE.[48]

In order for multiple cycles of the sulfotransferase reaction to occur, the persulfide on SufE Cys51 must then be released. *In vitro* this can be accomplished by the addition of reductants (DTT, TCEP) or by specific delivery of the persulfide to the Fe-S cluster scaffold.[45-47, 50] It was shown that SufE specifically donates persulfide to the SufB protein, which is the proposed scaffold of the Suf system (see below) [53]. The transfer of sulfur from SufS to SufE to SufB recycles SufS and SufE to their resting states ready for another round of desulfurase reaction.[46, 47, 53] The interaction of SufE with SufB is enhanced if SufC is present and has formed a complex with SufB (either as $SufB_2C_2$ or $SufBC_2D$).[46, 53]

SufB accepts persulfide sulfur from SufE, can bind a [4Fe-4S] cluster, and can transfer the cluster acceptor Fe-S proteins.[53-56] Based on these studies, it has been proposed that SufB is the scaffold for Fe-S cluster assembly in Suf pathway. SufB is not homologous to the IscU scaffold of the Isc system and represents a distinct class of scaffold protein. The two scaffold proteins also show differences in their de novo cluster assembly steps. IscU can form stable a [2Fe-2S] cluster intermediate or can undergo reductive coupling of 2 x [2Fe-2S] clusters to form a [4Fe-4S] cluster.[57] In contrast SufB does not seem to proceed through the same semi-stable intermediates to reach a [4Fe-4S] cluster, although the [4Fe-4S] cluster on SufB can be converted into the [2Fe-2S] form upon air exposure.[53, 56, 58] It was also shown that the IscU [2Fe-2S] cluster is less stable than the SufB [2Fe-2S] cluster in the presence of hydrogen peroxide, oxygen, and iron chelators, providing a partial biochemical rationale for use of the Suf system under stress conditions *in vivo*.[58]

SufC has a nucleotide hydrolysis domain homologous to that of the ATP-binding cassette (ABC) family of transporters that utilize ATP hydrolysis for transport across cellular membranes.[18, 59-61] However, SufC is expressed as a soluble cytoplasmic protein and is not part of a membrane bound ABC transport system. The exact role of SufC as an ATPase is still unknown, but mutations in the ATP binding site abolish the *in vivo* Fe-S cluster formation of the Suf pathway.[18, 19, 55] The reason for this appears to be that the Suf pathway may demand the activity of SufC ATPase and SufD to efficiently acquire iron *in vivo*.[55]

Interactions among the SufB, SufC, and SufD proteins result in three stable complexes: $SufBC_2D$, $SufB_2C_2$, and $SufC_2D_2$.[46, 55, 59, 62-65] SufD is paralogous to SufB and there is considerable C-terminal sequence similarity between SufB and SufD. This region of shared homology includes a C-terminal region of the overall the β-helix core as well as the specific C-terminal α-helices where both SufB and SufD interact with SufC.[64, 65] While SufD is a paralogue of SufB it does not seem to function directly as a Fe-S cluster scaffold. SufD may assist iron entry into the $SufBC_2D$ complex in conjunction with the ATPase activity of SufC.[55] $SufBC_2D$ also can bind one equivalent of $FADH_2$, which raises the possibility that the cofactor $FADH_2$ may serve as an electron donor to reduce ferric iron or persulfide during Fe-S cluster assembly on SufB.[56]

While $SufB_2C_2$, and $SufC_2D_2$ can be isolated under some conditions, $SufBC_2D$ is the primary complex resulting from the co-expression of the entire *sufABCDSE* operon in *E. coli*, which suggests that it is the most stable form of the three complexes.[46, 56, 65] The SufB protein itself is unstable and tends to form a heterogeneous oligomer when it is expressed alone.[53, 62, 63] SufC and SufB can interact to form $SufB_2C_2$, which is capable of

creating and transferring Fe-S clusters to apoproteins and is more efficient than $SufBC_2D$ in de novo Fe-S cluster assembly on ferredoxin *in vitro* using readily available iron salts as the iron source.[53, 55, 59, 63, 66] It is possible that $SufB_2C_2$ may act as the final scaffold and $SufBC_2D$ may be used as a distinct step for Fe-S cluster formation before the assembly of the final cluster on $SufB_2C_2$.[66] Although $SufB_2C_2$ can assembly Fe-S clusters *in vitro* using iron salts, labile iron is tightly controlled in vivo. Furthermore, $SufB_2C_2$ does not appear to be efficient at building Fe-S clusters when expressed *in vivo* without SufD.[55]

Therefore, formation of $SufBC_2D$ may be specifically required for iron mobilization from specific donors or storage sites in the cell. This model in consistent with the need for SufD to build Fe-S clusters on SufB in vivo but requires further testing to be validated. One weakness in the model is that $SufB_2C_2$ has not been observed *in vivo* from native expression of the *suf* operon and can only be isolated if *sufB* and *sufC* are expressed without *sufD* from a plasmid construct. The third complex, $SufC_2D_2$, is formed when *sufC* and *sufD* are co-expressed in the absence of *sufB*.[63, 64] To date no functional role has been assigned to $SufC_2D_2$ and it has not been observed in vivo from native expression of the *suf* operon.

The crystal structures of $SufC_2D_2$ and $SufBC_2D$ from *E. coli* have been solved.[64, 65] Both structures show that the interaction of SufB or SufD remodels the ATP catalytic site of SufC (Figure 1.9). Binding to SufB or SufD makes the ATP binding site of SufC more accessible, which could facilitate ATP binding and hydrolysis. These structural observations are consistent with that fact that in *Thermotoga maritima*, the interaction of SufB with SufC can enhance the low basal ATPase activity of SufC.[59] Similar effects have also been found when comparing the low ATPase activity of *E. coli* SufC with the

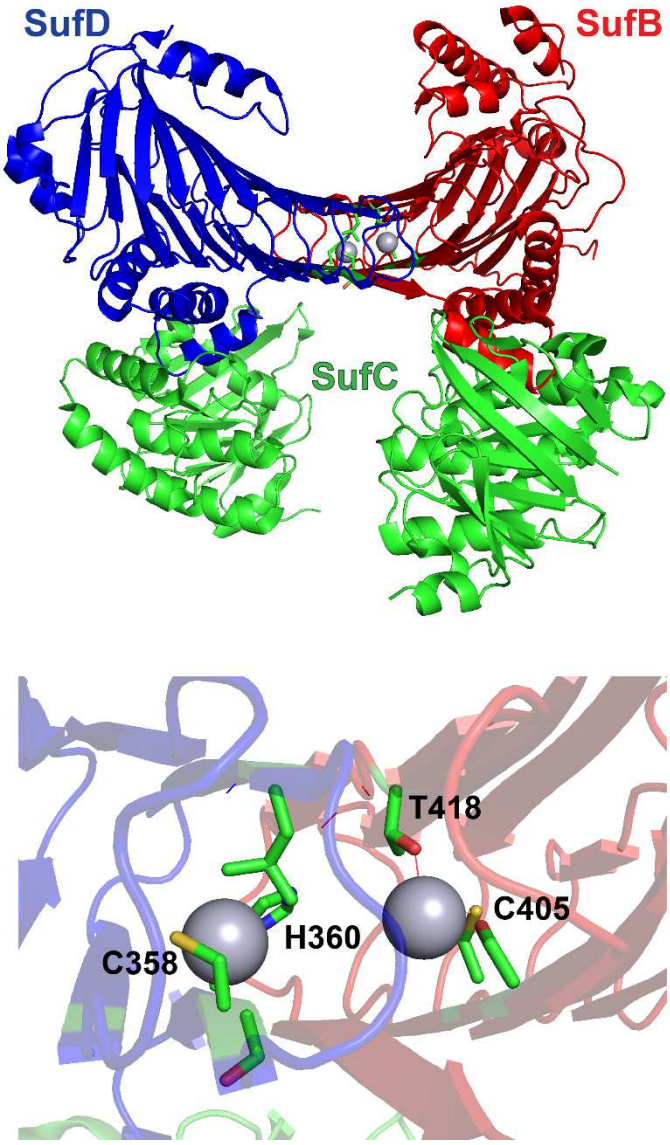

Figure 1.9. *Top*, overall structure of SufBC$_2$D with Hg^{2+} shown as grey spheres (from PDB 5AWG). *Bottom*, zoom of the metal binding site at the SufB – SufD interface with residues (sticks) labeled.

enhanced ATPase activity observed in both $SufB_2C_2$ and $SufBC_2D$ (unpublished data from F. W. Outten and K. S. Thomas). In addition to the conformational changes caused in SufC, it has been proposed that ATP-induced dimerization of SufC could alter the SufB and SufD proteins in the complex.[64, 65] During ATP binding and hydrolysis SufC likely forms a transient head to tail dimer within the $SufBC_2D$ complex, which may induce a gross conformational change of SufB and SufD, leading to an exposure of Cys405 of SufB and Cys358 of SufD in the heterodimer interface. These two residues bind an adventitious Hg^{2+} ion in the $SufBC_2D$ structure, indicating that they may be positioned to provide partial ligands for iron or Fe-S cluster binding.[65] His360 of SufD is also in the vicinity of the Hg^{2+} binding site near the interface of SufB and SufD. Mutation of SufB Cys405 or SufD His360 led to disruption of *in vivo* cluster assembly (although strangely mutation of SufD Cys358 had no obvious effect).[65] SufD is not required for SufB to bind an Fe-S cluster in vitro but it may provide transient ligands during iron trafficking into the cluster binding site in vivo or during cluster transfer to an acceptor protein.

The final protein in the Suf Fe-S cluster biogenesis pathway, SufA, belongs to the A-type carrier (ATC) family, which are proposed to deliver Fe-S clusters to apoproteins.[54, 67-73] Fe-S clusters can be reconstituted on SufA *in vitro* and the cluster binds to SufA through three conserved cysteine residues.[67, 68] *In vivo* studies show that when SufA is co-expressed with the whole *suf* operon, it purifies bound to a [2Fe-2S] cluster[71] and this form of SufA can transfer its Fe-S cluster to both [2Fe-2S] and [4Fe-4S] apoproteins. Elegant analysis of the ^{Nif}IscA homologue of SufA from *A. vinelandii* shows the protein can interconvert from a [2Fe-2S] cluster form under aerobic conditions to a [4Fe-4S] form under anaerobic, reducing conditions.[74] This cluster conversion activity could be important

for responding to changes in oxygen availability and/or altering the pool of available clusters to fit demand for specific cluster types. *In vitro*, Fe-S clusters can be transferred from the $SufBC_2D$ scaffold to SufA while the transfer in the reverse direction does not occur.[54] SufA physically interacts with SufB and this interaction is promoted if SufB is part of the $SufBC_2D$ complex and if $SufBC_2D$ is in the Fe-S cluster (holo) form.[54] Reactions containing all the components show that SufA can accept Fe-S clusters from SufB and move them to downstream target enzymes, supporting a role for SufA as an Fe-S cluster trafficking protein.[66, 71]

These *in vitro* studies are supported by characterization of Δ*sufA* mutant strains *in vivo*. The growth defect of a Δ*sufA* single mutant is mild but the growth defects are enhanced if the Δ*sufA* mutation is combined with deletions of *iscA* and/or *erpA*, two paralogues of SufA.[11, 19, 20, 72, 73]. Defects in Fe-S cluster biogenesis in these strains are more pronounced under aerobic conditions, where cluster turnover would be expected to increase due to damage from reactive oxygen species, and seem to be largely confined to the [4Fe-4S] proteins.[72, 73] Therefore it seems that the ATC family of proteins likely provides advantages for Fe-S cluster trafficking under aerobic conditions.

SufA and its paralogue IscA can also bind and donate iron in vitro for cluster assembly on the IscU scaffold.[75-80] ^{Nif}IscA from *A. vinelandii* binds Fe(III) in a 5-coordinate site with two or three cysteinate ligands and can bind Fe(II) with three cysteinate and 1-2 oxygenic ligands in a site similar to reduced rubredoxins or rubredoxin variants.[80] The iron-donation activity of SufA and IscA may be an artifact since iron release is mediated by L-cysteine present during the *in vitro* reaction and does not appear to be a specific donation process directly to the scaffold.[75, 77, 78, 80] While an *in vivo* role for

SufA/IscA for iron donation has not been conclusively demonstrated, it was shown that an IscA Y40F mutant that cannot bind mononuclear iron also cannot restore growth of the Δ*iscA*Δ*sufA* double mutant strain.[70] A recent study in *E. coli* shows that deletion of *iscA* and *sufA* or addition of a cell-permeable iron chelator results in accumulation of a red intermediate in recombinant IscS that is being over-expressed in that strain.[81] This IscS intermediate is likely a trapped alanine-quinonoid intermediate of the cysteine desulfurase reaction, suggesting that the ATC proteins are needed for the early steps of Fe-S cluster biogenesis to progress.[81] However, it is not clear from those studies if the intermediate accumulates due to a downstream block in cluster release from the scaffold protein IscU to the ATC proteins or if it occurs due to a direct role for the ATC proteins during cluster assembly. When considering all of the published studies on ATC proteins, it seems reasonable to hypothesize that they may have multiple functions or that their Fe-S cluster carrier function could be modulated by iron binding. For example, the iron-binding activity of SufA and IscA may have a physiological role in regulating Fe-S cluster biogenesis in response to iron availability in vivo or the ATC proteins may serve as ferric iron "reservoirs" that can release iron into a labile pool to help indirectly drive Fe-S cluster biogenesis.

Interactions among the multi-protein Suf complexes are important for regulating the stepwise assembly of Fe-S clusters. SufS relies on SufE to amplify its low basal activity, both by acting as a substrate as well as by allosterically influencing the SufS active site. The sulfotransferase activity of the SufS – SufE pair is itself significantly increased in the presence of $SufBC_2D$ or $SufB_2C_2$ but not if SufB alone is added. Similarly, the ATPase activity of SufC is low unless it is bound to its partner proteins, SufB and/or SufD.

Finally, SufA interactions with SufB are enhanced if SufB binds an Fe-S cluster as part of the $SufBC_2D$ complex. These interactions provide tight regulation to protect sensitive reaction intermediates (such as enzyme-bound persulfide and/or nascent Fe-S moieties) from oxidative stress. It is likely that these characteristics are biochemical adaptations that allow the Suf pathway to maintain Fe-S cluster biogenesis under stress. *In vitro* and *in vivo* it is clear that the IscS cysteine desulfurase and IscU scaffold of the Isc pathway are more sensitive to inactivation by oxidants and chelators compared with the SufS-SufE-$SufBC_2D$ super complex.[15, 50, 58]

REFERENCE

1. E. M. Shepard, E. S. Boyd, J. B. Broderick and J. W. Peters, Curr. Opin. Chem. Biol., 2011, 15: 319-327.

2. Y. Hu and M. W. Ribbe, Angew. Chem. Int. Ed. Engl., 2016, 55, 8216-8226.

3. Y. Hu and M. W. Ribbe, Annu. Rev. Biochem., 2016, 85, 455-483.

4. D. H. Flint, J. F. Tuminello and M. H. Emptage, J. Biol. Chem., 1993, 268, 22369-22376.

5. P. R. Gardner and I. Fridovich, J. Biol. Chem., 1991, 266, 19328-19333.

6. P. R. Gardner and I. Fridovich, J. Biol. Chem., 1991, 266, 1478-1483.

7. L. Macomber and J. A. Imlay, Proc. Natl. Acad. Sci. U. S. A., 2009, 106, 8344-8349.

8. C. Ranquet, S. Ollagnier de Choudens, L. Loiseau, F. Barras and M. Fontecave, J. Biol. Chem., 2007, 282, 30442-30451.

9. F. F. Xu and J. A. Imlay, Appl. Environ. Microbiol., 2012, 78, 3614-3621.

10. E. S. Boyd, K. M. Thomas, Y. Dai, J. M. Boyd and F. W. Outten, Biochemistry, 2014, 53, 5834-5847.

11. Y. Takahashi and U. Tokumoto, J. Biol. Chem., 2002, 277, 28380-28383.

12. B. Roche, L. Aussel, B. Ezraty, P. Mandin, B. Py and F. Barras, Biochim. Biophys. Acta, 2013, 1827, 455-469.

13. S. I. Patzer and K. Hantke, J. Bacteriol., 1999, 181, 3307-3309.

14. M. Zheng, X. Wang, L. J. Templeton, D. R. Smulski, R. A. LaRossa and G. Storz, J. Bacteriol., 2001, 183, 4562-4570.

15. S. Jang and J. A. Imlay, Mol. Microbiol., 2010, 78, 1448-1467.

16. J. H. Lee, W. S. Yeo and J. H. Roe, Mol. Microbiol., 2004, 51, 1745-1755.

17. L. Nachin, M. El Hassouni, L. Loiseau, D. Expert and F. Barras, Mol. Microbiol., 2001, 39, 960-972.

18. L. Nachin, L. Loiseau, D. Expert and F. Barras, EMBO J., 2003, 22, 427-437.

19. F. W. Outten, O. Djaman and G. Storz, Mol. Microbiol., 2004, 52, 861-872.

20. U. Tokumoto, S. Kitamura, K. Fukuyama and Y. Takahashi, J. Biochem., 2004, 136, 199-209.

21. L. Loiseau, C. Gerez, M. Bekker, S. Ollagnier-de Choudens, B. Py, Y. Sanakis, J. Teixeira de Mattos, M. Fontecave, et al., Proc. Natl. Acad. Sci. U. S. A., 2007, 104, 13626-13631.

22. K. C. Lee, W. S. Yeo and J. H. Roe, J. Bacteriol., 2008, 190, 8244-8247.

23. C. J. Schwartz, J. L. Giel, T. Patschkowski, C. Luther, F. J. Ruzicka, H. Beinert and P. J. Kiley, Proc. Natl. Acad. Sci. U. S. A., 2001, 98, 14895-14900.

24. J. L. Giel, D. Rodionov, M. Liu, F. R. Blattner and P. J. Kiley, Mol. Microbiol., 2006, 60, 1058-1075.

25. W. S. Yeo, J. H. Lee, K. C. Lee and J. H. Roe, Mol. Microbiol., 2006, 61, 206-218.

26. A. D. Nesbit, J. L. Giel, J. C. Rose and P. J. Kiley, J. Mol. Biol., 2009, 387, 28-41.

27. J. L. Giel, A. D. Nesbit, E. L. Mettert, A. S. Fleischhacker, B. T. Wanta and P. J. Kiley, Mol. Microbiol., 2013, 87, 478-492.

28. S. Rajagopalan, S. J. Teter, P. H. Zwart, R. G. Brennan, K. J. Phillips and P. J. Kiley, Nat. Struct. Mol. Biol., 2013, 20, 740-747.

29. E. Masse and S. Gottesman, Proc. Natl. Acad. Sci. U. S. A., 2002, 99, 4620-4625.

30. E. Masse, C. K. Vanderpool and S. Gottesman, J. Bacteriol., 2005, 187, 6962-6971.

31. G. Desnoyers, A. Morissette, K. Prevost and E. Masse, EMBO J., 2009, 28, 1551-1561.

32. F. Barras and M. Fontecave, Metallomics, 2011, 3, 1130-1134.

33. L. Loiseau, S. Ollagnier-de-Choudens, L. Nachin, M. Fontecave and F. Barras, J. Biol. Chem., 2003, 278, 38352-38359.

34. H. Mihara, M. Maeda, T. Fujii, T. Kurihara, Y. Hata and N. Esaki, J. Biol. Chem., 1999, 274, 14768-14772.

35. C. J. Schwartz, O. Djaman, J. A. Imlay and P. J. Kiley, Proc. Natl. Acad. Sci. U. S. A., 2000, 97, 9009-9014.

36. L. Zheng, R. H. White, V. L. Cash and D. R. Dean, Biochemistry, 1994, 33, 4714-4720.

37. L. Zheng, R. H. White, V. L. Cash, R. F. Jack and D. R. Dean, Proc. Natl. Acad. Sci. U. S. A., 1993, 90, 2754-2758.

38. H. Mihara and N. Esaki, Appl. Microbiol. Biotechnol., 2002, 60, 12-23.

39. T. Fujii, M. Maeda, H. Mihara, T. Kurihara, N. Esaki and Y. Hata, Biochemistry, 2000, 39, 1263-1273.

40. C. D. Lima, J. Mol. Biol., 2002, 315, 1199-1208.

41. H. Mihara, T. Fujii, S. Kato, T. Kurihara, Y. Hata and N. Esaki, J. Biochem., 2002, 131, 679-685.

42. J. R. Cupp-Vickery, H. Urbina and L. E. Vickery, J. Mol. Biol., 2003, 330, 1049-1059.

43. R. Shi, A. Proteau, M. Villarroya, I. Moukadiri, L. Zhang, J. F. Trempe, A. Matte, M. E. Armengod, et al., PLoS Biol., 2010, 8, e1000354.

44. H. D. Urbina, J. R. Cupp-Vickery and L. E. Vickery, Acta Crystallogr. D Biol. Crystallogr., 2002, 58, 1224-1225.

45. S. Ollagnier-de-Choudens, D. Lascoux, L. Loiseau, F. Barras, E. Forest and M. Fontecave, FEBS Lett., 2003, 555, 263-267.

46. F. W. Outten, M. J. Wood, F. M. Munoz and G. Storz, J. Biol. Chem., 2003, 278, 45713-45719.

47. B. P. Selbach, P. K. Pradhan and P. C. Dos Santos, Biochemistry, 2013, 52, 4089-4096.

48. Y. Dai, D. Kim, G. Dong, L. S. Busenlehner, P. A. Frantom and F. W. Outten, Biochemistry, 2015, 54, 4824-4833.

49. S. Goldsmith-Fischman, A. Kuzin, W. C. Edstrom, J. Benach, R. Shastry, R. Xiao, T. B. Acton, B. Honig, et al., J. Mol. Biol., 2004, 344, 549-565.

50. Y. Dai and F. W. Outten, FEBS Lett., 2012, 586, 4016-4022.

51. H. Singh, Y. Dai, F. W. Outten and L. S. Busenlehner, J. Biol. Chem., 2013, 288, 36189-36200.

52. S. Kim and S. Park, J. Biol. Chem., 2013, 288, 27172-27180.

53. G. Layer, S. A. Gaddam, C. N. Ayala-Castro, S. Ollagnier-de Choudens, D. Lascoux, M. Fontecave and F. W. Outten, J. Biol. Chem., 2007, 282, 13342-13350.

54. H. K. Chahal, Y. Dai, A. Saini, C. Ayala-Castro and F. W. Outten, Biochemistry, 2009, 48, 10644-10653.

55. A. Saini, D. T. Mapolelo, H. K. Chahal, M. K. Johnson and F. W. Outten, Biochemistry, 2010, 49, 9402-9412.

56. S. Wollers, G. Layer, R. Garcia-Serres, L. Signor, M. Clemancey, J. M. Latour, M. Fontecave and S. Ollagnier de Choudens, J. Biol. Chem., 2010, 285, 23331-23341.

57. J. N. Agar, C. Krebs, J. Frazzon, B. H. Huynh, D. R. Dean and M. K. Johnson, Biochemistry, 2000, 39, 7856-7862.

58. B. Blanc, M. Clemancey, J. M. Latour, M. Fontecave and S. Ollagnier de Choudens, Biochemistry, 2014, 53, 7867-7869.

59. K. Rangachari, C. T. Davis, J. F. Eccleston, E. M. Hirst, J. W. Saldanha, M. Strath and R. J. Wilson, FEBS Lett., 2002, 514, 225-228.

60. S. Watanabe, A. Kita and K. Miki, J. Mol. Biol., 2005, 353, 1043-1054.

61. S. Kitaoka, K. Wada, Y. Hasegawa, Y. Minami, K. Fukuyama and Y. Takahashi, FEBS Lett., 2006, 580, 137-143.

62. J. F. Eccleston, A. Petrovic, C. T. Davis, K. Rangachari and R. J. Wilson, J. Biol. Chem., 2006, 281, 8371-8378.

63. A. Petrovic, C. T. Davis, K. Rangachari, B. Clough, R. J. Wilson and J. F. Eccleston, Protein Sci., 2008, 17, 1264-1274.

64. K. Wada, N. Sumi, R. Nagai, K. Iwasaki, T. Sato, K. Suzuki, Y. Hasegawa, S. Kitaoka, et al., J. Mol. Biol., 2009, 387, 245-258.

65. K. Hirabayashi, E. Yuda, N. Tanaka, S. Katayama, K. Iwasaki, T. Matsumoto, G. Kurisu, F. W. Outten, et al., J. Biol. Chem., 2015, 290, 29717-29731.

66. H. K. Chahal and F. W. Outten, J. Inorg. Biochem., 2012, 116, 126-134.

67. S. Ollagnier-de Choudens, L. Nachin, Y. Sanakis, L. Loiseau, F. Barras and M. Fontecave, J. Biol. Chem., 2003, 278, 17993-18001.

68. S. Ollagnier-de-Choudens, Y. Sanakis and M. Fontecave, J. Biol. Inorg. Chem., 2004, 9, 828-838.

69. K. Wada, Y. Hasegawa, Z. Gong, Y. Minami, K. Fukuyama and Y. Takahashi, FEBS Lett., 2005, 579, 6543-6548.

70. J. Lu, J. Yang, G. Tan and H. Ding, Biochem. J., 2008, 409, 535-543.

71. V. Gupta, M. Sendra, S. G. Naik, H. K. Chahal, B. H. Huynh, F. W. Outten, M. Fontecave and S. Ollagnier de Choudens, J. Am. Chem. Soc., 2009, 131, 6149-6153.

72. G. Tan, J. Lu, J. P. Bitoun, H. Huang and H. Ding, Biochem. J., 2009, 420, 463-472.

73. D. Vinella, C. Brochier-Armanet, L. Loiseau, E. Talla and F. Barras, Plos Genetics, 2009, 5, e1000497.

74. D. T. Mapolelo, B. Zhang, S. G. Naik, B. H. Huynh and M. K. Johnson, Biochemistry, 2012, 51, 8071-8084.

75. B. Ding, E. S. Smith and H. Ding, Biochem. J., 2005, 389, 797-802.

76. H. Ding and R. J. Clark, Biochem. J., 2004, 379, 433-440.

77. H. Ding, R. J. Clark and B. Ding, J. Biol. Chem., 2004, 279, 37499-37504.

78. H. Ding, K. Harrison and J. Lu, J. Biol. Chem., 2005, 280, 30432-30437.

79. H. Ding, J. Yang, L. C. Coleman and S. Yeung, J. Biol. Chem., 2007, 282, 7997-8004.

80. D. T. Mapolelo, B. Zhang, S. G. Naik, B. H. Huynh and M. K. Johnson, Biochemistry, 2012, 51, 8056-8070.

81. J. Yang, G. Tan, T. Zhang, R. H. White, J. Lu and H. Ding, J. Biol. Chem., 2015, 290, 14226-14234.

CHAPTER 2
MECHANISM OF ACTIVATION OF SUFS BY SUFE: EQULIBRIUM AND PRE-EQUILIBRIUM KINETIC ANALYSIS

ABSTRACT

SufS is a cysteine desulfurase to abstract sulfur from L-cysteine and provides a sulfur source for the Fe-S cluster biosynthesis. SufE interacts with SufS to accept sulfur from SufS, which turnovers SufS and enhances its activity. This interaction also induces allosteric changes in the structure of SufS. To investigate the effects of these changes on the catalytic mechanism, we applied ^{31}P NMR, stopped flow spectra absorption, and site mutagenesis. The result shows that the binding of SufE causes a conformational change of the PLP cofactor in SufS, which may provide a better orientation for the reaction with L-cysteine. The reaction of L-cysteine and SufS is a biphasic process including the fast phase (formation of external aldimine) and slow phase (formation of external ketimine). The binding of SufE facilitates the formation of external ketimine. We mutated the His123 of SufS to Ala, which removed the enhancement of SufE to the activity of SufS and the facilitating effect for the formation of external ketimine. Finally, the binding of SufE increases the formation of the persulfide in SufS. Together, these results clarify the role of

SufE in the persulfide formation of the reaction between SufS and L-cysteine, which provides a clearer picture of the effect of the interaction between SufS and SufE.

INTRODUCTION

Cysteine desulfurases are the class of enzymes that promote the abstraction of sulfur from L-cysteine and transfer it to the acceptor molecules for the biosynthesis of sulfur-containing cofactors such as thiamin, molybdenum cofactor, thionucleotides in tRNA, biotin, and iron-sulfur clusters[1-3]. All cysteine desulfurases studied so far are related in evolution and display similar structures that each monomer of the homodimer contains both the active site Cys-thiol and a PLP cofactor bound to a strictly conserved Lys residue via a Schiff base (internal aldimine)[4]. Cysteine desulfurases can be divided into group I and group II based on sequence analysis and the key difference is the structure of the active site[4]. SufS acts as the cysteine desulfurase in the Suf pathway of *E. coli*, which produces Fe-S clusters under oxidative stress and iron starvation conditions[5]. SufS is a group II desulfurase enzyme and Cys364, its active site residue, locates on a rigid loop with a hydrophobic environment while IscS and other group I desulfurases have a flexible catalytic cysteine loop exposed to the environment, which may be one part of the reason why the basal activity of IscS is much higher than SufS[6-8]. SufS has a specific sulfur acceptor SufE whose coding gene *sufE* is adjacent to *sufS*. SufE interacts with SufS to accept the sulfide from SufS. It activates SufS to enhance its activity to a level comparable to IscS. And SufS-SufE sulfur transfer system is more resistant to oxidative stress than IscS[9]. However, the catalytic mechanisms of the effects of SufE on SufS except accepting sulfur are not completely clear.

Enzymology, site-directed mutagenesis, ITC, X-ray crystallography and so on have been used to clarify the reaction of L-cysteine and SufS in the presence of SufE[9-12]. L-cysteine is activated by binding to the PLP cofactor before the C-S bond of L-cysteine is cleaved by a nucleophilic attack from the active site Cys364 residue, which results in the formation of a persulfide at the active site (Cys364-S-SH)[10]. SufE binds to SufS to accept the sulfide. It allows SufS to fully turn over, consequently enhancing its activity[9]. Also, the binding of SufE initiates allosteric changes in the SufS structure including the peptide containing the conserved Lys residue that forms the Schiff base with the PLP cofactor. This allosteric change facilitates the binding of L-cysteine to the enzyme to form external aldimine or other reaction intermediate[11]. This finding leads us to investigate the role of SufE in enhancing the activity of SufS beyond accepting sulfide from SufS.

In this study, we reported that the effects of the binding of SufE on the PLP conformation, the pre-steady-state and steady-state kinetics of the reactions between SufS and L-cysteine in the presence or absence of SufE in a one turnover model, and the role of the binding of SufE on the persulfide formation. The results show that the interaction between SufE and SufS can cause a conformational change of the PLP cofactor in SufS, which may provide an appropriate orientation for its reaction with L-cysteine. The reaction of L-cysteine and SufS is a biphasic process including the fast phase (the pre-steady state) and slow phase (the steady state). External aldimine is produced in the fast phase and external ketimine is produced in the steady state. The binding of SufE facilitates the formation of external ketimine. Also, we used site-directed mutagenesis to investigate the possible catalytic mechanism of the effects of the SufE binding. Our result suggests His123 of SufS plays an important role in the reaction of SufS and L-cysteine in the presence of

SufE. The mutant SufS H123A cannot be enhanced by SufE in the desulfurase reaction. Also SufE cannot facilitate the formation of external aldimine in SufS H123A. Finally, we investigated the formation of persulfide in SufS and found that the binding of SufE enhances the formation of persulfide. Together with the finding that SufE binding induces allosteric changes in SufS, the present results demonstrate that SufE activates SufS by both accepting sulfur as well as by promoting the first step of the ping-pong reaction.

MATERIALS AND METHODS

Strains, Plasmids and Site-mutagenesis

SufS, SufS H123A, SufS C364A, SufE, and SufE C51A were expressed in BL21(DE3). The expression plasmids are constructed in the following steps. We used MG1655 chromosomal DNA as the template for PCR. The fragment of *sufS* was digested with XhoI and BamHI. After the digestion, the *sufS* fragment was ligated into the corresponding sites of the plasmid *pET-21a* (Invitrogen) to generate *pET-21a_sufS*. The fragment of *sufE* was digested with BamHI and NdeI. Then it was cloned into the corresponding site of *pET-21a* to make *pET-21a_sufE*.

The SufS H123A, SufS C364A used *pET-21a_sufS* as the template. The SufE C51A used *pET-21a_sufE* as the template. The substitution was introduced by the site-directed mutagenesis using the QuikChange kit (Stratagene). All the primer sequences are described in Table 2.1.

Protein expression and purification

E. coli BL21(DE3) containing *pET-21a_sufS, pET-21a_sufS H123A* or *pET-21a_sufS C364A* was grown in LB with 100 μg/mL ampicillin at 37 ˚C for overnight, diluted by 100 fold into LB, incubated with shaking to reach an OD_{600} of 0.4 – 0.6 before induced by 500 μM IPTG at 18 ˚C overnight. Cells were harvested and lysed in 25 mM Tris-HCl, pH 8.0, 5 mM DTT, and 1 mM PMSF via sonication. After centrifugation at 14000 rpm for 30min, the lysate was loaded on the columns. The WT SufS or the SufS mutants were purified through Q-sepharose, phenyl and Superdex 200 chromatography resins in sequence. The Q-sepharose column used a linear gradient from 25 mM Tris-HCl, pH 8.0, 10 mM βME to 25 mM Tris-HCl, pH 8.0, 1 M NaCl, 10 mM βME. The phenyl column utilized a linear gradient from 25 mM Tris-HCl, pH 8.0, 100mM NaCl, 1M ammonium sulfate, 10 mM βME to 25 mM Tris-HCl, pH 8.0, 10 mM βME. The Superdex column run with 25mM Tris-HCl, pH 8.0, 150mM NaCl, 10 mM βME. Purified proteins were concentrated, frozen as drops in liquid nitrogen, and stored at – 80 ˚C degrees until further use.

E. coli BL21(DE3) containing *pET-21a_sufE* or *pET-21a_sufE C51A* was grown in LB with 100 μg/ml ampicillin at 37 ˚C for overnight, diluted 100 fold into LB, incubated with shaking to reach an OD_{600} of 0.4 – 0.6 before induced by 500 μM IPTG at 37 ˚C for 3 hours. Cells were harvested and lysed in 25mM Tris-HCl, pH 8.0, 5mM DTT, and 1 mM PMSF via sonication. After centrifugation at 14000 rpm for 30min, the lysate was loaded on the columns. The WT SufE or SufE C51A was purified through Q-sepharose and Superdex 200 chromatography resins in sequence. The Q-sepharose column used a linear

Table 2.1 Primer sequences for plasmid construction of *pET21a_sufS*, *pET21a_sufE*[9] and site-directed mutagenesis for construction of *pET21a_SufS H123A*, *pET21a_SufS C364A*, *pET21a_SufE C51A*

Protein	Primer sequence
SufS	5'-GAGGGGATCATGATTTTTTCCGTCGACAA-3' 5'-TGCCCTCGAGTTATCCCAGCAAACGGTGAA-3'
SufE	5'-AGGCCATATGGCTTTATTGCCGGATAA-3' 5'-TCCTGGATCCTTAGCTAAGTGCAGCGGCTT-3'
SufS H123A	5'-CATCAGTCAGATGGAGGCCCACGCTAACATTGTTC-3' 5'-GAACAATGTTAGCGTGGGCCTCCATCTGACTGATG-3'
SufS C364A	5'-CGTACCGGACATCACGCCGCAATGCCATTGATG-3' 5'-CATCAATGGCATTGCGGCGTGATGTCCGGTACG-3'
SufE C51A	5'- CAAAATAGCATTCAGGGCGCACAGAGTCAGGTGTGGATTG-3' 5'-CAATCCACACCTGACTCTGTGCGCCCTGAATGCTATTTTG-3'

gradient from 25 mM Tris-HCl, pH 8.0, 10 mM βME to 25 mM Tris-HCl, pH 8.0, 1 M NaCl, 10 mM βME. The Superdex column run with 25mM Tris-HCl, pH 8.0, 150 mM NaCl, 10 mM βME. Purified proteins were concentrated, frozen as drops in liquid nitrogen, and stored at – 80 Celsius degrees until further use.

^{31}P NMR Spectroscopy

Fourier-transform ^{31}P NMR spectra was collected at 121.497 MHz on a Bruker 400 MHz super wide-bore superconducting spectrometer using a 5-mm multinuclear probehead with broadband 1H decoupling. The NMR tube contained the sample (2 mL) and $^{2}H_2O$ (0.2 mL) as field/frequency lock and was maintained at 15 Celsius degrees using a thermostated continuous air flow. The protein concentration was 1 mM subunits. A spectral width of 2000 Hz was acquired in 8K data points with a pulse angle of 60 degrees. The exponential line broadening used prior to Fourier transformation was 10 Hz. The acquisition times were in the range of 1 to 15 hour with a repetition time of 2 s. Positive chemical shifts in ppm are downfield changes with respect to 85% H_3PO_4. Monoprotic titiration curves were calculated by least squares analysis.

Cysteine Binding Assays

All assays were conduct at room temperature in 25 mM Tris-HCl, pH 7.4, 150 mM NaCl. The binding between SufS and L-cysteine was evaluated by monitoring the immediate ΔA_{340} elicited by the addition of increasing concentrations of L-cysteine to 25 μM WT SufS or 25 uM WT SufS with an equal amount of SufE C51A using a BECKMAN COULTER DU 800 spectrophotometer. Protein and L-cysteine were added into the

cuvettes and mixed for around 5 s before the wavelength scan from 200 to 650 nm. Data were analyzed with the GraphPad Prism software. ΔA340 was best fit with the one-site-specific binding model.

Stopped-flow Absorption Spectroscopic Analysis

Stopped-flow absorption experiments were performed on an Applied Photophysics Ltd. SX20 stopped-flow spectrophotometer. 25 μM WT SufS or 25 μM WT SufS with an equal amount of SufE C51A or 25 μM SufS H123A with an equal amount of SufE C51A was rapidly mixed with increased concentration of L-cysteine. The reaction was performed in the buffer 25 mM Tris-HCl, pH 7.4, 150 mM NaCl. Single wavelength traces were taken by a photomultiplier tube. Full spectrum data were collected by photodiode array. The single wavelength data at 370 nm were best fit to the double exponential model using Pro Data Viewer version 4.2.18.

Cysteine Desulfurase Activity Assay

Cysteine desulfurase activity was measured through the formation of methylene blue with NNDP and $FeCl_3$ using the protocol below. Reactions were conduct aerobically in 25mM Tris-HCl, pH 7.4, 150 mM NaCl at room temperature. 0.5 μM SufS or SufS mutants and 2 μM SufE were incubated in the buffer for 5 min before the addition of 2mM L-cysteine and 2mM DTT. The total volume of the reaction system was 800 μL. Reactions proceeded for 10 min and were quenched by adding 100 μL 20mM NNDP in 7.2 M HCl and 100 μL 30 mM $FeCl_3$ in 1.2 M HCl. The mixture was incubated in the dark for 30 min to produce methylene blue. Precipitated protein was removed by 1 min centrifugation at

13000 rpm and the methylene blue was measured at 670 nm. A Na_2S standard line was made for calibration of the content of sulfur product from this reaction.

Identification of the SufS-Bound Persulfide

The SufS-bound persulfide was identified using a slightly modified published protocol. 50 nmol SufS or SufS mutants was incubated with 400 nmol L-cysteine in 25 mM Tris-HCl, pH 8.0, 150 mM NaCl for 20s before 300 nmol of 1,5-I-AEDANS was added. The reaction proceeded for 30 min. Then the excess of the 1,5-I-AEDANS was removed by washing three times with the above buffer using the centrifugal filter (Amicon Ultra - 15). The samples were brought to 1 mL with the buffer and then equally divided to 500 uL. An aliquot of 1 M DTT (55.6 µL) was added to one sample (500 µL) to give a final concentration of 5 mM to reduce any formed persulfide (disulfide bond) from SufS and the fluorescent compound. The other half was not reduced by DTT and served as a control. The incubation time with DTT was 30 min. Then, small molecules were separated from protein by washing three times with the above buffer by using the centrifugal filter. Finally, all the samples were brought to 500 µL with the buffer and the relative persulfide percentage was determined spectrofluorometrically with the BioTek Synergy H1 Hybrid Reader. The λ_{ex} was 336 nm and the λ_{em} was 490 nm.

RESULTS

Binding of SufE changes the conformation of PLP in SufS

Our former research proved that the binding of SufE to SufS leads to conformational changes within the peptide of SufS including the Lys226 that forms a Schiff

base with the PLP cofactor[11]. Thus it is reasonable to hypothesize the binding of SufE changes the conformation of the PLP cofactor of SufS. To further test if the binding of SufE can cause a conformational change of PLP, ^{31}P NMR spectroscopy was applied. The ^{31}P NMR allows monitoring of the microenvironment around the 5'-phosphate group of the enzyme-bound PLP by detecting its chemical shift under different conditions (Figure 2.1). It is acquired with ^{1}H decoupling, which produces a single resonance line for the ^{31}P nucleus of PLP. If the line width of the single resonance is narrow, then this indicates that there is free rotation around the C5'-O4' bond of the phosphate group. Alternatively, observing an increased line width suggests this rotation is restricted. A typical ^{31}P NMR spectrum analysis includes matching the expected chemical shifts to the expected moieties. Each type of signal has a characteristic chemical shift range. Important factors influencing chemical shift include the electron density and electronegativity of neighboring groups. The decreasing of the electron density can cause a downfield shift in the NMR spectrum.

For SufS alone, there are two ^{31}P NMR signals at 3.4 ppm (60%) and 2.4 ppm (40%). The presence of SufE shifts the ^{31}P NMR signals to 3.3 ppm (95%) with a small portion (5%) still present at 2.4 ppm (Figure 2.2). In both the absence and presence of SufE, line widths are consistent with restricted rotation about the C5'-O bond linking the phosphate ester to the pyridine moiety of the cofactor. This result indicates that the binding of SufE changes the microenvironment of the phosphorus in the cofactor PLP, possibly to obtain the proper conformation for the reaction of the PLP cofactor and the substrate L-cysteine.

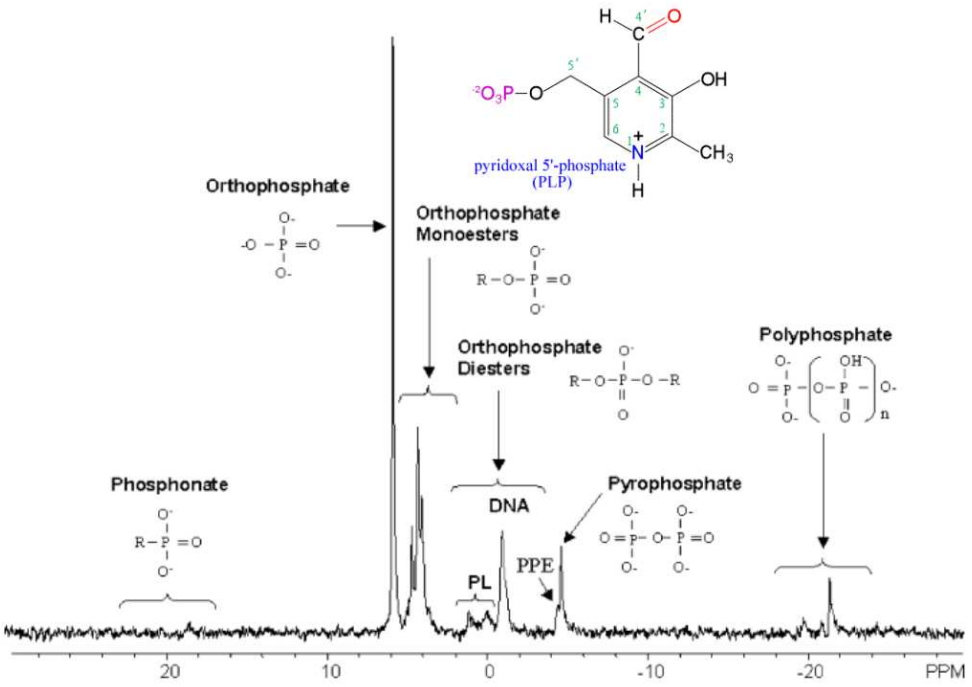

Figure 2.1. Chemical shift of phosphorus-containing group and PLP. PLP is one type of orthophosphate monoesters whose chemical shift is between 2 ppm – 6 ppm[19].

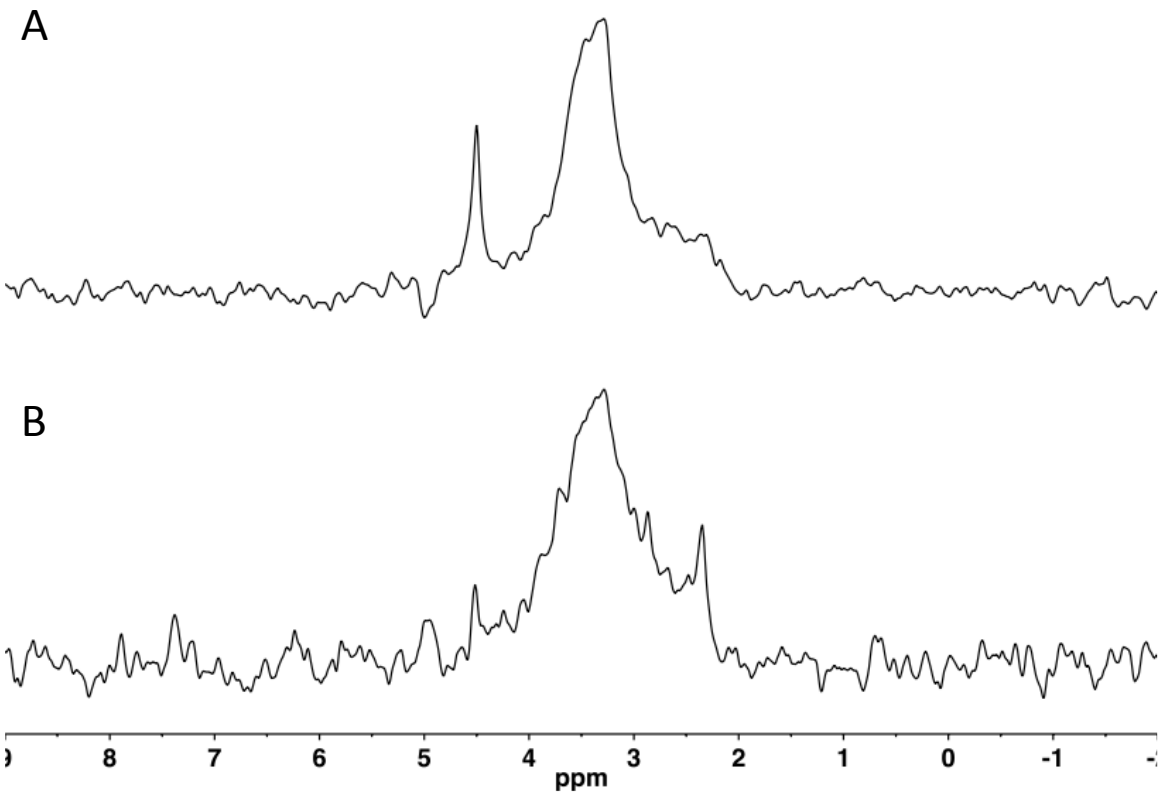

Figure 2.2. ^{31}P NMR spectra of SufS in the absence and presence of SufE. (A) ^{31}P NMR spectrum of 500 µM SufS in 25 mM Tris-HCl, 50 mM NaCl buffer, pH 8.0. (B) ^{31}P NMR spectrum of 500 µM SufS and 500 µM SufE in 25 mM Tris-HCl, 50 mM NaCl buffer, pH 8.0. The signal at 4.5 ppm is considered to be an impurity containing phosphorus from protein purification.

Kinetics of Reaction of SufS with L-Cysteine with/without SufE C51A

In the study of the L-cysteine binding to SufS, we already showed that the presence of SufE facilitates the formation of a L-cysteine-SufS PLP intermediate(s) with an absorption maximum at 340 nm under the steady state[11]. Here stopped-flow experiments were applied to investigate the kinetics of the binding of L-cysteine to SufS under the pre-steady state and the effects of SufE in this reaction. The stopped-flow experiment is to use a rapid mixing device to study the chemical kinetics of the fast reaction. The half-lives of the fastest reaction that the stopped-flow instrument can study can be as short as a few milliseconds. In a stopped flow experiment (Figure 2.3), the substrates and enzymes are forced from two separated syringes into a mixing chamber. After a very short period of flow, the flow is stopped and the mixture is observed by the monitoring probe. The dead time is the period between the end of mixing and the beginning of the observation of the kinetics for the reaction, which is usually 1-2 ms.

The active site of SufE, Cys 51, was mutated to Ala (SufE C51A), which prevents the sulfur transfer from SufS to SufE and blocks SufE enhancement of SufS turnover (Figure 2.4). However, SufE C51 still binds to SufS thus allowing us to exclusively investigate the effect of SufE binding on the initial reaction of L-cysteine and SufS to form a SufS-persulfide intermediate. We observe that SufE C51A can still facilitate the formation of the intermediate(s) at 340 nm under the steady state similar to what we observed previously for SufE (Figure 2.5).

Interrogation of the reaction of SufS with L-cysteine by the stopped-flow absorption spectrophotometry revealed the decay of internal aldimine at 420 nm and the

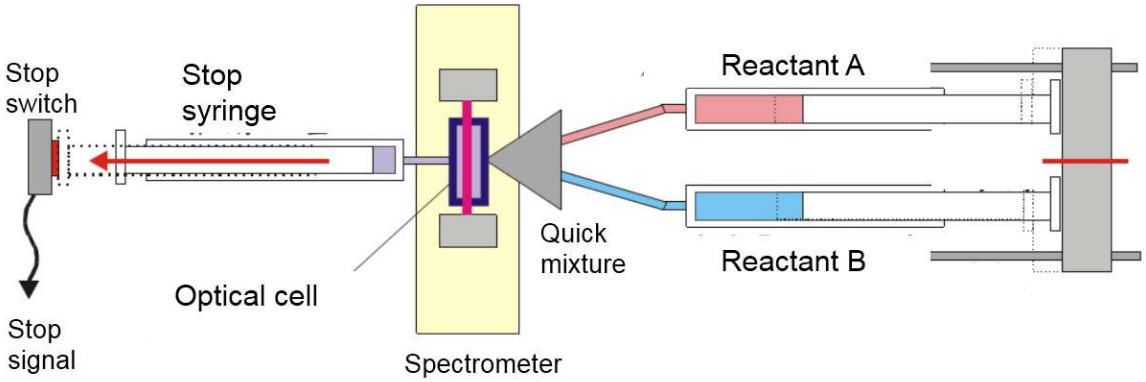

Figure 2.3. Model of a stopped-flow device.

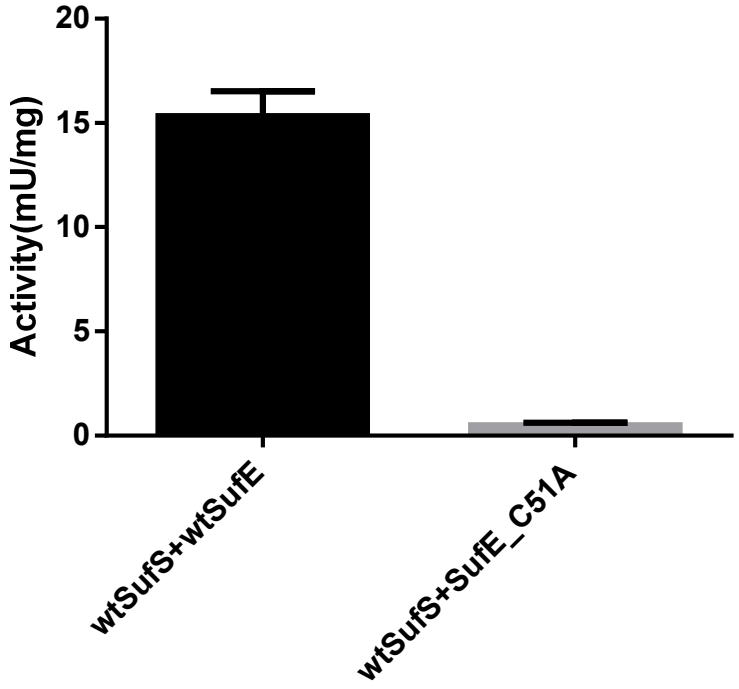

Figure 2.4. Comparison of the activities of WT SufS with WT SufE/SufE C51A. 0.5 µM SufS reacts with 2 µM WT SufS or 2 µM SufE C51A.

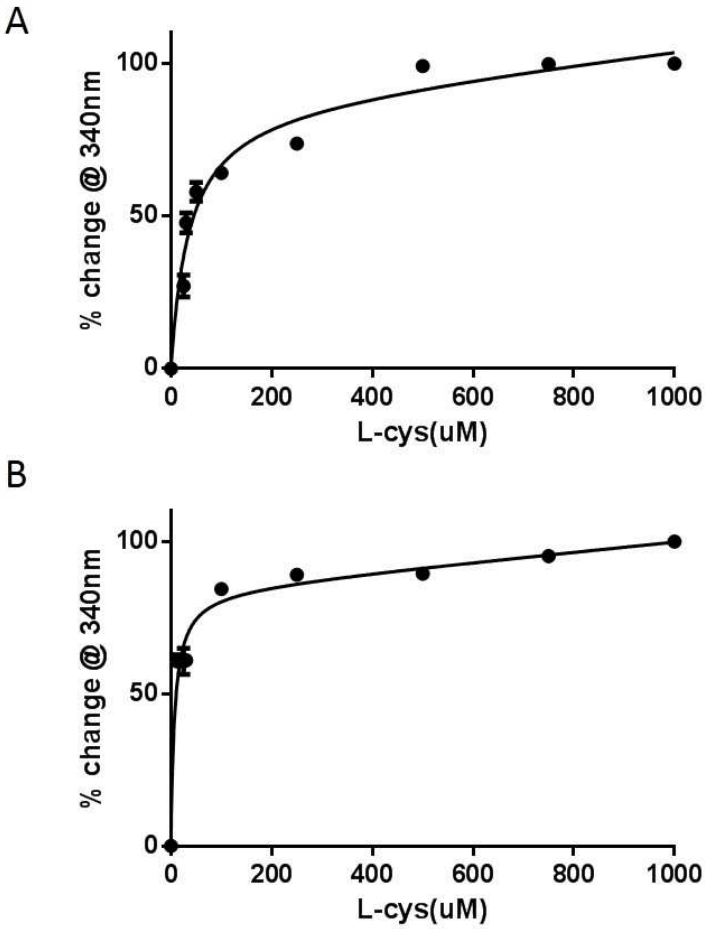

Figure 2.5. Formation of intermediate(s) upon addition of L-cysteine to SufS in the absence and presence of SufE C51A. (A) Percentage of change at 340 nm after adding increasing concentration of L-cysteine to 25 μM SufS. The solid line is fit of one-site binding model and corresponds to a Kd value of 35 ± 8 μM. (B) Percentage of change at 340 nm after adding increasing concentration of L-cysteine to 25 μM SufS and 25 μM SufE C51A. The solid line is fit of one-site binding model and corresponds to a Kd value of 7 ± 1 μM.

accumulation of an intermediate(s) at 340 nm (Figure 2.6). Fitting the time course for the intermediate(s) at 340 nm using regression methods required a double exponential (two phase association) model with observed rate constants (k_{obs}) $k_1 = 7.35 \pm 0.12\ s^{-1}$ and $k_2 = 0.16 \pm 0.0044\ s^{-1}$ (Figure 2.7). The complex biphasic kinetic behavior for the formation of the intermediate(s) at 340 nm may be attributed to multiple populations of one intermediate reacting at different rates, or may alternatively occur because there are two different intermediates that both absorb at the same wavelength (340 nm).

Based on the accepted mechanism of the reaction between cysteine desulfurase and L-cysteine[13,14](Figure 2.8), a PLP transsulfuration begins when the internal aldimine that absorbs at 420 nm shifts to the external aldimine Schiff base that absorbs at 340 nm. Then the α proton of the substrate is abstracted by an enzyme residue serving as a general base to form the external ketimine via a transient intermediate Cys-PLP quinonoid. It is postulated that during our single-turnover reaction we observe the accumulation of both the external aldimine and the external ketamine intermediates, which forms a mixture in equilibrium at 340 nm.

To test if two intermediates may be present, singular value decomposition (SVD) was applied to the complex photodiode array (PDA) data. SVD is a mathematical method which is a factorization of a complex matix. It can decompose a normal matrix to any m * n matrix via an extension of polar decomposition. We utilized SVD to decompose the matrix of the PDA data where the number of singular values (number of the decomposed matrixes) equals the number of intermediates in this stopped-flow experiment. In our experiment, three singular values were obtained, which represents three species in this reaction (Figure 2.9). Using global analysis methods, the pure optical spectra for external

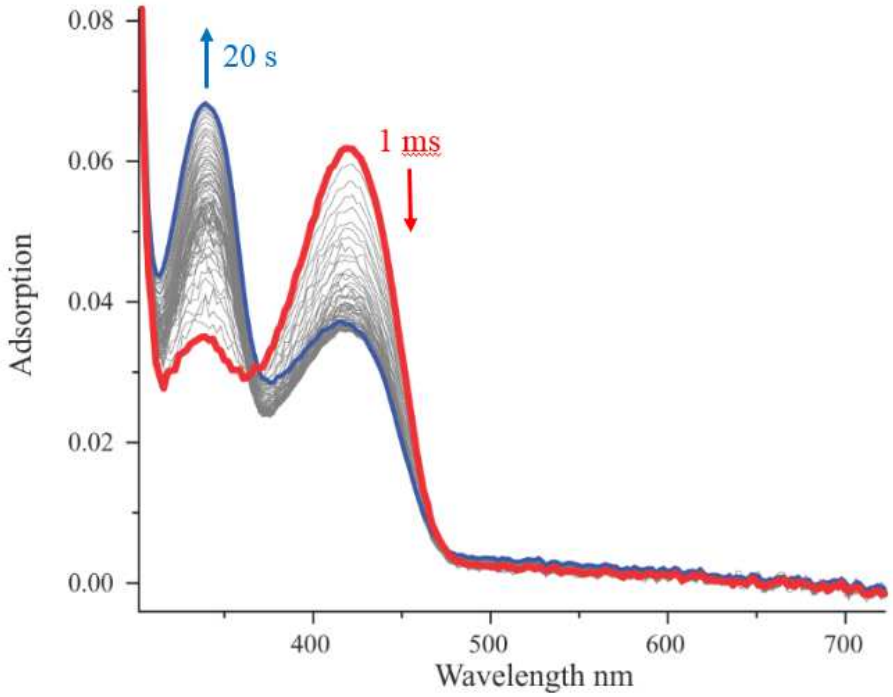

Figure 2.6. Stopped-flow absorption spectrophotometry of SufS and L-cysteine. PDA spectrum of a single turnover reaction of 25 μM SufS and 1 M L-cysteine.

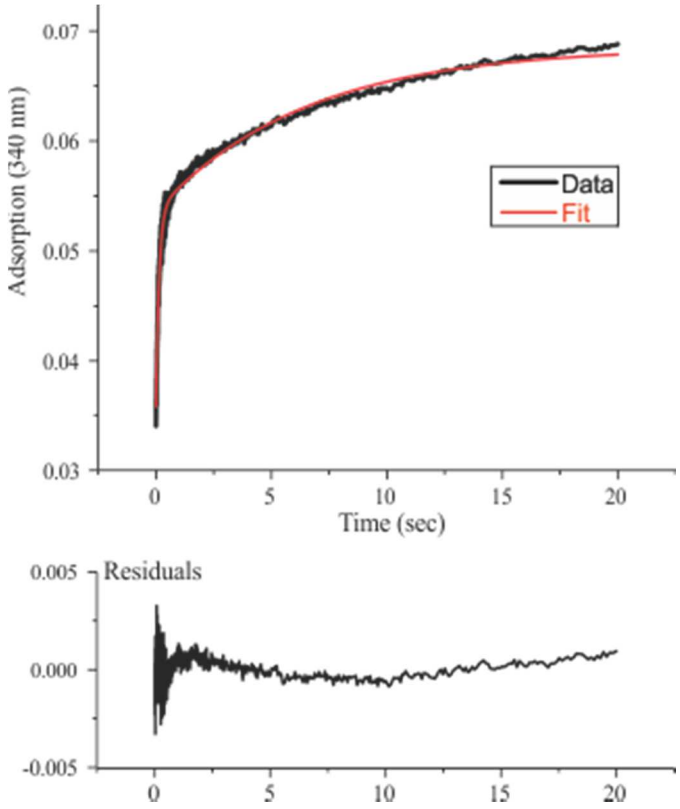

Figure 2.7. Representative single-wavelength (340 nm) time course for the reaction of 25 μM SufS and 1M L-cysteine. The red line represents the double exponential fits to the data.

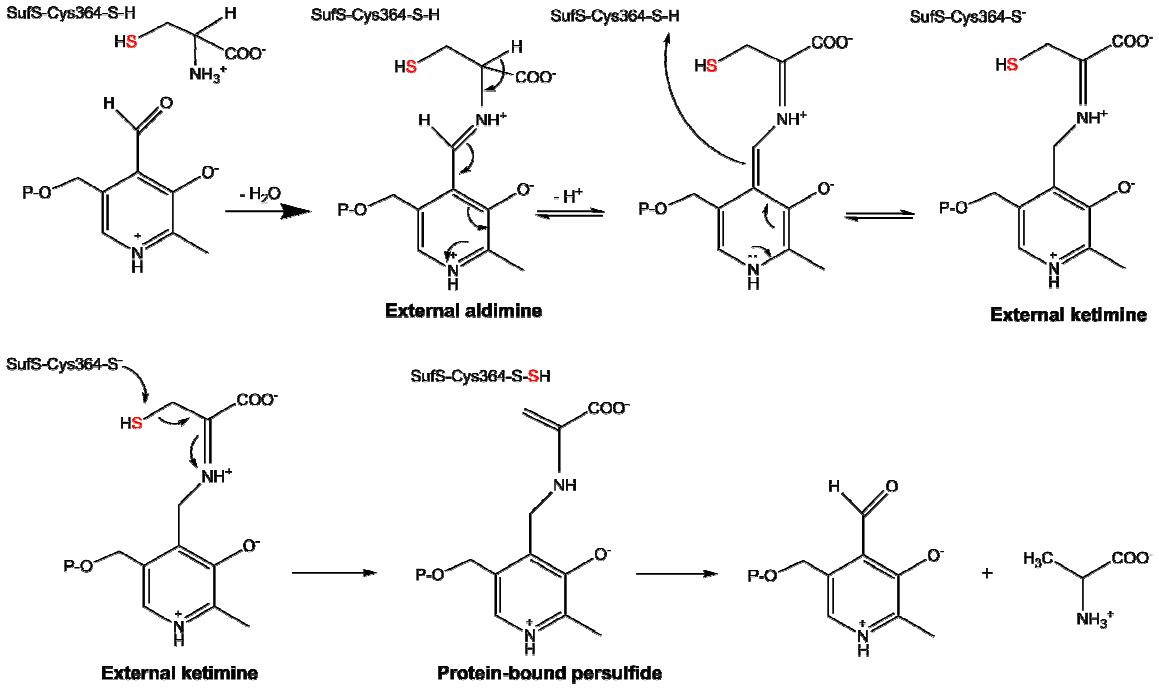

Figure 2.8. Proposed mechanism of the desulfurase reaction between SufS and L-cysteine. External aldimine is obtained through a transimination reaction. After deprotonation, external ketimine was formed before the persulfide formation.

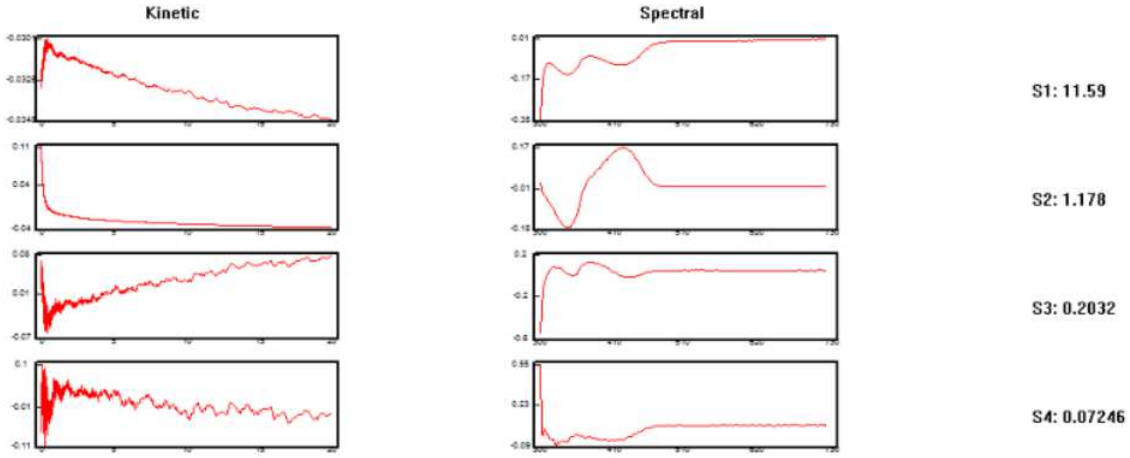

Figure 2.9. SVD basis vectors after SVD calculation for the PDA data of the reaction between 25 µM SufS and 1 M L-cysteine. S1 – S4 are the singular values. S4 is much smaller than the rest of singular values, which is considered to be noise.

aldimine and a species we assign as the external ketimine were extracted (Figure 2.10). Both the pure external aldimine and the pure external ketamine have similar absorption features around 340 nm. Based on the observed rate constants in the fast phase and slow phase, we computed the three intermediates in the reaction of SufS and L-cysteine (Figure 2.11). The pure optical spectrum at 364 nm showed two phases together: the first one is for the absorbance decreasing from decomposition of the internal aldimine to external aldimine; the second phase is going up from external aldimine to an intermediate that we assign as the external ketimine (Figure 2.12). It is consistent with the spectrum of the time course at 364 nm from the PDA data (Figure. 2.13), which further supports that external aldimine and external ketimine may exist as a mixture at 340 nm.

To delineate the kinetics of this whole reaction from internal aldimine to external ketimine, the dependence of both k_{obs} in the fast and slow phases at various L-cysteine concentrations was examined in either the absence or presence of SufE C51A. The k_{obs} of the fast phase shows a linear dependence on L-cysteine concentration with or without SufE C51A. In the absence of SufE C51A, the forward and reverse rate constants for the formation of external aldimine are provided by the slope (k_1 = 0.012 $\mu M^{-1}s^{-1}$) and the intercept (k_{-1} = 0.46 s^{-1}), which gives an equilibrium dissociation constant K_D = 37.6 μM (k_{-1}/ k_1). This value is lower than that measured in the presence of SufE C51A where k_1 = 0.0055 $\mu M^{-1}s^{-1}$, k_{-1} = 0.45 s^{-1}, and K_D = 82.9 μM (Figure 2.14). The kinetics indicate that SufE does not enhance the formation of external aldimine in the fast phase. The k_{obs} of the slow phase shows a hyperbolic dependence on L-cysteine concentration regardless of the presence of SufE C51A. Results from the hyperbolic fit of the L-cysteine concentration dependence show that the y intercept of the plot is zero, which corresponds to the reverse

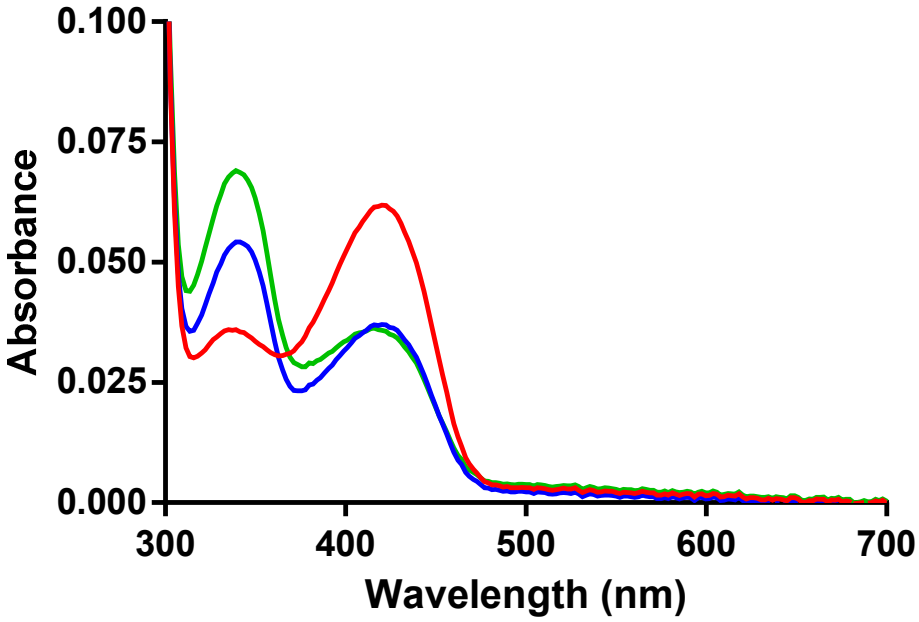

Figure 2.10. Pure components of spectra of internal aldimine (red), external aldimine (blue), and external ketimine (green) obtained from global fitting analysis of PDA data. The internal aldimine has a minimal absorption at 340 nm due to the dead time of the stopped-flow experiment.

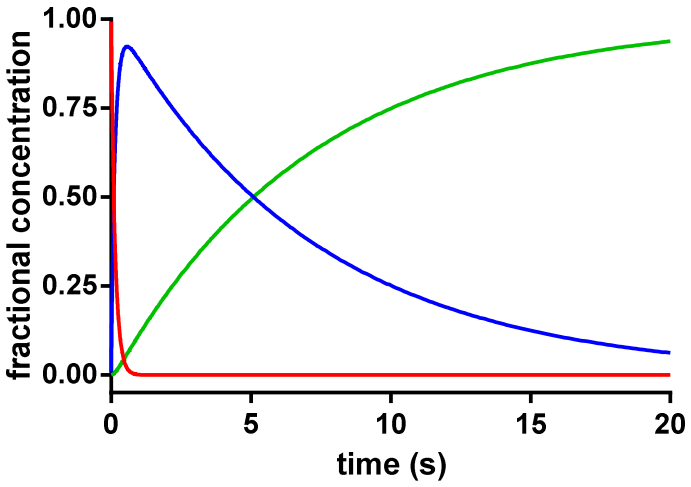

Figure 2.11: Speciation plots of the fractional concentrations of intermediates computed using the rate constants determined in the PDA study of 25 μM SufS and 1 M L-cysteine. Internal aldimine is red, the external aldimine is blue, and external ketimine is green.

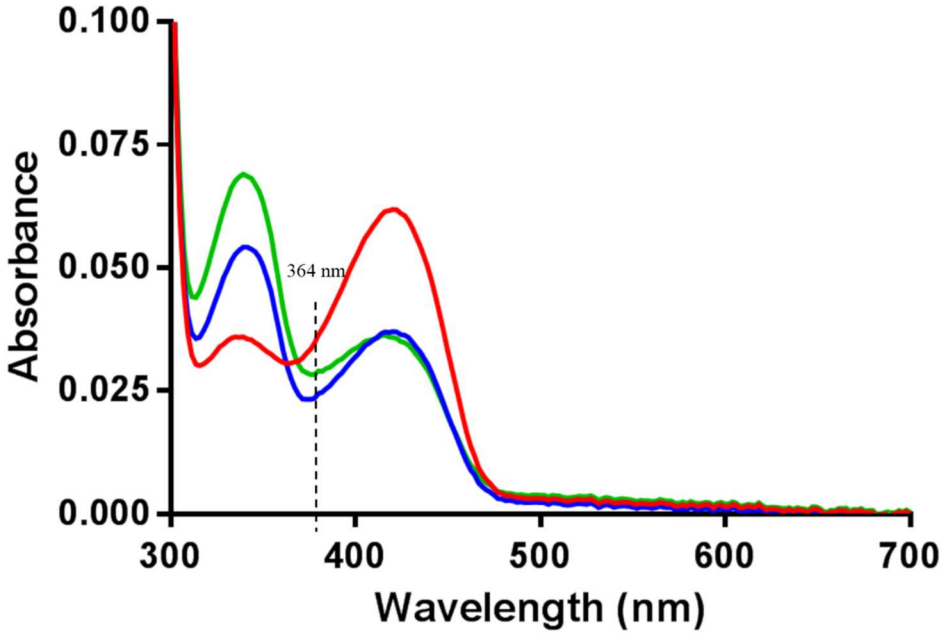

Figure 2.12. The spectrum at 364 nm in the pure components of spectra of internal aldimine (red), external aldimine (blue), and external ketimine (green). The absorption of internal aldimine decreases due to the formation of external aldimine and increases due to the formation of external ketimine.

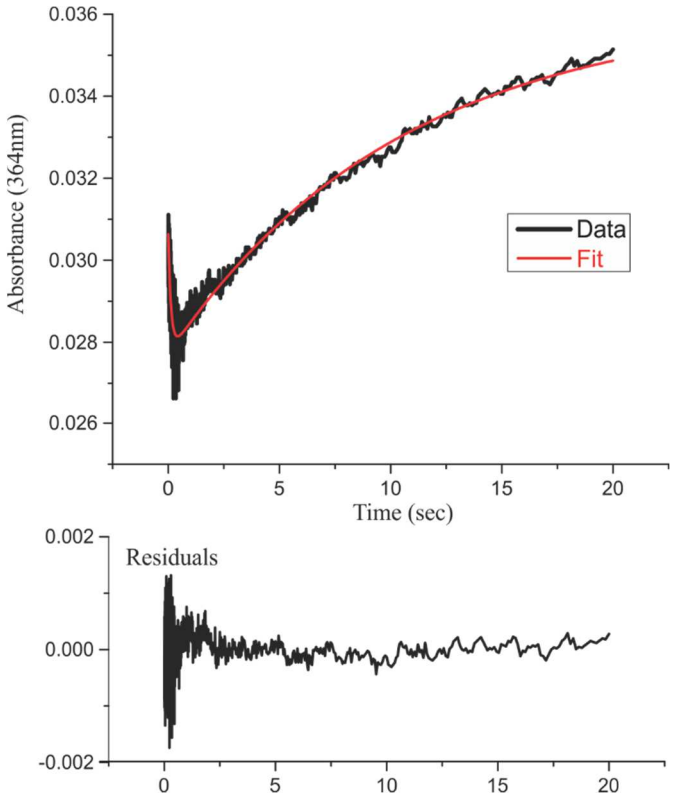

Figure 2.13. The single-wavelength time course for the reaction of decay of internal aldimine to external aldimine and formation of external ketimine monitored at 364 nm.

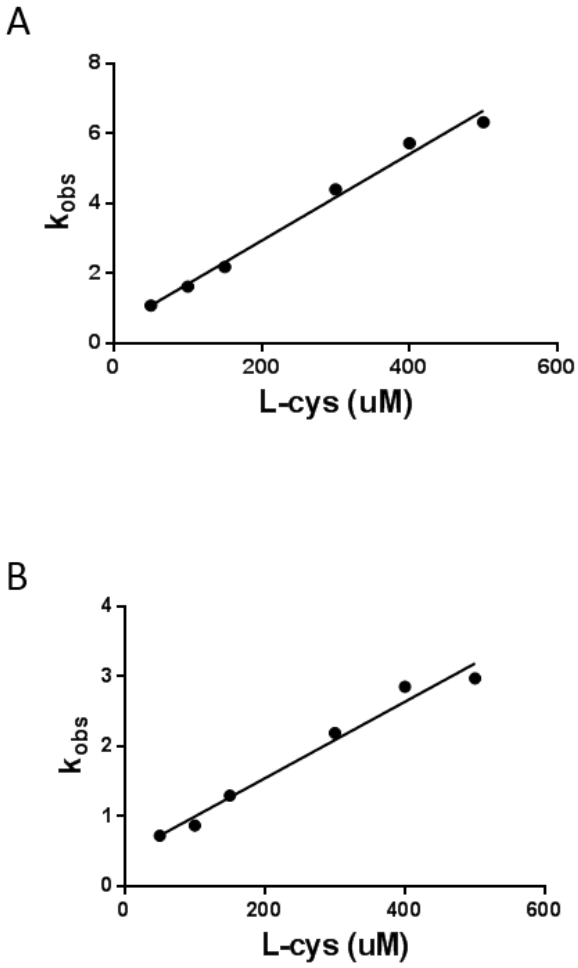

Figure 2.14. Kinetic analysis of the formation of external aldimine at 340 nm at the fast phase (pre-equilibrium state). (A) k_{obs} of the fast phase for 25 µM WT SufS alone following increasing concentrations of L-cysteine. (B) k_{obs} of the fast phase for 25 µM WT SufS and 25 µM SufE C51A following increasing concentrations of L-cysteine.

rate constant for the formation step of the second intermediate, which we assign as the ketimine formed from L-cysteine ($k_{-2} = 0$). The asymptote of the plot was used to obtain the formation rate constant for this putative Cys ketimine. We found that $k_2 = 0.5111\ s^{-1}$ in the absence of SufE C51A giving a $K_D = 82.94\ \mu M$. In contrast, when SufE C51A was present the $k_2 = 0.24\ s^{-1}$ resulting in a $K_D = 22.02\ \mu M$ (Figure 2.15). These results from the kinetic analysis of the slow phase indicate that the formation of the second intermediate, which we assign as the external ketimine, is an irreversible step which is enhanced 4-fold by SufE C51A.

His123 of SufS plays a critical role in the promotion of SufE to the formation of external ketimine

According to the accepted mechanism of the reaction between cysteine desulfurase and L-cysteine, an enzyme residue serving as a general base is used to abstract a proton from the α carbon of the external aldimine, which is critical for the conversion from external aldimine to Cys ketimine[14]. If SufE enhances this step of the desulfurase reaction in SufS, then SufE enhancement should be blocked by mutation of the catalytic base in SufS. His123 is a conserved His residue located between the PLP cofactor and the active site of SufS (Figure 2.16), suggesting its potential role as a general base during the abstraction of the substrate α proton[14]. To test this hypothesis, we mutated His123 to Ala (SufS H123A) and analyzed the desulfurase reaction in the mutant SufS. The desulfurase assay showed that SufE can no longer enhance the SufS H123A activity compared with WT SufS (Figure 2.17). However, this mutant still kept the basal activity (1.41 mU/mg) which is similar as SufS alone (1.30 mU/mg). Stopped-flow spectroscopy of SufS H123A

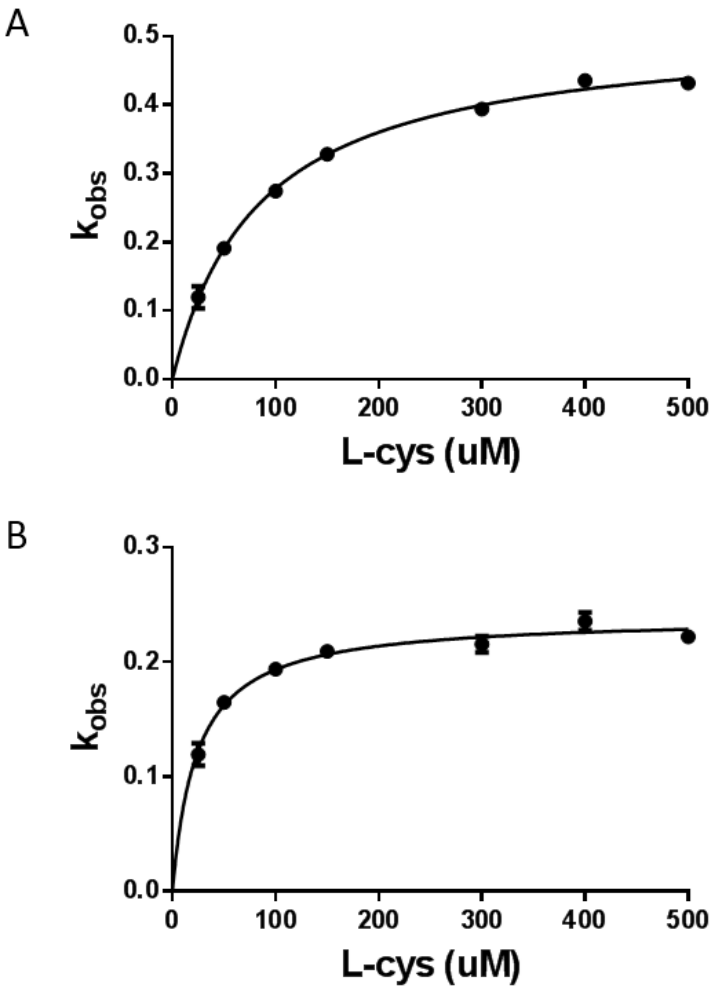

Figure 2.15. Kinetic analysis of the formation of external ketimine at 340 nm at the slow phase (equilibrium state). (A) k_{obs} of the slow phase for 25 μM WT SufS alone following increasing concentrations of L-cysteine. (B) k_{obs} of the slow phase for 25 μM WT SufS and 25 μM SufE C51A following increasing concentrations of L-cysteine.

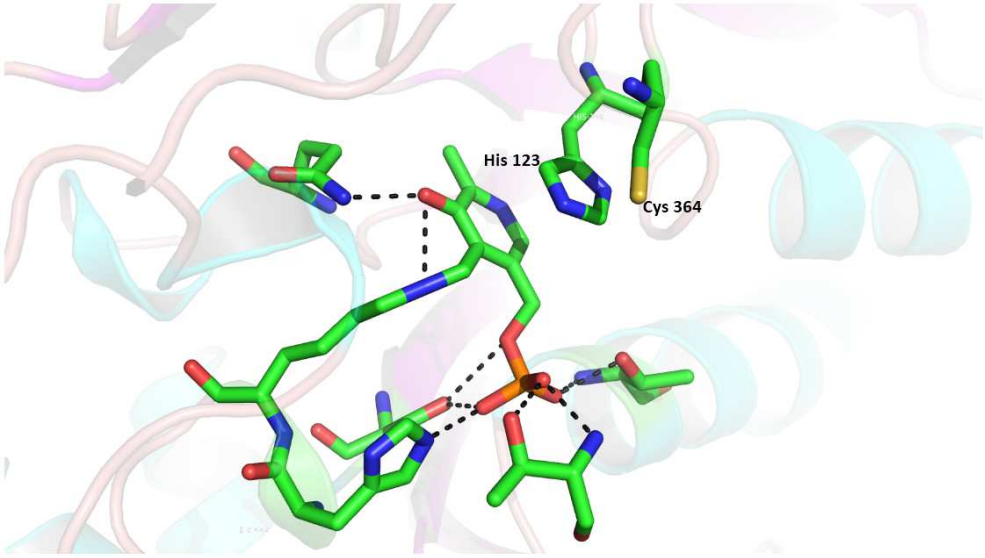

Figure 2.16. The location of His123 in the active site of SufS.

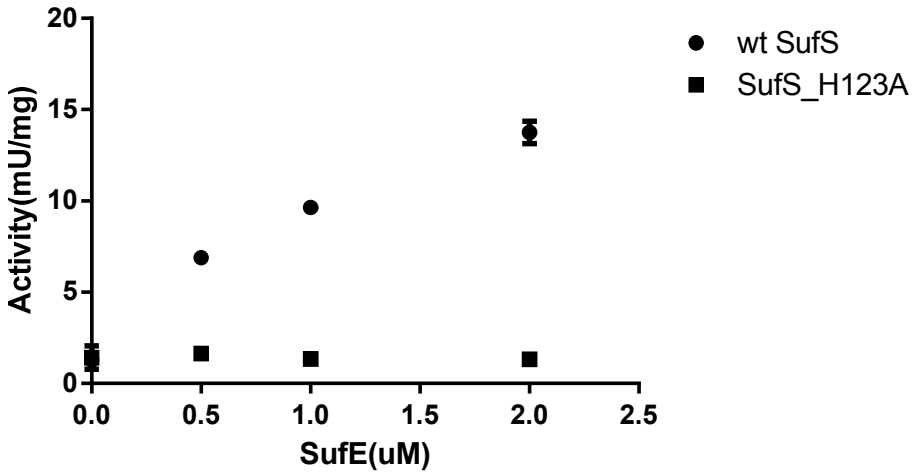

Figure 2.17. Comparison of the activity of 0.5 μM WT SufS and 0.5 μM SufS H123A in the presence of 2 μM WT SufE.

and L-cysteine with or without SufE C51A also showed a biphasic process. The fast phase was similar as the WT SufS indicating that H123A does not interfere with formation of the external aldimine between L-cysteine and SufS PLP. The slow phase still had a hyperbolic fit, but the k_2 = 0.5789 s^{-1} and K_D = 330.7 μM in the presence of SufE C51A, which is much larger than WT SufS with SufE C51A (K_D = 22.02 μM) (Figure 2.18). The slow phase of SufS H123A alone shows k_2 = 0.6642 and K_D = 225.5 μM, which is similar as SufS H123A in the presence of SufE C51A, indicating that SufE cannot enhance the formation of external ketimine in SufS H123A. This result indicates that His123 is required for SufE to facilitate formation of the external ketimine and that this activity of SufE in the first half of the desulfurase ping-pong reaction is a key part of SufE enhancement of SufS.

SufE enhances the formation of persulfide

According to the proposed mechanism of SufS as a desulfurase, L-cysteine can form a cysteine PLP adduct with the SufS cofactor PLP. The active site Cys364 thiolate of SufS starts a nucleophilic attack on this adduct to make remove sulfur from L-cysteine. A persulfide is formed on the active site Cys364 as an intermediate in this reaction[10]. The presence of SufE enhances the desulfurase activity of SufS in part by transferring the persulfide sulfur from the SufS Cys364 to SufBCD[15]. If SufE does enhance the formation of the ketimine intermediate in SufS as we propose here, then the presence of SufE should also enhance persulfide formation on SufS Cys364, which is stable enzyme intermediate formed upon completion of the first half of the ping-pong desulfurase reaction. To test if SufE can facilitate the formation of persulfide of SufS, we used SufE C51A, which still

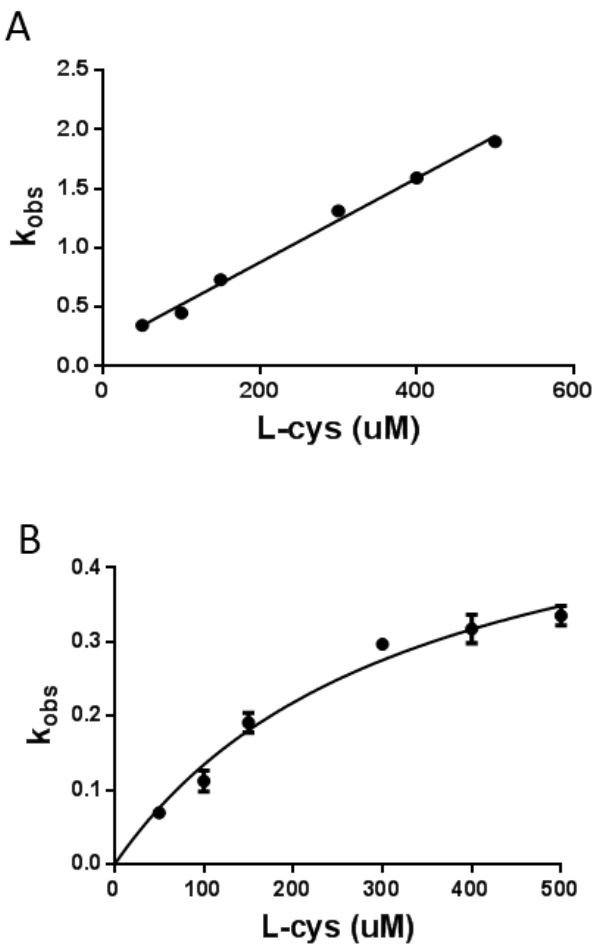

Figure 2.18. Kinetic analysis of the formation of intermediates at 340 nm from SufS H123A and L-cysteine in the presence of SufE C51A. (A) k_{obs} of the fast phase for 25 µM SufS H123A and 25 µM SufE C51A following increasing concentrations of L-cysteine. (B) k_{obs} of the slow phase for 25 µM SufS H123A and 25 µM SufE C51A following increasing concentrations of L-cysteine.

interacts with SufS but cannot remove persulfide from SufS, thus we are only analyzing the effect of SufE on that first half of the reaction. After mixing L-cysteine and SufS with or with SufE C51A, the fluorescent alkylating reagent 1,5-I-AEDANS was added to alkylate exposed thiol or persulfide sulfurs. Excess IAEDANS was removed by extensive washing. If there is no persulfide present a stable thioether derivative will be formed between IAEDANS and residues such as Cys364, which cannot not be broken using the reductant DTT[13] (Figure 2.19). However, if IAEDANS alkylates an enzyme-bound persulfide at Cys364 then the addition of DTT will reduce the persulfide and release the IAEDANS, resulting in a loss of fluorescent signal from the IAEDANS. We also mutated the active site of SufS from Cys to Ala (SufS C364A) and alkylated this mutant mixed with SufE C51A with IAEDANS to measure the background alkylation signal from the other 3 Cys residues in SufS and the one additional Cys residue in SufE C51A (none of which are directly involved in the desulfurase reaction). The results showed that the reaction of 1,5-I-AEDANS with a mixture containing SufS, SufE C51A, and L-cysteine results in the formation of a DTT-reducible persulfide species at the active site of SufS in 91.1% of the enzyme (compared with the control with SufS C364A and SufE C51A). If SufE C51A is omitted from the reaction, the DTT-reducible persulfide formation at the SufS active site of this enzyme is decreased to 62.4% (Figure 2.20). We extended the reaction time from 20s to 3 min and this percentage remained the same in both presence and absence of SufE C51A, which means an equilibrium was formed. Without the treatment with DTT, the total fluorescence signals of the SufS with/without SufE C51A were similar to each other. These results indicate that the presence of SufE facilitates the formation of persulfide in the early

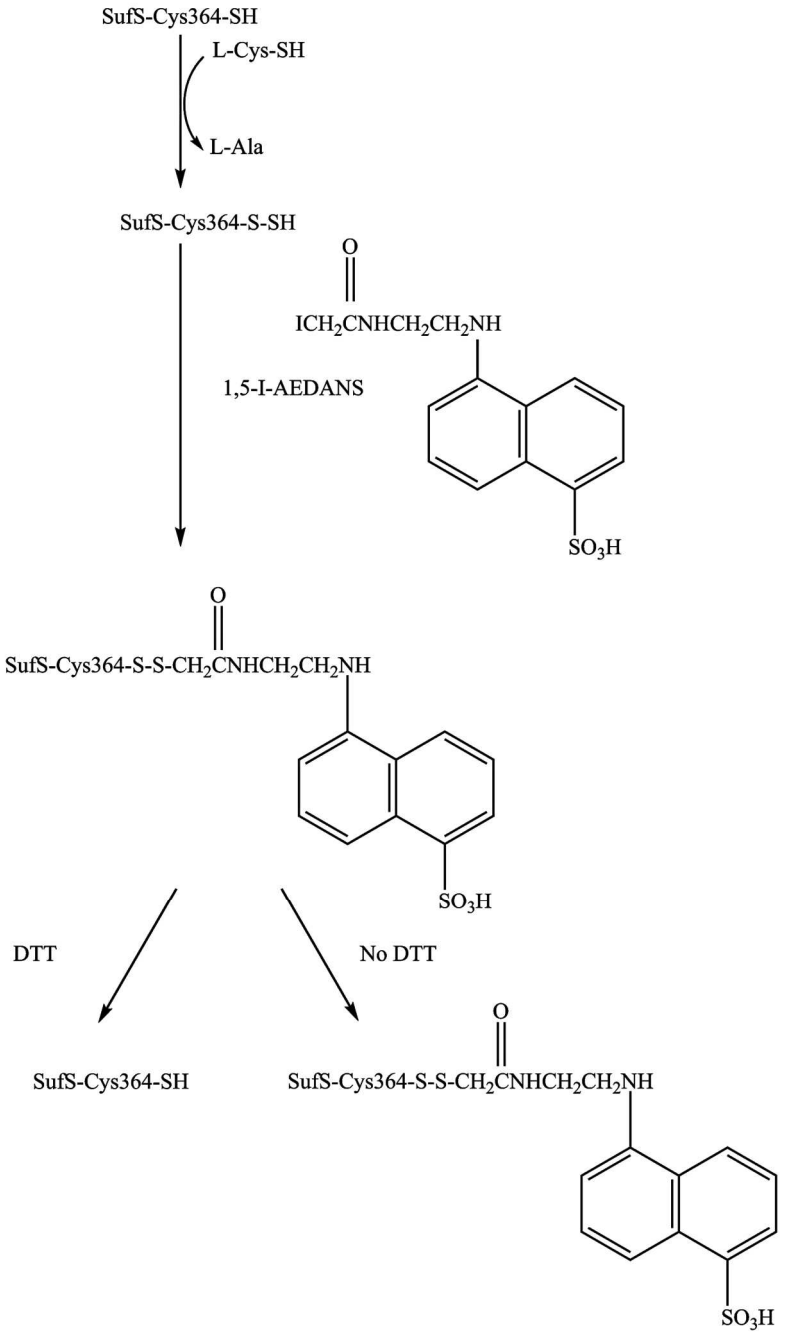

Figure 2.19. Scheme for the identification of a SufS-bound persulfide.

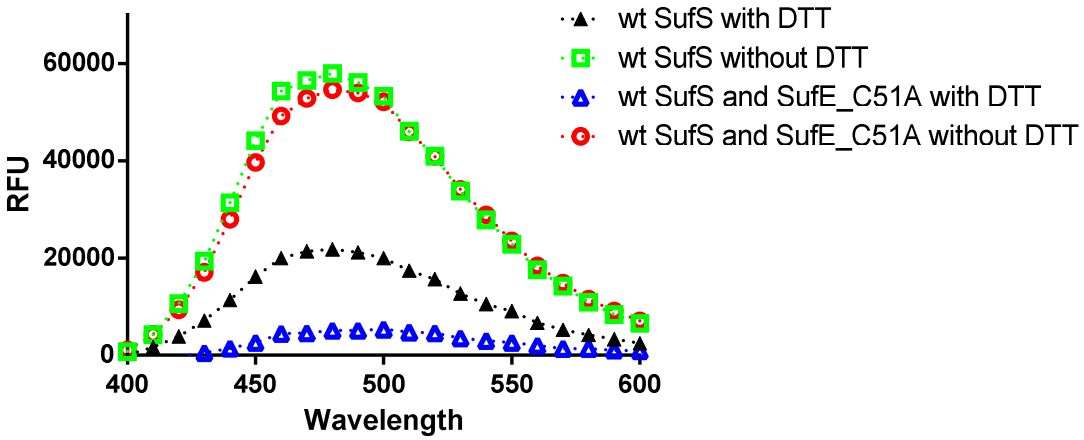

Figure 2.20. Fluorescence spectrum of SufS and L-cys with/without SufE C51A. SufS reacted with L-cys with/without SufE C51A. The samples incubated with 1,5-I-AEDANS. Then they were treated with/without DTT. 1,5-I-AEDNAS can react with cysteine residue to form a sulfide derivative which cannot be released by DTT. It can also react with persulfide to form a persulfide derivative which can be released by DTT. SufS C364A has no persulfide formation because the active site is mutated, which reacts with L-cysteine to provide the blank control.

steps of the reaction between SufS and L-cysteine even if SufE is not competent to remove the persulfide from SufS due to the C51A mutation.

DISCUSSION

It has been proven that SufE enhances the activity of SufS by removing the Cys364 persulfide to make it turnover[9]. We have previously shown that the binding of SufE initiated allosteric change in SufS including the peptide containing the conserved Lys residue that forms Shiff base with the PLP cofactor, which facilitates the binding of L-cysteine to the PLP cofactor[11]. Our current hypothesis is that binding of SufE can also promote the formation of an enzyme-bound persulfide by facilitating the production of intermediates in the reaction between SufS and L-cysteine. In the present study, we proved that the binding of SufE causes conformational change of the PLP cofactor through ^{31}P NMR, which may provide a more favored orientation of the PLP to react with L-cysteine. To elaborate the influence of the SufE binding to the reaction mechanism, we applied stopped-flow experiment to study the pre-steady state. We showed a model that describes the proposed mechanism for the reaction of SufS and L-cysteine and proved that the presence of SufE facilitates the formation of an intermediate beyond the external aldimine which we assign as the Cys ketimine. To further clarify this mechanism, we mutated the His123 to Ala in SufS. This mutation blocked the enhancement of SufS by SufE, which demonstrated that His123 plays an important role in the catalytic mechanism. Finally, we observed that the binding of SufE C51A increases the formation of the persulfide in SufS, which is consistent with our hypothesis.

To our knowledge the pre-steady-state kinetics of the group II cysteine desulfurase like SufS and L-cysteine with/without SufE is not described previously. The result demonstrates biphasic kinetics in the accumulation of the intermediate(s) at 340 nm. The SVD calculation shows 3 singular values that implies three intermediates in the whole reaction[16]. Taken together, there may be two intermediates in the growing absorption at 340 nm. Traditionally, external aldimine of cysteine is believed to absorb at 340 nm according to spectral change and the accepted reaction mechanism of cysteine desulfurase. In our former kinetic research under the steady state, we indicate that external aldimine of L-cysteine is absorbed at 340 nm. However, in the kinetic analysis in the cysteine desulfurase CD 0387 from Synechocystis sp. PCC 6803, Cys ketimine is proved to exist at 340 nm at the steady state by the deuterium equilibrium isotope effect[17]. Here we show that the accumulation of external Cys aldimine is fast, which gives rise to the initial observable fast phase of the reaction at 340 nm. However, the reaction that produces Cys ketimine produces a slow phase at 340 nm at the steady state. The structures of external aldimine and ketimine are very similar except the position of the double bond, which may explain the similarity of their spectral absorption. The quinonoid (506nm) in the reaction mechanism is observed in the group I cysteine desulfurase[17,18]. However, we do not observe a quinonoid intermediate between the aldimine and ketimine in the stopped flow experiments with SufS and L-cysteine regardless of the presence of SufE. The reason may be due to the difference in the structures of group I and group II cysteine desulfurases that group I cysteine desulfurase may better stabilize the short-lived quinonoid intermediate.

Catalytic activity of many enzymes is sensitive to conformational dynamics that can be influenced by allosteric regulation. Previously we demonstrated the binding of SufE

caused highly localized dynamic perturbations within residues 225-236 (including the Lys binding to PLP) and 356-366 (the loop including the active site Cys364)[11]. Since residues 225-236 locates deeply in the active site cavity, its conformational change around PLP upon SufE binding may be transmitted via the 356-366 loop with the active site. Here our data provides direct evidence to the allosteric change of the PLP cofactor in SufS upon SufE binding. The pre-steady-state kinetic research demonstrates that the SufE binding actually facilitates the formation of Cys ketimine that is the intermediate after the formation of external Cys aldimine. The external Cys aldimine in SufS seems to have a similar absorbance as the Cys ketimine, such that they are not easily distinguished in a steady-state experiment and were observable here using SVD analysis of pre-steady state data. We also demonstrate the critical role of His123 in the reaction mechanism. It is possible that the SufE binding shifts the PLP cofactor to an optimal orientation that facilitates the general base, His123, to abstract the α proton from the external Cys aldimine, which shifts the SufS active site equilibrium toward the formation of Cys ketimine. The finding that SufE increases the persulfide formation supports this theory since shifting the reaction forward to the ketimine should promote formation of the final persulfide product.

In summary, we clarified the role of the SufE binding in persulfide formation of the reaction of SufS and L-cysteine. The observed changes in the PLP conformation and pre-steady-state kinetics suggest that SufE actively promotes the Cys ketimine formation. The site directed mutagenesis proves that His123 plays an important role in the process above, likely by acting as a catalytic base. Finally, the changes SufE binding induces increase the persulfide formation. Based on our former research, this study further elucidates the catalytic mechanism of SufS as cysteine desulfurase and the role of SufE in both persulfide

formation and sulfur transfer, which provides a clearer picture of the interaction between SufS and SufE.

REFERENCE

1. C.J. Schwartz, O. Djaman, J.A. Imlay, P.J. Kiley, Proc. Natl. Acad. Sci. U. S. A., 2000, 97, 9009–9014.

2. C.T. Lauhon, R. Kambampati, J. Biol. Chem., 2000, 275, 20096–20103.

3. C.T. Lauhon, J. Bacteriol., 2002, 184, 6820–6829.

4. H. Mihara, N. Esaki, Appl. Microbiol. Biotechnol., 2002, 60, 12–23.

5. F.W. Outten, O. Djaman, G. Storz, Mol. Microbiol., 2004, 52, 861–872.

6. Fujii, T., Maeda, M., Mihara, H., Kurihara, T., Esaki, N., Hata, Y, Biochemistry, 2000, 39, 1263-1273.

7. R. Shi, A. Proteau, M. Villarroya, I. Moukadiri, L. Zhang, J.F. Trempe, PLoS Biol, 2010, 8, e1000354.

8. B.P. Selbach, P.K. Pradhan, P.C. Dos Santos, Biochemistry, 2013, 52, 4089–4096.

9. Dai Y, Outten FW, FEBS Lett., 2012, 586 (22), 4016-4022.

10. Lima, C.D., J. Mol. Biol., 2002, 315, 1199-1208.

11. Singh H, Dai Y, Outten FW, Busenlehner LS., J. Biol. Chem., 2013, 288 (51), 36189-36200.

12. Dai Y, Kim D, Dong G, Busenlehner LS, Frantom PA, Outten FW, Biochemistry, 2015, 11, 54 (31), 4824-4833.

13. Limin Zheng, Robert H. White, Valerie L. Cash, and Dennis R. Dean, Biochemistry, 1994, 33, 4714-4720.

14. Katherine A. Black, Patricia C. Dos Santos. Biochimica et Biophysica Acta., 2015, 1853, 1470-1480.

15. Outten FW, Wood MJ, Munoz FM, Storz G, J. Biol. Chem., 2003, 278 (46), 45713-45719.

16. László Zimányi, Ágnes Kulcsár, Janos K. Lanyi, Donald F. Sears, Jr. and Jack Saltiel, Proc Natl Acad Sci U S A. 1999, 96 (8), 4408–4413.

17. Elhanm Behshad and J. Martin Bollinger, Jr., Biochemistry, 2009, 48, 12014-12023.

18. Jing Yang, Guoqiang Tan, Ting Zhang, Robert H. White, Jianxin Lu, and Huangen Ding, J. Biol. Chem., 2015, 290 (22), 14226–14234.

19. Klaus D. Schnackerz, Babak Andi, Paul F. Cook, Biochimica et Biophysica Acta., 2011, 1814, 1447-1458.

CHAPTER 3
CHARACTERIZATION OF THE INTERACTION INTERFACE OF SUFS AND SUFE

ABSTRACT

Fe-S clusters are one major type of the sulfur-containing cofactors, which conduct essential functions in organisms. SufS is a cysteine desulfurase that provides sulfur for the formation of Fe-S cluster. It is the beginning of the Suf pathway, which forms Fe-S clusters for *E. coli* under iron limitation and oxidative stress. The basal activity of SufS is quite low and it needs the interaction of SufE for activation. The interaction of SufE is essential for the normal activity of SufS. The study on the interaction of SufS and SufE may lead to a design of protein-protein interaction inhibitors to disturb the binding of SufE to SufS, which may shut down Suf pathway with a potential of a new type of antibiotic. We generated the Y345A/D346A mutations in SufS and applied PLP quantification, analytical gel filtration, UV-visible spectroscopic analysis and circular dichroism to confirm this mutant still keeps the structural integrity. The basal activity of SufS Y345A/D346A is similar as that of WT SufS but SufE cannot enhance the activity of this mutant. The results of ITC show that there is no more interaction between this mutant and SufE. SufS residues Ser262 and Glu263 are other candidates for the interaction with SufE. However, the

S262A/E263A mutations on SufS do not alter enhancement by SufE. Based on the research above, a structural modeling of the SufS-SufE interaction was made through protein-protein docking, which clarifies more details in this interaction.

INTRODUCTION

Sulfur containing cofactors are essential in many biochemical reactions and distributed widely in nature. Fe-S clusters are one major type of the sulfur-containing cofactors, which are made up of Fe^{2+} or Fe^{3+} bounded to sulfides that bridge the iron ions. They coordinate to proteins through cysteine residues. [4Fe - 4S] is the most abundant type in metalloproteins. They are stable at multiple oxidation states with physiologically relevant redox potentials. Fe-S clusters perform important functions in cells such as substrate binding and catalysis, electron transfer, sensing reactive oxygen and nitrogen species, genetic regulation in transcription and translation[1,2]. The biogenesis of Fe-S clusters *in vivo* is undertaken by a series of proteins working cooperatively and the core steps include sulfur mobilization, iron donation, assembly of Fe-S clusters on a scaffold protein, and Fe-S cluster trafficking from scaffold protein to target proteins[1]. These core steps form a framework for Fe-S cluster formation, which is universal in various organisms. Currently three main Fe-S cluster assembly systems are identified in bacteria including the *isc*, *nif* and *suf* pathways[3,4]. The *nif* pathway assemblies Fe-S clusters in the nitrogenase enzymes. The *isc* pathway is found in both procaryotic cells and the mitochondria of eukaryotic cells to generate various Fe-S clusters for metalloproteins. The *suf* pathway is present in many gram-negative and the plant chloroplast. In some bacteria, *suf* pathway can

undertake the biogenesis of Fe-S clusters under oxidative stress and iron limitation[5]. *E. coli* has both *isc* and *suf* pathways for the Fe-S cluster assembly[6]. All of the three pathways utilize cystine desulfurase like NifS, IscS, and SufS individually to abstract sulfur from L-cysteine. Then the sulfur is transferred to the scaffold protein where nascent Fe-s clusters are assembled after iron donation[7]. NifU and IscU act as the scaffold proteins in the nif and isc pathways. SufU is homologous to IscU, which can form $[4Fe - 4S]^{2+}$ clusters in *B. Subtilis*[8]. In *E. coli*, $SufBC_2D$ replaces SufS to act as the scaffold protein in *suf* pathway[9].

E. coli is the model organism we use to investigate the mechanism of the Fe-S cluster assembly. There are *isc* and *suf* pathways together in *E. coli* (Figure 3.1). Isc pathway is the housekeeping pathway for Fe-S cluster assembly while Suf pathway produces Fe-S clusters under oxidative stress and iron starvation. The Suf pathway is encoded by the *suf* operon composed by *sufABCDSE* (Figure 3.2). SufS is homologous to IscS as cysteine desulfurase to extract sulfur from L-cysteine, which forms a persulfide on its active site (Cys364-S-SH). Then the sulfur is transferred to the active site of SufE (Cys51-S-SH), which transfers this sulfur atom to the scaffold protein $SufBC_2D$ as a sulfur shuttle. In the Suf pathway, $SufBC_2D$ acts as the scaffold protein where the nascent Fe-S cluster is formed with Fe donation. SufA is homologous to IscA, which is a shuttle of the Fe-S cluster from the scaffold protein to the target apo protein[6,10]. The basal activity of SufS is low that the activity of IscS is up to 20-fold higher than SufS. SufE can enhance the activity of SufS to a level comparable to IscS[11]. $SufBC_2D$ can further increase the activity of SufS-SufE complex[12]. Under stress conditions, both IscS and IscS-IscU complex are much more sensitive to H_2O_2 exposure than SufS-SufE complex that still maintains a high activity as the concentration of H_2O_2 increases. The active site of SufS is

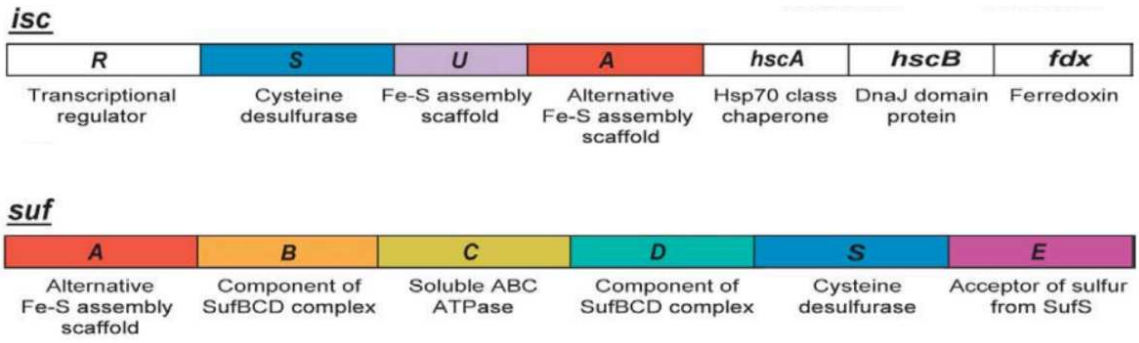

Figure 3.1 Comparison of isc and suf pathway and the function of each component.

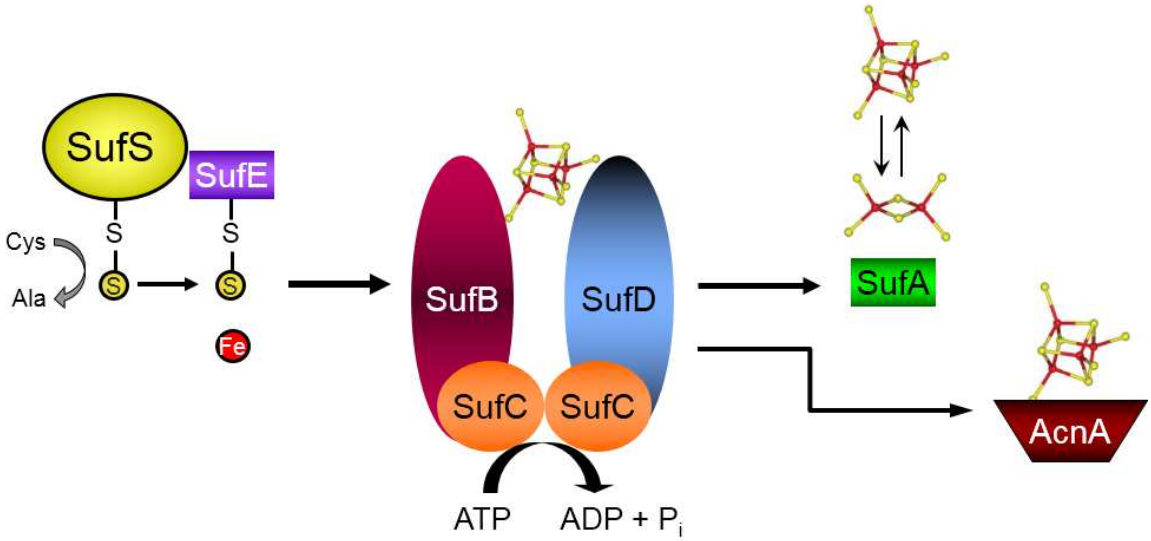

Figure 3.2. Current model of Suf pathway.

more resistant to oxidation modification in the presence of SufE. The interaction of SufS and SufE is essential to activate SufS and provide protection against oxidative stress[11]. However, the interface of this interaction is still unknown. This research on the interface of the interaction between SufS and SufE has a potential to develop an inhibitor to disrupt the binding of SufE in order to decrease the activity of SufS, which has biomedical relevance. The *suf* pathway is conserved in various bacteria like *Mycobacterium tuberculosis*, *Shigella* and even our model system, *E. coli.* They are important infectious pathogens. It has been shown that the *suf* pathway is essential for bacterial survival under iron deprivation conditions, which is a common setting bacteria confront in the human body. Because of lack of direct homologs of Suf proteins in humans, disruption of the Suf pathway with novel antibiotics should have minimal side effects[13].

CsdA and CsdE are homologous to SufS and SufE individually. Both CsdA and SufS belong to the group II cysteine desulfurase with ~ 43% sequence identity (Figure 3.3). CsdE and SufE have ~ 35% sequence identity (Figure 3.4). The sequence similarity suggests that CsdA/CsdE and SufS/SufE are closely relative. The crystal structure of the complex of CsdA-CsdE has been resolved. The helix16, helix18 β sheets and the active site loop of CsdA are the main parts of the interaction with CsdE (helix-II, active site loop, helix-III and a part of helix-VI) (Figure 3.5). This interaction causes a significant conformational change of the active site loop of CsdE from being buried in the hydrophobic pocket to shift towards CsdA by moving ~ 11 angstroms upon binding of CsdA. The residues in the interface of CsdA-CsdE interaction are highly conservative in SufS and SufE, which suggests the SufS-SufE interface may resemble that of CsdA-CsdE[14]. Amide hydrogen/deuterium exchange mass spectrometry (HDX-MS) is used to characterize the

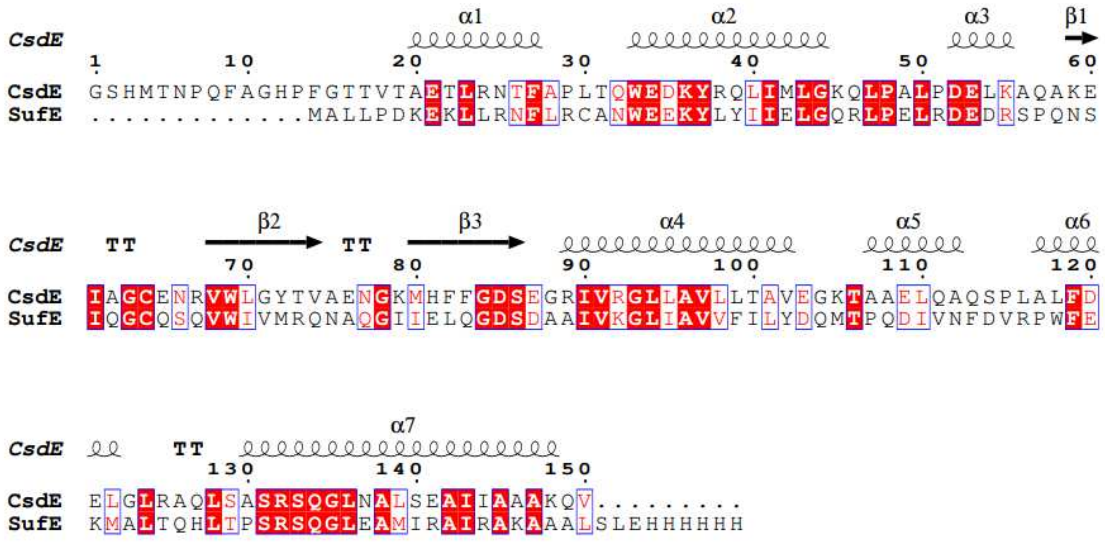

Figure 3.3. Alignment of CsdE and SufE. The secondary structure of CsdE was shown using the CsdE pdb file 5EEP.

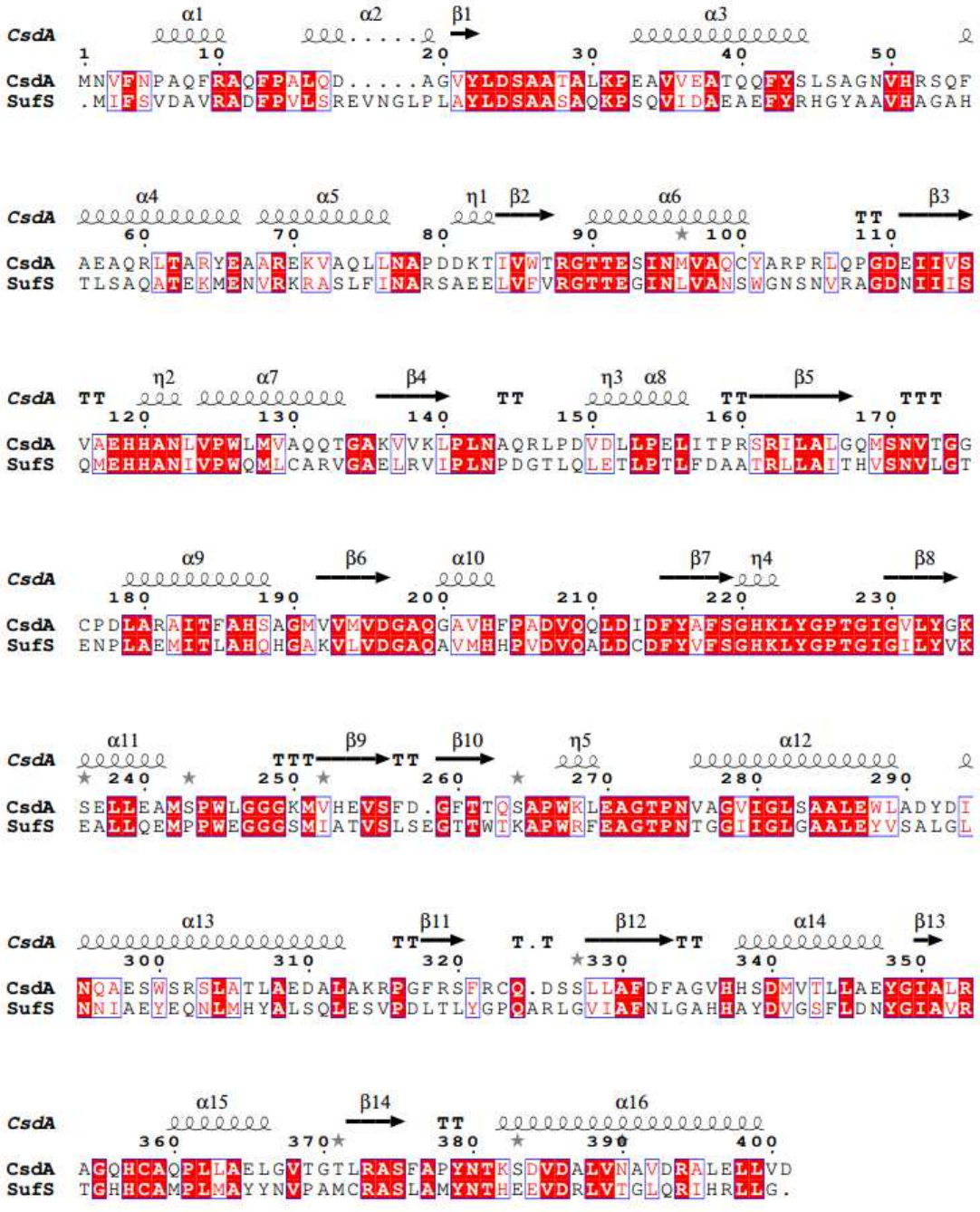

Figure 3.4. Alignment of CsdA and SufS. The secondary structure of CsdA was shown using the CsdA pdb file 5FT4.

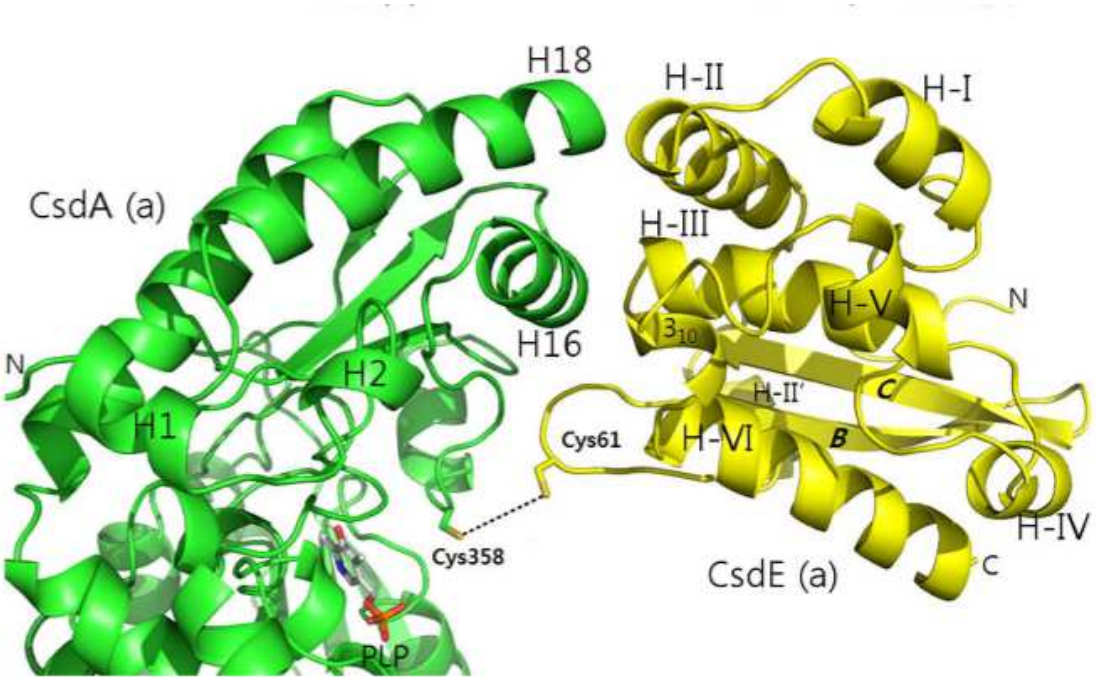

Figure 3.5. Interface of the interaction between CsdA and CsdE[14]. CsdA is green. CsdE is yellow.

SufS and SufE interaction. The result shows residue 38 – 56 and/or 66 – 83 of SufE, 225 – 236 and 356 – 366 of SufS, have altered deuterium uptake, which means conformational change after the interaction[15]. Residue 38 – 56 and 66 – 83 of SufE are corresponding to the interface region of CsdE. Reside 356 – 366 of SufS is the active site loop that corresponds one part of the interface regions of CsdA. Residue 225 – 236 locates in the deep cavity of the active site which is impossible to participate in the interaction but related in the activation mechanism of SufS. Based on the CsdA-CsdE co-structure, 343 – 354 (helix16) and 393 – 406 (helix18) of SufS are also possible to form hydrogen bonds and van der Waals with SufE but they do not show a significant change in the HDX-MS data of SufS-SufE interaction[15]. This finding led us to investigate the possible interface in the reaction of SufS and SufE.

Here we show the activity of SufS Y345A/D346A cannot be enhanced by SufE. And there is no interaction between SufS Y345A/D346A. Our results thus show that Tyr345 and Asp346 of SufS play an important role in the interface of the interaction of SufS and SufE. The binding of SufE to SufS is essential to its enhancement to the activity of SufS, which may be relative to the sulfur transfer from SufS to SufE. According to the current data, we propose a simulation of the interface of the interaction of SufS and SufE to further clarify this interaction.

MATERIALS AND METHODS

Plasmid and Site-mutagenesis

For mutagenesis of *sufS*, *pET21a_sufS* was used as the template plasmid. The SufS Y345A/D346A double mutation was introduced by site-directed mutagenesis using the QuikChange Kit (Stratagene) with primers 5'-AACACCACGCCGCTGCTGTTGGCAG-3' and its complementary primer 5'-CTGCCAACAGCAGCGGCGTGGTGTT-3' on pET21a_*sufS*. For the SufS S262A/E263A double mutation, the primer was 5'-CAGCCTGGCTGCAGGCACTA-3' and its complementary primer was 5'-TAGTGCCTGCAGCCAGGCTGA-3' on pET21a_sufS. The mutations were confirmed by DNA sequencing and alignment.

Protein expression and purification

E. coli SufS and SufE were independently expressed and purified as described previously. *E. coli* BL21(DE3) containing *pET-21a_SufS Y345A/D346A* or *pET-21a_SufS S262A/E263A* was grown in LB with 100 μg/ml ampicillin at 37 ˚C for overnight, diluted 100 fold into LB, incubated with shaking to reach an OD_{600} of 0.4 – 0.6 before induced by 500 μM IPTG at 18 ˚C for overnight. Cells were harvested and lysed in 25mM Tris-HCl, pH 8.0, 5mM DTT, and 1 mM PMSF via sonication. After centrifugation at 14000 rpm for 30min, the lysate was loaded on the columns. The SufS mutants were purified through Q-sepharose, phenyl and Superdex 200 chromatography resins in sequence. The Q-sepharose column used a linear gradient from 25 mM Tris-HCl, pH 8.0, 10 mM βME to 25 mM Tris-HCl, pH 8.0, 1 M NaCl, 10 mM βME. The phenyl column utilized a linear gradient from

25 mM Tris-HCl, pH 8.0, 100 mM NaCl, 1M ammonium sulfate, 10 mM βME to 25 mM Tris-HCl, pH 8.0, 10 mM βME. The Superdex column run with 25 mM Tris-HCl, pH 8.0, 150mM NaCl, 10 mM βME. Purified proteins were concentrated, frozen as drops in liquid nitrogen, and stored at – 80 ˚C until further use.

Ultraviolet-visible Spectroscopic Analysis

Ultraviolet-visible (UV-vis) spectra were measured by a BECKMAN COULTER DU 800 spectrophotometer. SufS Y345A/D346A and WT SufS were prepared at the concentration of 20 μM in 25 mM Tris-HCl, 150 mM NaCl, pH 8.0 buffer. 180 – 500 nm spectra were collected with a cuvette of 1 cm path length.

PLP quantification

The PLP cofactor is essential for the activity of SufS. PLP quantification can measure the percentage of PLP in SufS, which indicates the structural integrity of this enzyme. The protein was diluted into 1-2 mg/ml of 800 uL sample in 10 mM Tris-HCl, pH 8.0 buffer. 200 uL 5M NaOH was added and incubated at 75 ˚C for 10 min. Then 85 μL 12 M HCl was added. The sample was centrifuged at the highest rpm for 2 min. The UV-visible absorption was read at 390 nm. A PLP quantification standard line (Figure 3.6) was used to calculate the concentration of PLP in the sample.

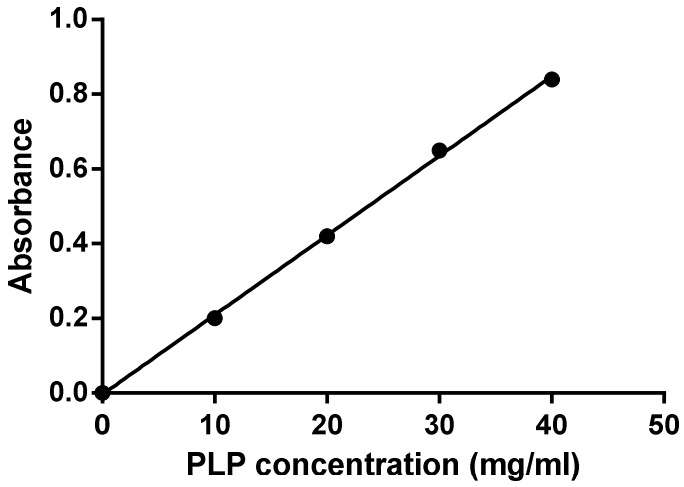

Figure 3.6. PLP quantification standard line and its linear fitting. The fitting line is y = 0.0211x + 0.0026.

Analytical gel filtration analysis

Analytical Superdex 200 gel filtration column (GE Healthcare) was used for the analytical gel filtration analysis to compare the molecular weight (MW) of WT SufS and SufS Y345A/D346A. The sample volume is 25 uL and the amount of protein is 1 mg. The flow rate is 0.5 mL/min and the elution buffer is 10 mM Tris-HCl, 150 mM NaCl, pH 8.0. The standard line was used to calculate the MW of the protein.

Circular Dichroism Spectroscopic Analysis

Circular dichroism (CD) spectra were measured by a JASCO J815 spectropolarimeter (JASCO, Essex, UK) at 20 ˚C. SufS Y345A/D346A and WT SufS were prepared at the concentration of 20 µM in 25 mM boric acid, pH 8.0 buffer. Far-ultraviolet (180 - 300 nm) spectra were collected with a cuvette of 1 cm path length.

Isothermal Titration Calorimetry

Isothermal titration calorimetry (ITC) measurements were performed on a VP-ITC calorimeter (MicroCal) at 20 ˚C. In the SufS/SufS Y345A/D346A and SufE ITC experiment, 1.44 ml 50 µM SufS or SufS Y345A/D346A present in the cell was titrated with 45 x 6uL injections of 1.1 mM SufE (10-fold molar excess over SufS/SufS Y345A/D346A). The duration of each injection was 7.2 s (1.2 s/µL), with an interval of 200 s between injections. Each experiment was corrected by the endothermic heat of

injection resulting from the titration of SufE into the buffer without protein. SufS/SufS Y345A/D346A ITC data wre analyzed in MicroCal Origin.

Cysteine Desulfurase Activity Assay

Cysteine desulfurase activity was measured through the formation of methylene blue with NNDP and $FeCl_3$ using the protocol below. Reactions were conduct aerobically in 25mM Tris-HCl, pH 7.4, 150 mM NaCl at room temperature. 0.5 μM proteins were incubated in the buffer for 5 min before the addition of 2 mM L-cysteine and 2 mM DTT. The reaction volume was 800 uL. Reactions proceeded for 10 min and were quenched by 100 uL 20mM NNDP in 7.2 M HCl and 100 uL 30 mM $FeCl_3$ in 1.2 M HCl. The mixture was incubated in the dark for 30 min to produce methylene blue. Precipitated protein was removed by 1 min centrifugation at 13000 rpm and the methylene blue was measured at 670 nm. A Na_2S standard line was made for calibration of the content of sulfur product from this reaction.

Protein-protein Interface Simulation through Protein Docking

To get an insight into the interaction interface of SufS and SufE, docking of SufS and SufE was performed with the GRAMMX server (http://vakser.bioinformatics.ku.edu/resources/gramm/grammx/), which applies extensive refinement, smoothed potentials, and knowledge-based scoring with fast Fourier transform global search methodology to predict the structure of a protein complex.

RESULTS

Structural integrity of SufS Y345A/D346A

The crystal structure of SufS shows that the PLP-binding site and active site residues are located in a narrow cavity within the SufS homodimer[16]. Around the cavity opening of SufS, there are several polar residues, like Tyr345/Asp346 (Fig. 3.7). Polar residues of amino acids may play a role in the interaction of proteins[17]. To check if Tyr345/Asp346 play a role in the binding of SufS and SufE, the Tyr345Ala and Asp346Ala double mutation of SufS was constructed through codon substitutions (SufS Y345A/D346A). Mutation may cause influence to the original structure, even breakdown of the tertiary and quarternary structures of a protein. To check its structural integrity, we checked the PLP occupancy of SufS Y345A/D346A through a PLP quantification assay and it turns out to be above 90%. The pure SufS Y345A/D346A also was analyzed by the analytical Superdex-200 gel filtration (Figure 3.8). The results show that the mutant SufS almost overlays WT SufS and the molecular weight of the mutant SufS is smaller than WT SufS, which is consistent with the calculation based on the protein sequence. We applied UV-vis spectrum analysis. SufS is a PLP-dependent enzyme with a UV-visible absorption at 420 nm which represents the internal aldimine. Internal aldimine is the Shiff base that PLP cofactor binds covalently with a SufS Lys residue. Any shift of this absorption peak means there is a significant change of the SufS structure, which may lead to loss of activity. The UV-vis spectrum of SufS Y345A/D346A shows that the mutant still has the PLP-characteristic absorption peak around 420 nm. It indicates that this mutation does not disturb the PLP cofactor of SufS (Figure 3.9).

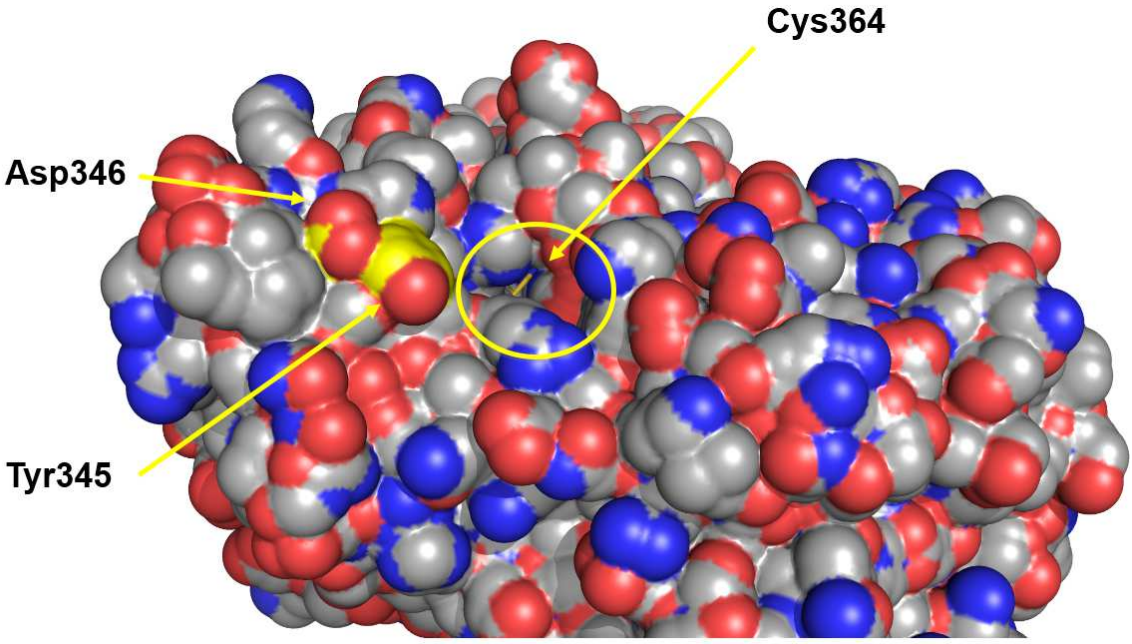

Fig. 3.7. Crystal structure of the polar residues around the cavity opening of the active site of SufS.

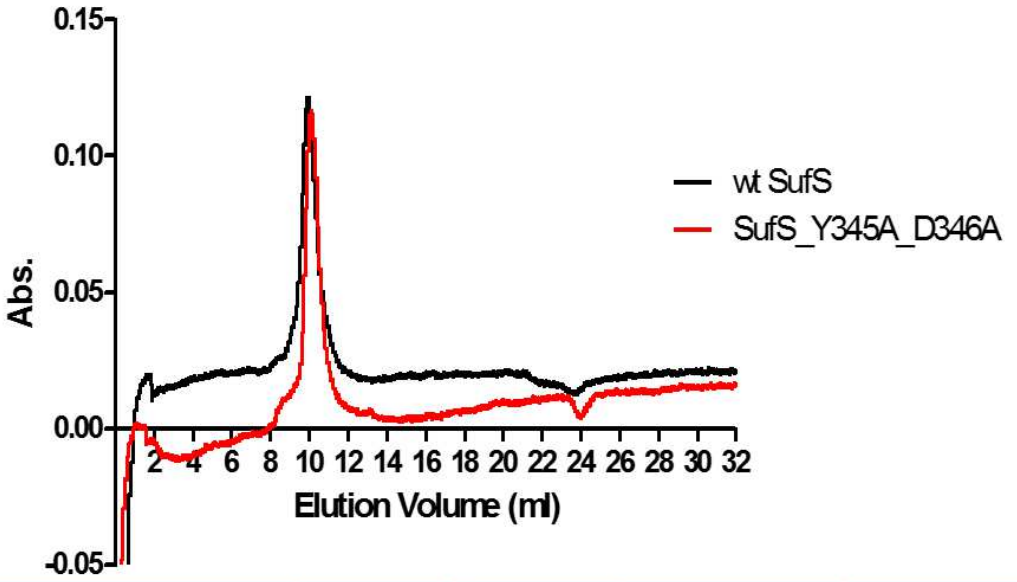

	Ve	Kav	MW	Theoretical MW
wt SufS	9.994ml	0.1091	56294	44434
SufS_Y345A_D346A	10.166ml	0.1200	52687	44298

Figure 3.8. Analytical gel filtration analysis of WT SufS and SufS Y345A/D346A. Ve is elution volume. Kav is an elution volume parameter.

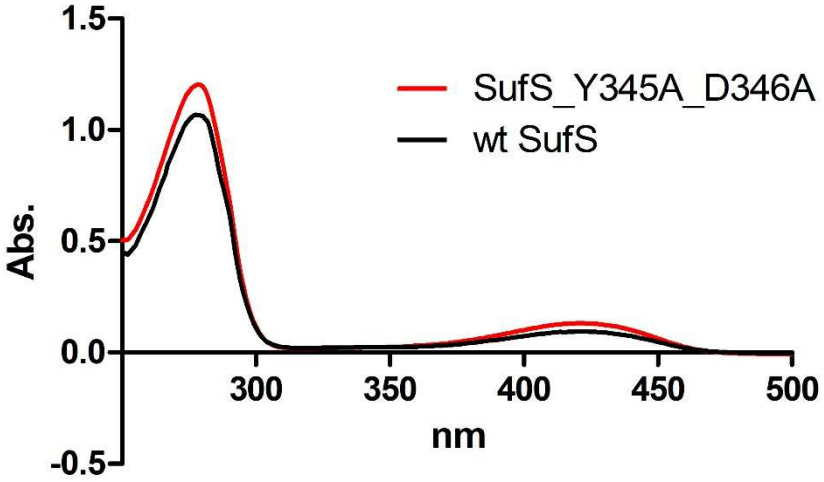

Figure 3.9. Overlay of the UV-visible spectra of WT SufS and SufS Y345A/D346A.

Circular dichroism (CD) is the difference in absorption between the left and right hand circularly polarized light in chiral molecules. The CD spectroscopy in the far UV region (180 nm – 250 nm) is used to probe the secondary structures of proteins[18]. To check if the double mutations change the secondary structure of SufS, we applied CD spectroscopy analysis to SufS Y345A/D346A. The result of CD shows that the spectra of WT SufS and SufS Y345A/D346A match each other well, which indicates that the double mutations do not disturb the secondary structure of SufS (Fig. 3.10).

Activity of SufS Y345A/D346A in the L-cysteine desulfurase reaction

To test the activity of SufS Y345A/D346A in the L-cysteine desulfurase reaction, we utilized the cysteine desulfurase assay to check the activity of SufS Y345A/D346A in the absence or presence of SufE. Cysteine desulfurases, like SufS, can mobilize the sulfur from L-cysteine to form alanine and a persulfide sulfur. The activity of the cysteine desulfurase can be determined by quantifying the amount of persulfide (S-SH) species on SufS after reduction to sulfide (SH) using DTT, TCEP, or excess L-cysteine. We first checked the activity of the SufS Y345A/D346A in function of various concentration of L-cysteine without the enhancement of SufE (Figure 3.11). The result suggests that the mutant SufS has a similar basal activity as WT SufS without the enhancement of SufE. Then we checked the enhancement of SufE to the activity of the mutant SufS (Figure 3.12). The result shows that as the concentration of SufE increases, the activity of WT SufS increases significantly while SufS Y345A/D346A does not respond to the presence of SufE. Thus SufE does not enhance the activity of SufS Y345A/D346A.

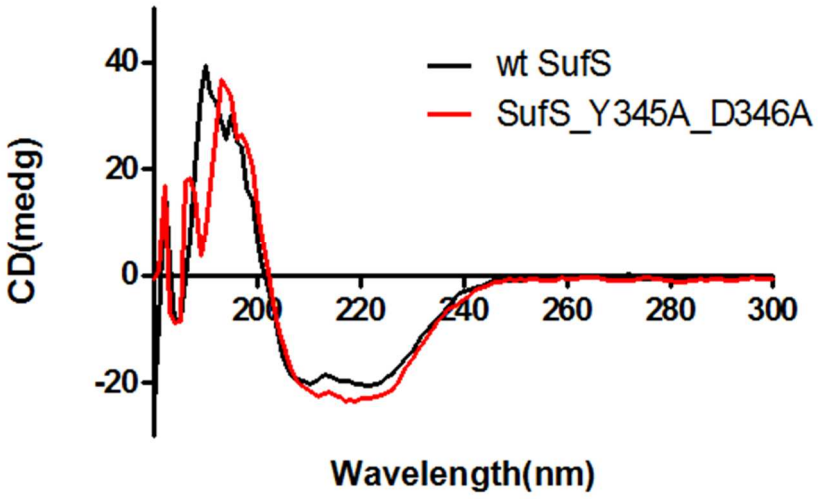

Fig. 3.10. Overlay of the CD spectra of WT SufS and SufS Y345A/D346A.

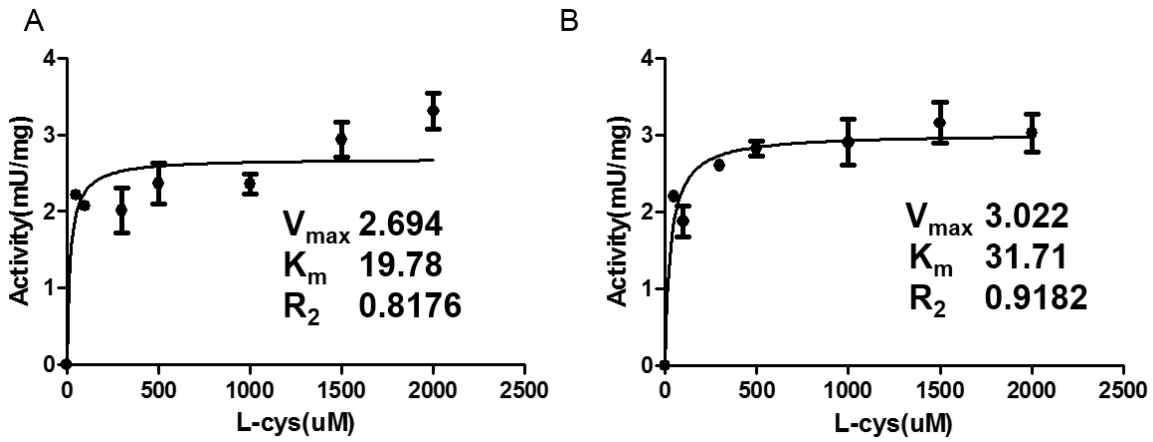

Figure 3.11. The comparison of activities of WT SufS and SufS Y345A/D346A in function of the concentration of L-cysteine in the absence of SufE. (A) Activity of WT SufS. (B) Activity of SufS Y345A/D346A.

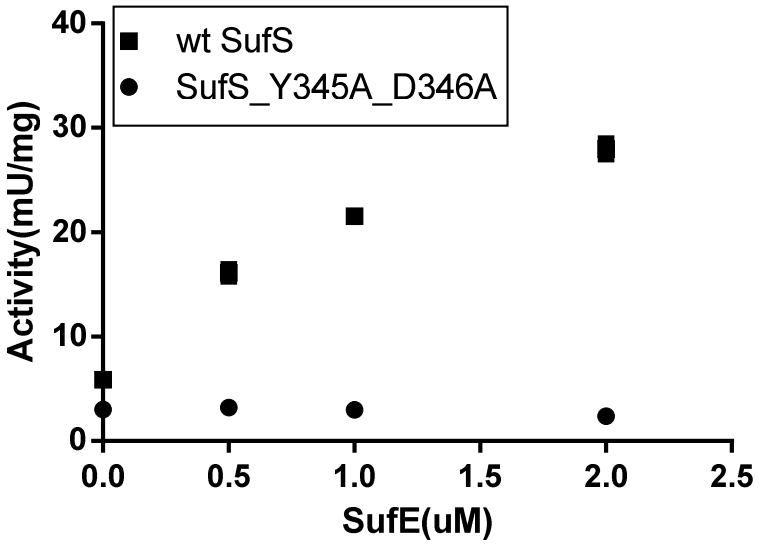

Figure 3.12. Comparison of activities of 0.5 µM WT SufS and 0.5uM SufS Y345A/D346A in the presence of various concentration of SufE.

Affinity of SufE to SufS Y345A/D346A

Isothermal titration calorimetry (ITC) directly measures the heat generated or absorbed when molecules interact and provides thermodynamic parameters like enthalpy, entropy, and kinetics of interactions like K_m, K_{cat}, and the heat rate in solution, which can indicate the interactions of molecules[19]. For the interaction, ITC can provide the number of binding site (n) and the dissociation constant (K_d). There is direct evidence from ITC that SufS binds to SufE[15]. To check the affinity between SufE and SufS Y345A/D346A, we used SufE to titrate SufS Y345A/D346A in ITC. The ITC result shows there is no obvious endothermic process during the whole titration and the data cannot fit any model, which indicates that no detectable interaction is observed (Figure 3.13). This result shows that the mutation of SufS Y345A/D346 inhibits the interaction with SufE so SufE cannot enhance the activity of the cysteine sulfurase, but we still cannot exclude the possibility that the mutation also disrupts the structure of SufS.

Activity of SufS S262A/E263A in L-cysteine desulfrase reaction

Like Tyr345/Asp346, Ser262/Glu263 are also located at the opening of the cavity containing the active site of SufS (Figure 3.14). The Location of Ser262 and Glu263 on polar "knob" present on the active site "lid" around the opening of the cavity containing the active site of SufS. The HDX-MS data shows that a slow H/D exchange was observed in the region of residue 262-274 of SufS (Figure 3.15). Ser262/Glu263 are polar residues which may form hydrogen bonds with SufE and contribute to the interaction between SufS and SufE. We mutated both Ser262 and Glu263 to Ala (SufS S262A/E263A) and checked

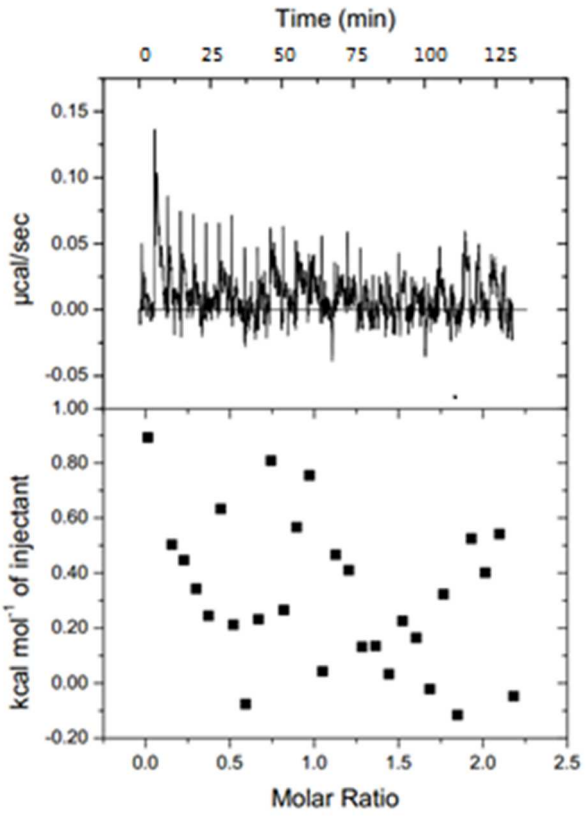

Figure 3.13. Analysis of the binding of SufS Y345A/D346A and WT SufE by isothermal titration calorimetry. The integrated heats of the binding plotted against the molar ratio of SufE added to the mutant SufS showed random dots, which indicates there is no interaction between the two proteins above.

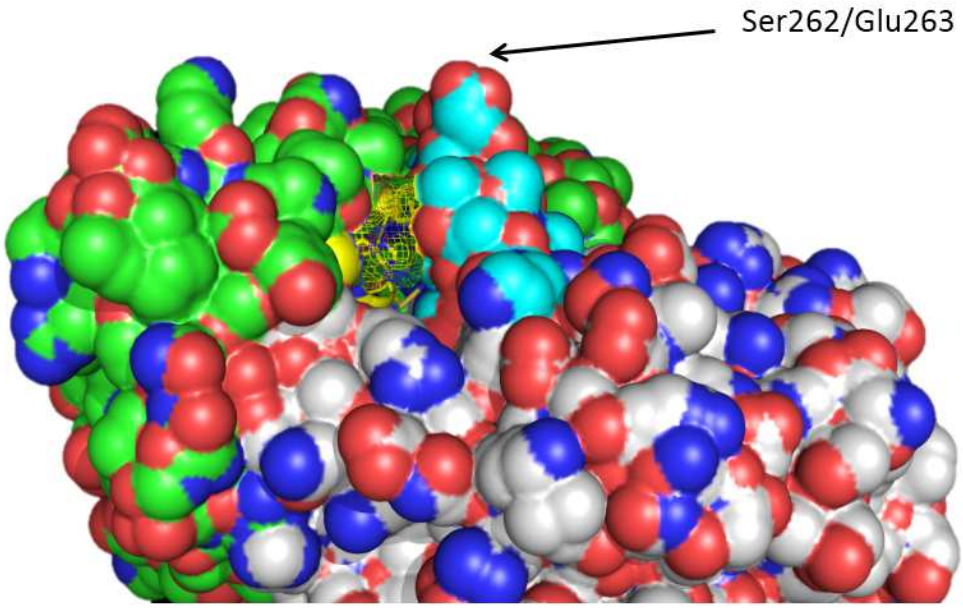

Figure 3.14. Location of Ser262/Glu263 on the surface of SufS. The cyan part is the "lid" around the opening of the active site of SufS.

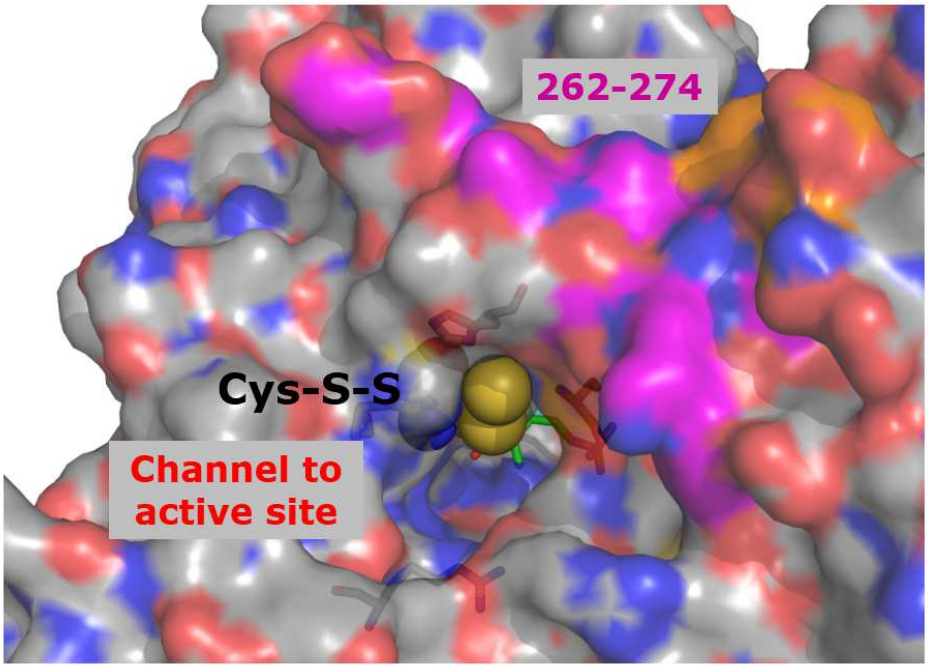

Figure 3.15. Crystal structure of the surface of SufS. The pink region (Residue 262-274) shows a slower H/D change.

its influence on SufS activity. The result shows that SufE can still enhance the activity of SufS S262A/E263A (Figure 3.16). Compared with the data of SufS Y345A/D346A, Ser262 and GLu263 may not participate in the interaction of SufS and SufE.

Structural modeling of the SufS-SufE interaction

Since the crystallography structure of a SufS-SufE complex is not solved yet, we used the crystal structure of SufS (PDB accession NO. 1C0N) and SufE (PDB accession NO. 1MZG) of *E. coli* to predict the interaction between SufS and SufE by protein-protein docking with the GRAMM-X docking server. 30 possible solutions for the SufS-SufE interaction were generated, one of which was selected based on the similarity as the interaction of CsdA-CsdE[14], the HDX-MS data of the apo SufS and the apo SufE[15] and the predicted proximity of the cysteine residues at the active sites of SufS and SufE (Figure 3.17). SufS and SufE are homodimers. In the interaction model, only one monomer of SufS interacts with one monomer of SufE. The other monomers of the homodimers have no interaction. The loop containing the active site Cys51 of SufE is flipped towards the active site Cys364 of SufS to reduce the distance between the sulfur atoms of the two cysteines, which is a better orientation for the transpersulfide reaction. The β helix containing Tyr345 and Asp346 of SufS is proximal to the helixes of SufE and hydrogen bonds are formed, which are essential for the interaction between SufS and SufE.

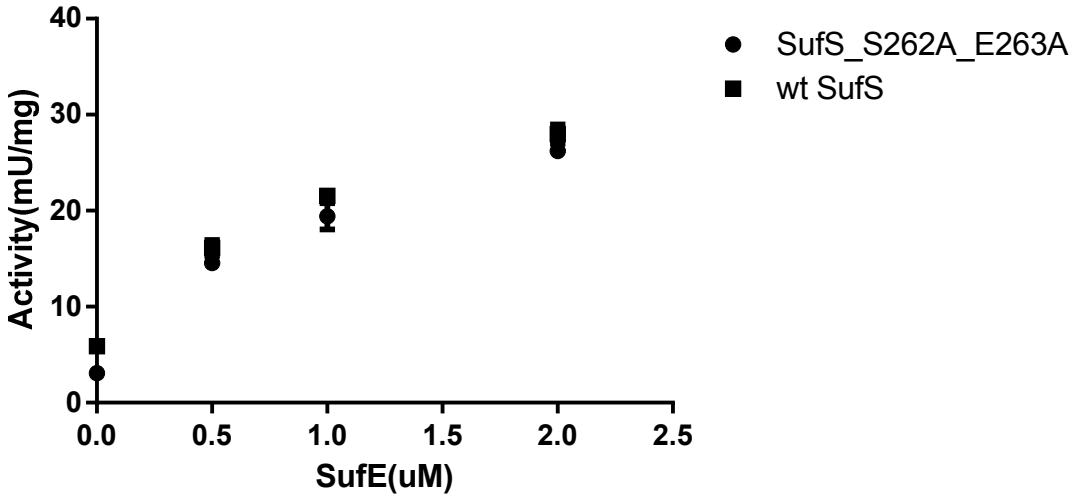

Figure 3.16. Comparison of activities of 0.5 μM WT SufS and 0.5uM SufS S262A/E263A in the presence of various concentration of SufE.

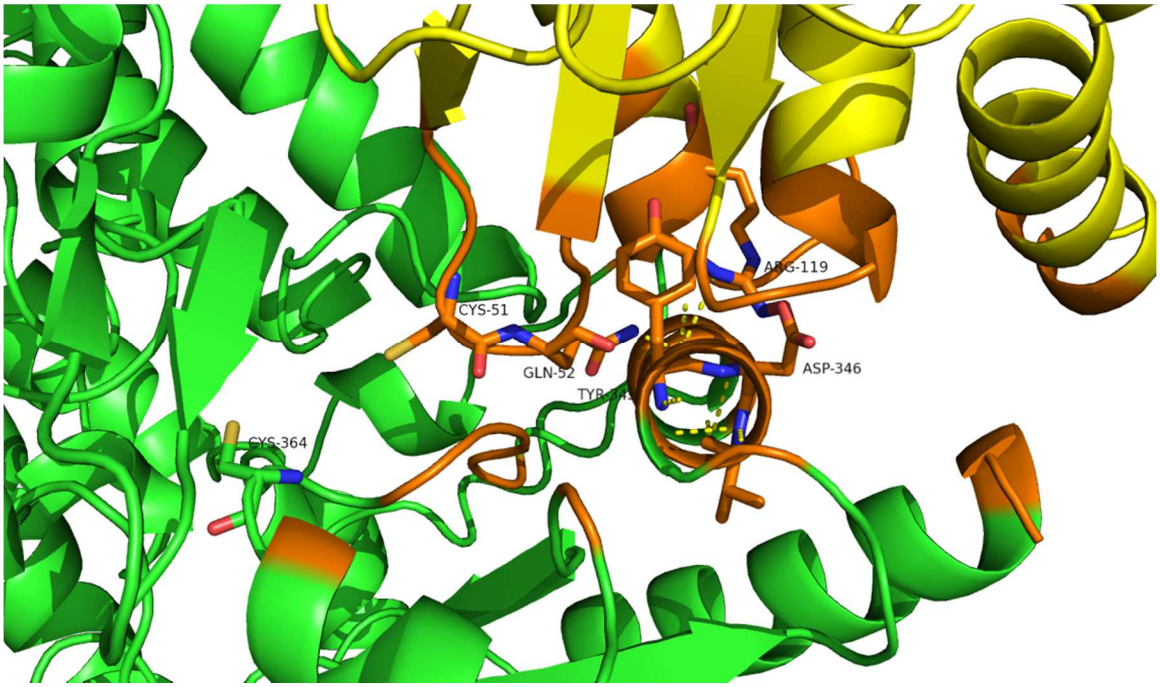

Figure 3.17. Binding interface simulation of the interaction of SufS and SufE through protein-protein docking. SufS is green. SufE is yellow. The orange part is the interface of the interaction.

DISCUSSION

Recent advances have made protein-protein interactions (PPIs) new targets for inhibitor design. Protein crystallography and mutational analysis have revealed that not all the residues at the interaction interface are critical but some "hot spot" residues provide most of the binding energy through hydrogen bonds and Van der Waals' forces[20]. Small molecules that bind to the hot spots can disrupt the PPI and inhibit the function of the protein-protein complex[21]. The research on the interaction of SufS and SufE has a potential to develop a type of PPI which can solve the problem of the specificity of the traditional SufS inhibitor. In this study, we proposed the hypothesis that the polar residues around the opening of the active site of SufS may participate in the interaction of SufS and SufE. To prove it, we applied site-directed mutagenesis and characterize the possible binding sites by CD, ITC, cysteine desulfurase assay and computational protein docking. The results show that the mutation of SufS Y345A/D346A keeps its structural integrity of the protein but it loses its affinity to SufE and it cannot be enhanced by SufE. The structural modeling of the SufS-SufE interaction by protein docking shows that the polar residues Tyr345 and Asp346 are located at a β helix beside the active site of SufE which is proximal to a helix of SufE and hydrogen bonds are formed. These findings are consistent with our hypothesis.

In our former research of the interaction between SufS and SufE, the ITC of apo SufS and apo SufE shows that there is a biphasic behavior in the binding process. At lower SufE concentration, it is an exothermic phase. At higher SufE concentration, it is an endothermic phase. The binding of SufE to SufS is best fit by a sequential two-site binding model with a higher affinity site and a lower affinity site[15]. It indicates that: first, SufE binds to SufS; second, each monomer of the homodimer of SufS has different affinity to

SufE. One SufE binding to one monomer of SufS can change the binding of the other monomer of SufS with another SufE. In the current study, we make the mutation of SufS Y345A/D346A. The ITC of apo SufE and apo SufS Y345A/D346A shows that there is no obvious binding between SufE and this mutant. It indicates that the double mutant breaks the interaction between SufS and SufE. We further checked the activity of SufS Y345A/D346A. The result shows that SufE cannot enhance the activity of the mutant SufS. The reason may be due to the loss of the interaction between them. So it is safe to say Tyr345 and Asp346 are important in the interaction of SufS and SufE. They are the "hot spot" residues that provide binding energy most likely from hydrogen bond in the SufS-SufE interaction and are candidates for the design of PPIs for SufS.

The crystal structure of CsdA-CsdE shows that the binding interface in CsdA includes helix16, helix18 and the active site loop[14]. CsdA and CsdE are homologous to SufS and SufE. Both CsdA and SufS are group II cysteine desulfurases. So the binding behaviors of CsdA has special meaning in the research of the binding of SufS and SufE. Based on the CsdA-CsdE crystal structure, the binding interface of SufS is supposed to be the residues of 343-354 (helix16), 355-378 (active site Cys364 loop), 393-406 (helix18). However, our former research on the SufS-SufE interaction through HDX-MS shows residue 356-366 of SufS are involved in the binding process[15]. The first explanation to this difference is that the SufS and SufE interaction may not be completely analogous to that of CsdA and CsdE. The second explanation may be that the binding of residue 343-354 and 393-406 may be not as significant as the residue 356-366. Our current study shows that Tyr345 and Asp346 in the residue 343-354 are essential for the interaction of SufS and SufE. It indicates that besides the residue 356-366, at least residue 343-354 also participate

in the binding. From our structural modeling of the SufS and SufE interaction, the loop containing the active site Cys364 of SufS is very close to the active site loop of SufE, which may provide larger binding energy compared with the rest binding interface. So our current research supports the second explanation of this difference.

In summary, we applied site-directed mutations and ITC to investigate the interaction of SufS and SufE. The UV-vis and CD show that the mutation still has the integral structure. The ITC shows that the mutation SufS Y345A/D346A loses its affinity with SufE. The cysteine desulfurase assay shows that SufE cannot enhance the activity of this mutant any more. Finally, we generated a structural binding model of SufS and SufE with computational protein docking. All the results above indicate that Tyr345 and Asp346 are essential in the binding of SufS and SufE. The interruption of the two residues above can make SufS-SufE complex lose its activity. Our further work will be required to further clarify this interaction and to screen or design the protein-protein inhibitor based on the interaction interface of SufS and SufE.

REFERENCE

1. Beinert, H., J Biol Inorg Chem., 2000, 5 (1), 2-15.
2. C. Ayala-Castro, A. Saini, F. W. Outten, Microbiol Mol Biol Rev., 2008, 72 (1), 110-125.
3. D. C. Johnson, D. R. Dean, A. D. Smith, M. K. Johnson, Annu. Rev. Biochem., 2005, 74, 247-281.
4. Limin Zheng, Robert H. White, Valerie L. Cash, and Dennis R. Dean, Biochemistry, 1994, 33, 4714-4720.
5. F.W. Outten, O. Djaman, G. Storz, Mol. Microbiol. 2004, 52, 861–872.
6. Outten FW, Biochim Biophys Acta., 2015, 1853 (6), 1464-1469
7. Mueller, E. G., Nat. Chem. Biol., 2006, 2, 185-194.
8. P. C. Dos Santos, A. D. Smith, J. Frazzon, V. L. Cash, M. K. Johnson, D. R. Dean, J. Biol. Chem., 2004, 279, 19705-19711.
9. A. G. Albrecht, D. J. Netz, M. Miethke, A. J. Pierik, Q. Burghaus, F. Peuckert, R. Lill, M. A. Marahiel, J Bacteriol., 2010, 192, 1641-1643.
10. Boyd ES, Thomas KM, Dai Y, Boyd JM, Outten FW, Biochemistry, 2014, 23, 53 (37), 5834-5847.
11. Dai Y, Outten FW, FEBS Lett., 2012, 586 (22), 4016-4022.
12. Outten FW, Wood MJ, Munoz FM, Storz G, J Biol Chem., 2003, 278 (46), 45713-45719.
13. Runyen-Janecky L, Daugherty A, Lloyd B, Wellington C, Eskandarian H, Sagransky M, Infect. Immun., 2008, 76 (3), 1083-1092.

14. Sunmin Kim and SangYoun Park, The Journal of Biological Chemistry, 2013, 288 (38) 27122-27180.

15. Singh H, Dai Y, Outten FW, Busenlehner LS, J Biol Chem., 2013 288 (51), 36189-36200.

16. Fujii, T., Maeda, M., Mihara, H., Kurihara, T., Esaki, N., Hata, Y., Biochemistry, 2000, 39, 1263-1273.

17. Lin Wang, Lin Li, and Emil Alexov, Proteins, 2015, 83 (12), 2186–2197.

18. Lee Whitmore, B. A. Wallace, Wiley InterScience. 2007, DOI 10.1002 / bip.20853.

19. Pierce, Michael M. Raman, C.S. Nall, Barry T., Methods, 1999, 19 (2), 213–221.

20. Arkin ME, Wells JA, Nat Rev Drug Discov Sci., 2004 3, 301–317.

21. Gadek TR, Burdick DJ, McDowell RS, Stanley MS, Marsters JC Jr, Paris KJ, Oare DA, Reynolds ME, Ladner C, Zioncheck KA, Lee WP, Gribling P, Dennis MS, Skelton NJ, Tumas DB, Clark KR, Keating SM, Beresini MH, Tilley JW, Presta LG, Bodary SC, Science. 2002, 295, 1086–1089.

22. Sharon Goldsmith-Fischman et al, J. Mol. Biol., 2004, 344, 549-565.

CHAPTER 4
EFFECTS OF PLP-BASED INHIBITORS CYCLOSERINE AGAINST SUFS AND SUFE AND THEIR MECHANISMS

ABSTRACT

Suf pathway is necessary for Fe-S cluster biogenesis under oxidative stress and iron-limiting conditions. It is a good target for novel antibiotic design. SufS is the cysteine desulfurase in Suf pathway to extract sulfur from L-cysteine. It needs the enhancement of its accessory protein, SufE. The PLP cofactor of SufS is essential to catalyze the β-elimination reaction of L-cysteine to extract the sulfur. Cycloserine has two enantiomers, D-cycloserine (DCS) and L-cysloserine (LCS), which are irreversible inhibitors of PLP dependent enzymes by forming a stable adduct with the PLP cofactors. To investigate if DCS/LCS can inhibit the activity of SufS, we checked the activity of SufS in the presence of either DCS or LCS. The results show that there is a dose-dependent inhibition of SufS activity by DCS. The 50% inhibitory concentration (IC_{50}) was calculated to be 1.98 mM. A dose-dependent inhibition of SufS by LCS was also observed and the IC_{50} is 306.1 μM Compared with DCS, LCS shows much better inhibitory effects. The small-molecular docking shows that the nitrogen of DCS to start the nucleophilic attack towards the Schiff base of the PLP and Lys226 is far away from its target, which is not a proper orientation for the transimination reaction. The docking of LCS shows that the nitrogen of LCS for the

nucleophilic attack is close to the Schiff base of Lys226 and PLP, which is a proper orientation for the following transimination reaction. The UV-visible spectra of SufS and DCS shows the degradation of internal aldimine and a new intermediate at 380 nm is formed. The spectrum of LCS shows the 380 nm peak is reduced but a 320 nm peak keeps growing, which indicates the intermediate at 320 nm is a stable adduct and it is hard to get rescued by excessive L-cysteine. A reaction mechanism is proposed to depict the reaction between SufS and DCS/LCS.

INTRODUCTION

Iron is essential for most organisms in which it performs a wide variety of vital cellular functions. Many of these functions depend on iron-sulfur (Fe-S) clusters. Fe-S clusters are key metal cofactors in electron transfer, catalysis, sensing of reactive oxygen, and genetic regulation[1]. The biosynthesis of Fe-S clusters is undertaken by a series of proteins working cooperatively. In *Escherichia coli* (*E. coli*), the Suf pathway is necessary for Fe-S cluster biogenesis under oxidative stress and iron-limiting conditions[2]. The Suf pathway is a good target for novel antibiotic design because: First, the Suf pathway is conserved in important pathogens like *Mycobacterium tuberculosis* and *Shigella* as well as in our model system, *E. coli*[3]. Second, the Suf pathway is essential under oxidative stress and iron limiting conditions which confront bacterial pathogens in the human body[4,5]. Third, humans lack direct homologues of most of the Suf proteins, so disruption of the Suf pathway should have minimal side effects[6]. SufS is the cysteine desulfurase in Suf pathway that extracts sulfur from the L-cysteine for sulfur donation to nascent Fe-S cluster formation. It has an important cofactor, pyridoxal-5'-phosphate (PLP), located in the active

site of SufS that plays a key role in the desulfurase reaction[7]. SufE is another protein from the same *suf* operon as SufS[8]. SufE interacts with SufS and this interaction enhances the activity of SufS by accelerating the sulfur release from SufS. SufS itself has low activity. SufE also protects the SufS active site from oxidative stress[5].

The cysteine desulfurase like SufS utilizes the PLP cofactor at the active site to catalyze the β-elimination reaction of L-cysteine to extract the sulfide from this amino acid[9]. The crystal structure of SufS from *E. coli* clearly shows that this cofactor covalently attached to the side-chain of a conserved Lys226 via a Schiff's bass (Figure 4.1). This is also known as an internal aldimine and is located at the cavity of the active site[10]. Transaldimination occurs when the L-cysteine substrate binds at the active site to form an external aldimine[11]. The crystal structure of external aldimine is not resolved due to the fast turnover. However, the structure of L-propargylglycine bound to PLP is resolved, which proves the presence of the transaldimination reaction[12] (Figure 4.2). The proposed steps subsequent to the formation of the external aldimine are (Figure 4.3): deprotonation at the α carbon of the external aldimine to form a quinonoid intermediate; the quinonoid is not stable and generates external ketimine; the active site Cys364 starts a nucleophilic attack to get the sulfide from external ketimine and the PLP is regenerated to release the Ala after a series of reactions[9]. PLP that plays an essential role in the desulfurase reaction is a good target for specific inhibitors.

Cycloserine has two enantiomers, D-cycloserine (DCS) and L-cysloserine (LCS) (Figure 4.4). Both of them can be used as cyclic analogues of cysteine, serine, and/or alanine. They have been shown to be irreversible inhibitors of many PLP-dependent enzymes like transaminases[13], racemases[14] and decarboxylases[15]. DCS also shows an

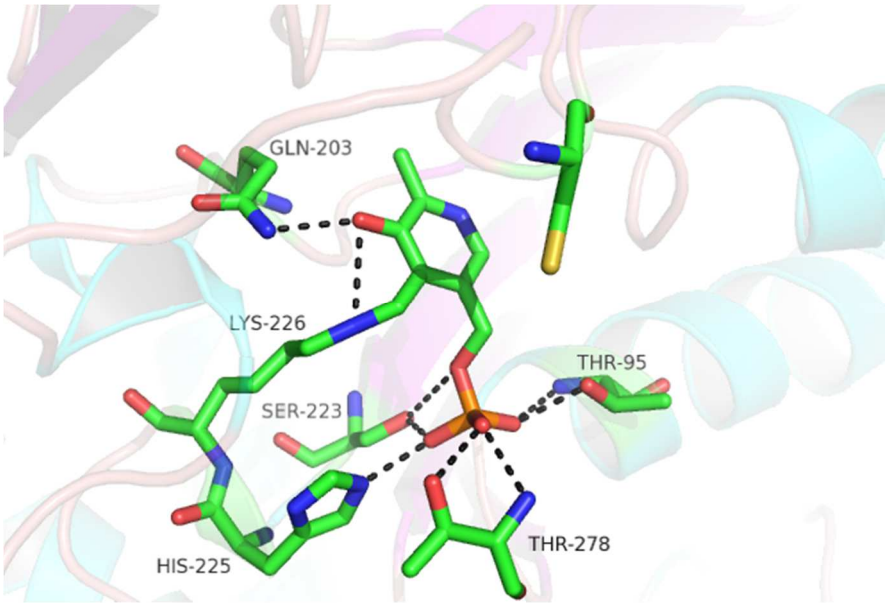

Figure 4.1 Crystal structure of internal aldimine in the active site of SufS.

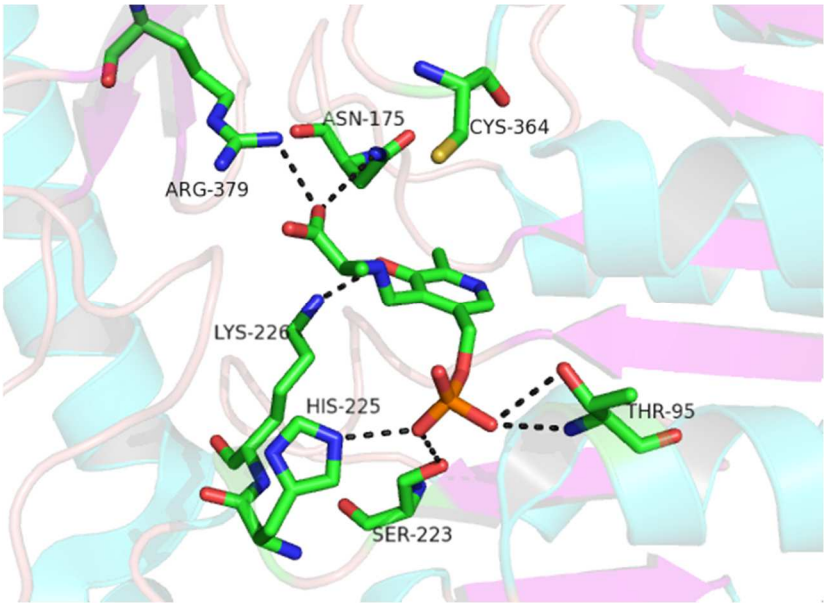

Figure 4.2. Crystal structure of L-propargylglycine bound to PLP in SufS.

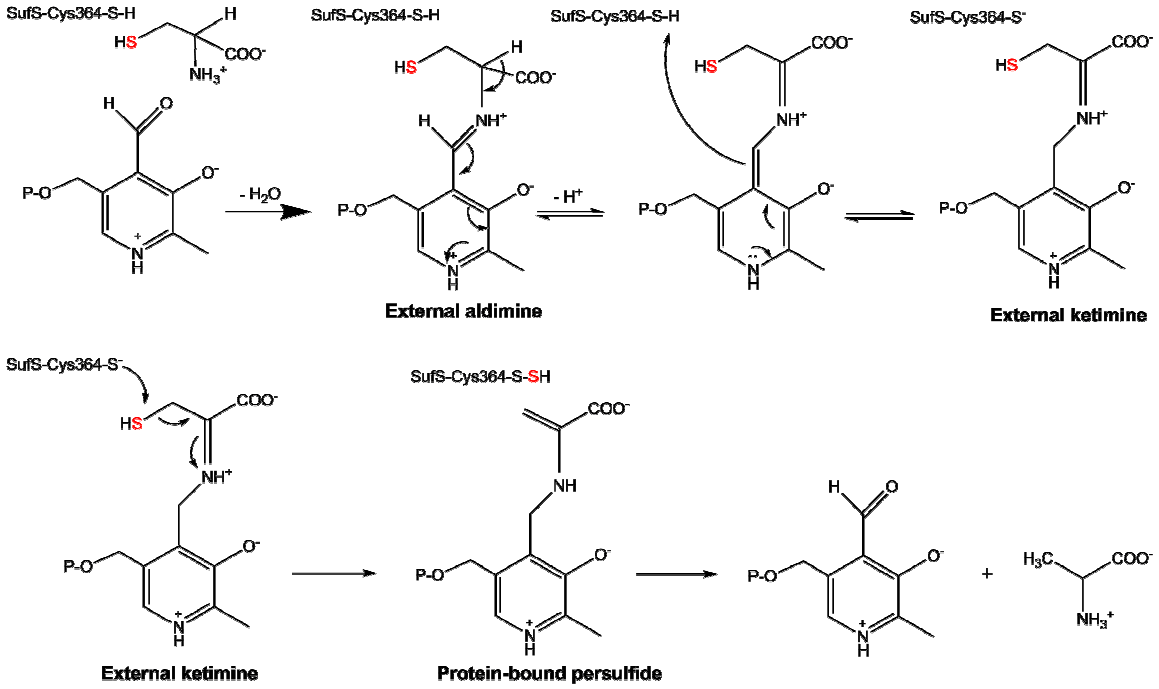

Figure 4.3 Proposed mechanism of the reaction between SufS and L-cysteine.

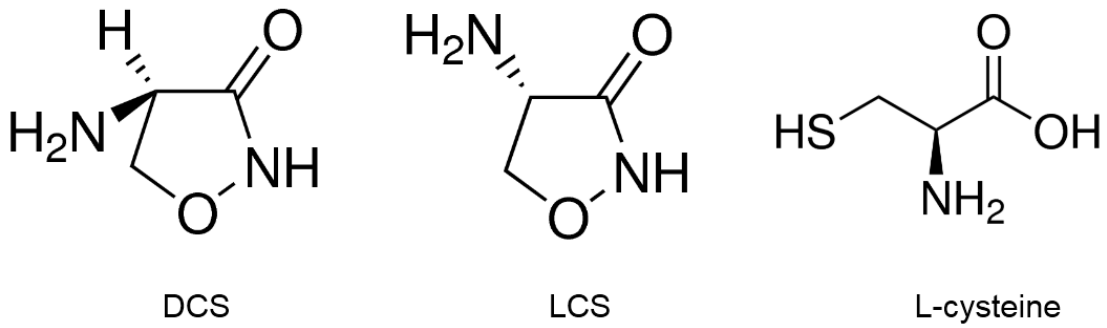

Figure 4.4. Chemical structures of DCS, LCS, and L-cysteine.

inhibitive effect on the desulfurase reaction of pSufS, which is the cysteine desulfurase in *Plasmodium falciparum*[16]. DCS is a natural product from *Streptomyces* strains and acts as a broad spectrum antibiotic, whereas LCS is synthesized chemically[17]. DCS has severe side effects so it is most commonly used as a second-line antibiotic in the combination therapy to treat tuberculosis[18]. Its main antibacterial target is the PLP-dependent alanine racemase which is an essential enzyme generating D-alanine for the formation of the D-alanyl-D-alanine dipeptide incorporated into the bacterial peptidoglycan layer[19]. DCS is also a potent agonist of N-methyl-D-aspartic acid (NMDA) receptor involved in human neurotransmission[20]. LCS commonly regulates the lipid metabolism but its mechanism of inhibition is still unknown. Unlike many irreversible inhibitors that inactivate their protein targets by covalent modification, cycloserine forms a stable adduct with the PLP cofactors to inhibit[16].

SufS is a PLP-dependent enzyme and PLP is essential for the desulfurase reaction. Cycloserine is a good candidate as a specific inhibitor to decrease the activity of SufS. In this study, we used a combination of enzyme kinetics, computational protein docking, and UV-vis spectroscopy to elucidate the mechanism of SufS inactivation by both enantiomers of cycloserine. We highlight differences in the inhibition from DCS and LCS and provide further insight in the PLP-dependent reaction.

MATERIALS AND METHODS

Strains and Plasmids

SufS and SufE were expressed in BL21(DE3). The construction of the vectors, *pET21a_sufS* and *pET21a_sufE*, were described before[5]. Cells that overexpress SufS and SufE were grown in Lennox Broth (LB). 100 mg/L ampicillin was used. All chemicals were obtained from Sigma unless otherwise indicated.

Protein Expression and Purification

E. coli BL21(DE3) containing *pET21a_sufS* and *pET21a_sufE* vectors was grown in LB at 37 ˚C until it reached an OD_{600} of 0.4 - 0.6. The overexpression was induced by addition of 500 µM IPTG. The condition for the induction of SufS is 18 ˚C overnight. The SufE induction condition is 37 ˚C for 3 hours. Cells were harvested and lysed in 25mM Tris-HCl, pH 8.0, 5mM DTT, and 1 mM PMSF via sonication. After centrifugation at 14000 rpm for 30min, the lysate was loaded on the columns. SufS was purified through Q-sepharose, phenyl and Superdex 200 chromatography resins in sequence. SufE was purified through Q-sepharose and Superdex 200 chromatography resins in sequence. The Q-sepharose column used a linear gradient from 25 mM Tris-HCl, pH 8.0, 10 mM βME to 25 mM Tris-HCl, pH 8.0, 1 M NaCl, 10 mM βME. The phenyl column utilized a linear gradient from 25 mM Tris-HCl, pH 8.0, 100 mM NaCl, 1M ammonium sulfate, 10 mM βME to 25 mM Tris-HCl, pH 8.0, 10 mM βME. The Superdex column run with 25 mM Tris-HCl, pH 8.0, 150mM NaCl, 10 mM βME. Purified proteins were concentrated, frozen as drops in liquid nitrogen, and stored at – 80 degrees until further use.

Rates of SufS-SufE inactivation by cycloserine using cysteine desulfurase assay

The activity of SufS and SufE was measured using the methylene blue assay as previously described[5]. Reactions were conduct aerobically in 25mM Tris-HCl, pH 7.4, 150 mM NaCl at room temperature. 0.5 μM SufS and 2 μM SufE proteins were incubated with DCS (0 μM, 10 μM, 50 μM, 100 μM, 500 μM, 1000 μM, 2000 μM, 5000uM) or LCS (0 μM, 10 μM, 50 μM, 100 μM, 500 μM, 1000 μM, 2000 μM, 5000uM) in the buffer for 5 min before the addition of 2mM L-cysteine and 2mM DTT. The reaction volume was 800 uL. Reactions proceeded for 10 min and were quenched by 100 uL 20mM NNDP in 7.2 M HCl and 100 uL 30 mM $FeCl_3$ in 1.2 M HCl. The mixture was incubated in the dark for 30 min to produce methylene blue. Precipitated protein was removed by 1 min centrifugation at 13000 rpm and the methylene blue was measured at 670 nm. A Na_2S standard line was made for calibration of the content of sulfur product from this reaction.

Docking study of cycloserine into SufS

Flexible-ligand docking studies were done by AutoDock 4.2 program. All the pre-processing steps for the ligand DCS/LCS and the receptor SufS crystallographic files were performed within the AutoDock Tools 1.5.4 program (ADT). All hydrogens were added to the receptor PDB file by the ADT program. For docked ligands, non-polar hydrogens were added; Gasteiger charges assigned and torsions degrees of freedom were also allocated by ADT program. A grid of 60 x 60 x 60 points in x, y, and z direction was built centered at

the center of the active site of SufS. Cluster analysis was performed on the docking results using an RMS tolerance of 2 angstroms.

UV-visible secptroscopy of SufS-SufE inhibition by cycloserine

Ultraviolet-visible (UV-vis) spectra were measured by a BECKMAN COULTER DU 800 spectrophotometer. 25 μM SufS, 100 μM SufE and 5mM DCS or LCS were prepared at the concentration of 20 μM in 25 mM Tris-HCl, 150 mM NaCl, pH 8.0 buffer. 180 – 500 nm spectra were collected with a cuvette of 1 cm path length at time intervals from 0 min to 2 hours.

RESULTS

Inhibitory effects of DCS and LCS on the activity of SufS in the presence of SufE

The native activity of SufS alone is very low compared with its homologue IscS. The SufS and SufE complex reaches a comparable level of activity with IscS[5]. So we used SufS and SufE with a 1:4 ratio in the cysteine desulfurase assay to check its activity. The active site of SufS includes the PLP cofactor bound to the conserved Lys226. Inhibitors of PLP-dependent enzymes that bind with this cofactor have been used as irreversible inhibitors for the activity of the enzyme. DCS reacts with the PLP fold type 1 enzymes like aspartate aminotransferase family to inhibit their activities[18,20,21]. Since cysteine desulfurase like SufS also belongs to the PLP fold type 1 enzymes[22], DCS may act as an inhibitor to SufS. The effect of DCS on the desulfurase activity of SufS was investigated. DCS was incubated with SufS and SufE. There was a dose-dependent inhibition of SufS

activity by DCS (Figure 4.5). The 50% inhibitory concentration (IC_{50}) was calculated to be 1.98 mM. The inhibitory effect of DCS on the desulfurase activity of SufS is poor. To further investigate the inhibitory mechanism of cycloserine on SufS, we used LCS that is an enantiomer to DCS with a chiral symmetry. A dose-dependent inhibition of SufS by LCS was also observed and the IC_{50} was 306.1 μM (Figure 4.6). Compared with DCS, LCS shows much better inhibitory effects.

Small-molecular docking of cycloserine into SufS

Docking is a method to predict the preferred orientation of one molecule to another to form a stable complex. It is commonly used in the field of molecular modeling. Small-molecular docking is used to predict the binding conformation of small molecule ligands to the target binding site[23]. In this study, we docked both DCS and LCS into SufS to investigate the difference of their inhibitory effects on SufS. We first docked the substrate L-cysteine into the active site of SufS as a control (Figure 4.7). L-cysteine is stabilized by His123, Arg359, and Thr278 (from the other monomer) through hydrogen bond. The nitrogen of the L-cysteine is at a proper orientation towards the Schiff base between the PLP cofactor and the conserved Lys226, which facilitates the reaction of transimination. DCS is a cyclic analogue of cysteine. After it is docked into the active site of SufS, it is also stabilized by His123, Arg359, and Thr278 (Figure 4.8). However, the nitrogen of DCS to start the nucleophilic attack towards the Schiff base of the PLP and Lys226 is far away from its target, which is not a proper orientation for the transimination reaction. The transimination reaction between DCS and the internal aldimine is hard to happen. It may

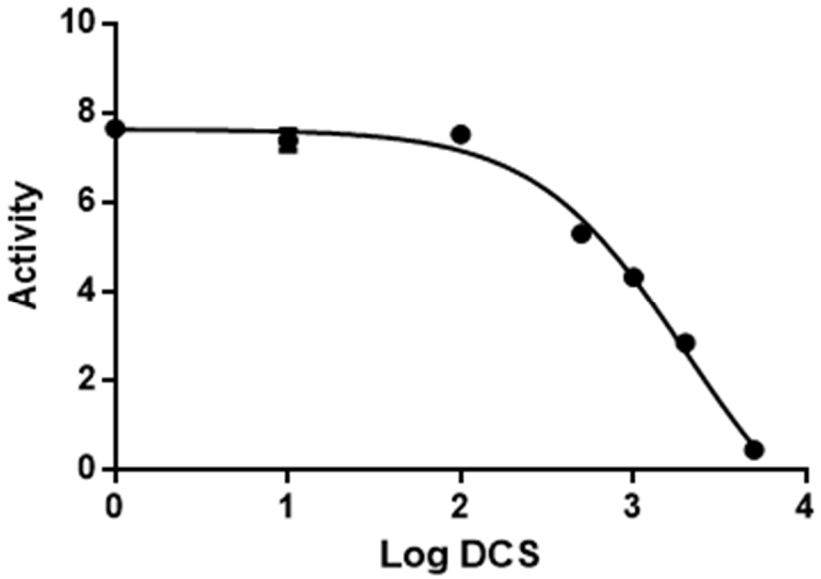

Fig. 4.5. Activity of 0.5 µM SufS and 2 µM SufE at various concentration of DCS.

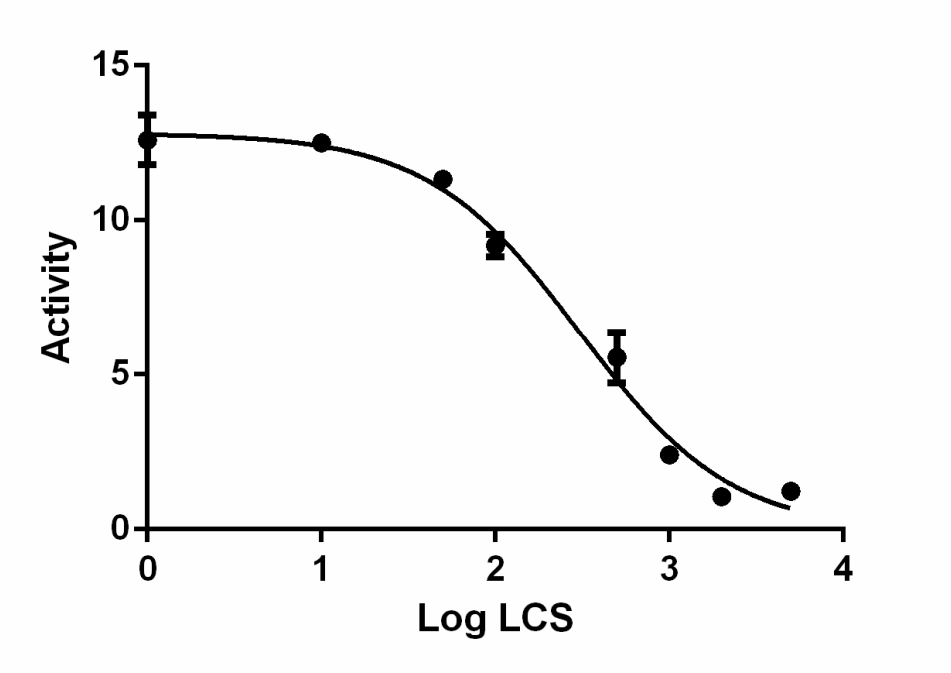

Figure 4.6. Activity of 0.5 µM SufS and 2 µM SufE at various concentration of LCS.

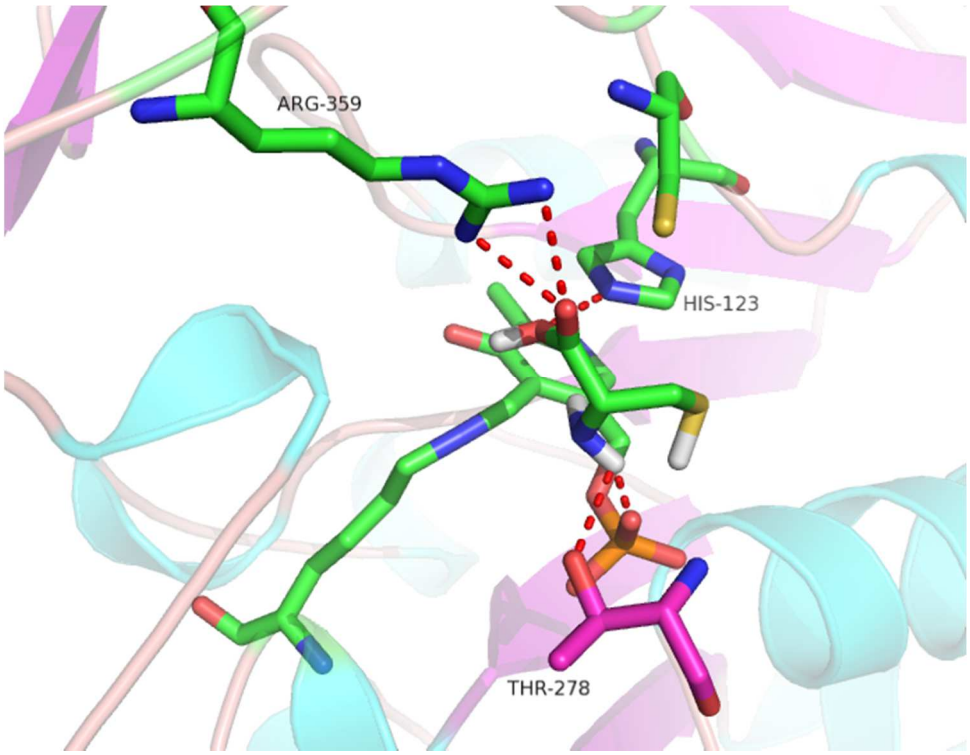

Figure 4.7. Docking model of L-cysteine as a substrate into the active site of SufS.

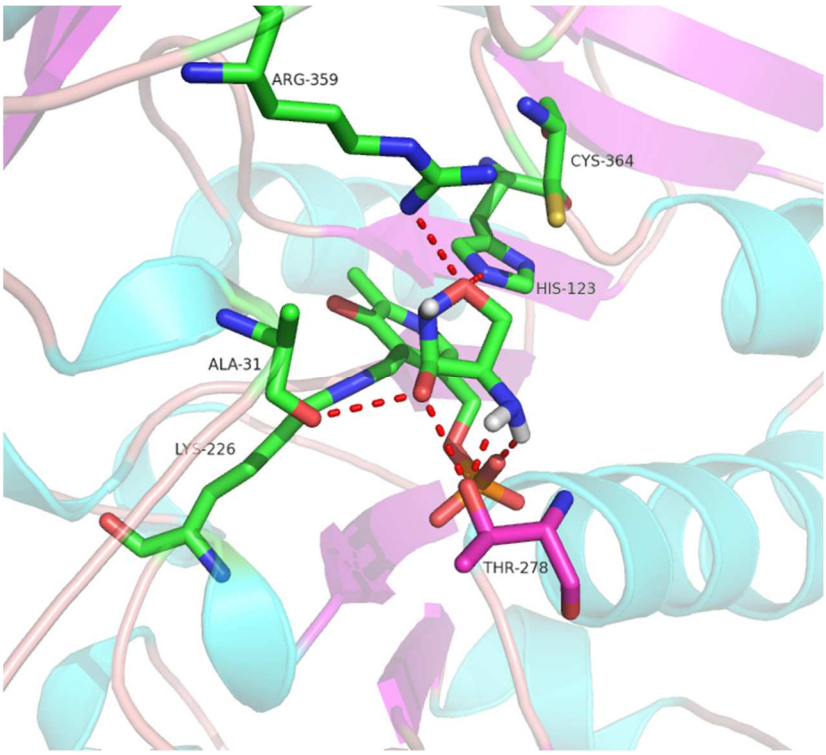

Figure 4.8. Docking model of DCS into the active site of SufS.

explain why the inhibitory effect of DCS on SufS is poor. LCS is an enantiomer to DCS and is chiral with DCS. The docking of LCS shows that the nitrogen of LCS for the nucleophilic attack is close to the Schiff base of Lys226 and PLP, which is a proper orientation for the following transimination reaction (Figure 4.9). It may explain why LCS shows a better inhibitory effect compared with DCS.

UV-vis spectroscopy analysis of DCS and LCS binding to SufS

The UV-visible spectrum of SufS displays absorbance maxima at 420 nm corresponding to the internal aldimine form of the PLP-bound enzyme. When DCS was added to SufS at pH 8.0 and 25 ˚C, notable changes in the 420 nm peak occurred (Figure 4.10), which suggests that DCS interacts with the PLP cofactor. Over a period of 1 hour, the internal aldimine peak (420 nm) was reduced to about 10% of its original value with simultaneous growth of a new peak at 380 nm. No new peak was observed when the sample was incubated for about 2 hours. It suggests that the PLP cofactor bound to the residue Lys226 as internal aldimine is replaced by one or more new species.

Significant changes in the PLP absorbance spectrum of SufS were also observed after the addition of LCS but the changes thereafter were much fast compared with DCS. The 420 nm peak went down to about 10% of its original value within 5 min (Figure 4.11), which indicates the internal aldimine reacts with LCS to get a new adduct. This spectroscopic change correlates with the observation that LCS has a much smaller IC_{50} compared with DCS because it is easier to conduct the tranimination reaction with the internal aldimine. Meanwhile, two new peaks, 380nm and 320 nm, are formed. Over time

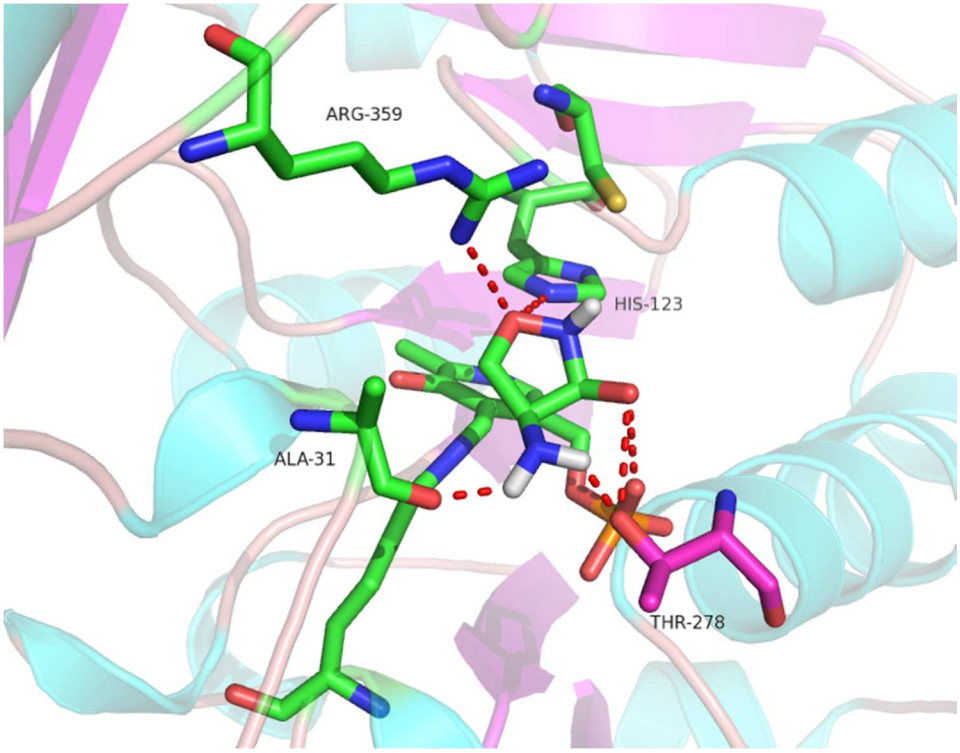

Figure 4.9 Docking model of LCS into the active site of SufS.

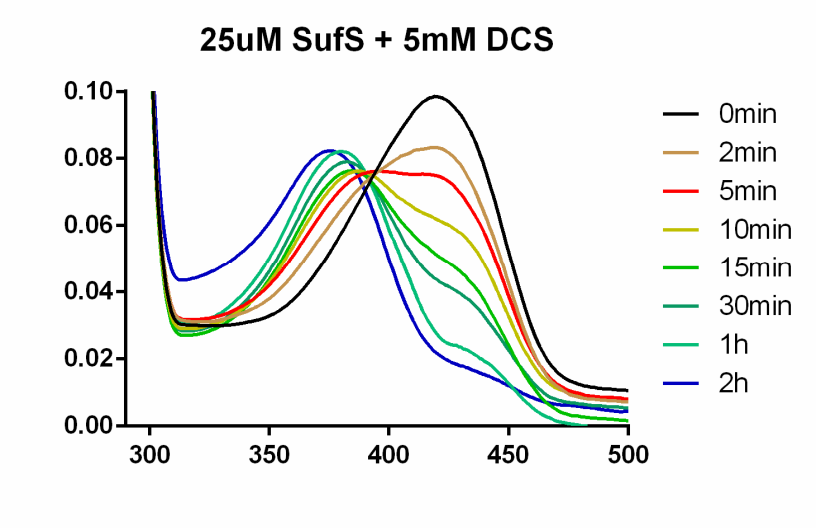

Figure 4.10. UV-visible spectra of addition of 5 mM DCS into 25 µM SufS at various time points.

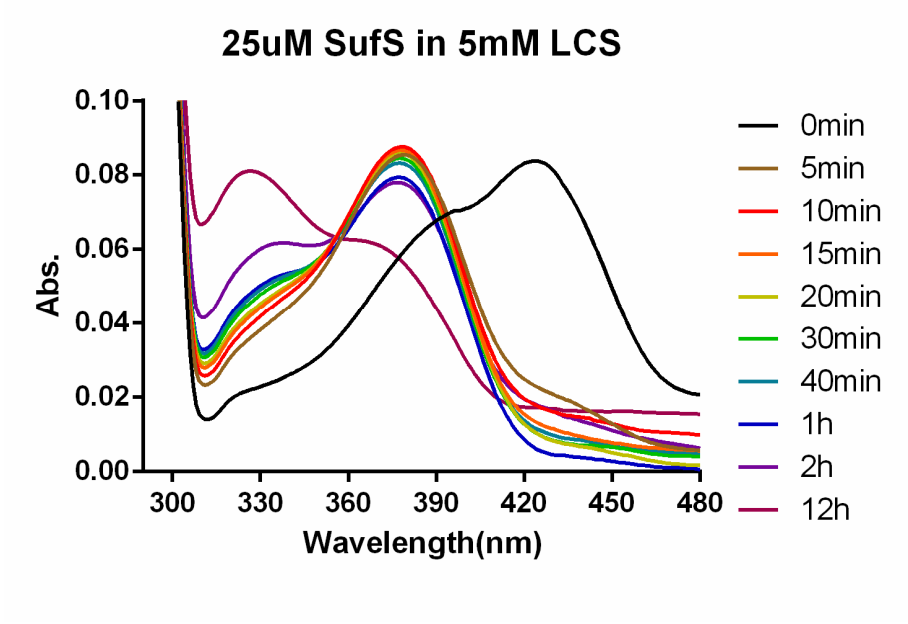

Figure 4.11. UV-visible spectra of addition of 5 mM LCS into 25 µM SufS at various time points.

(2 hours to 12 hours), the 380 nm peak is reduced but the 320 nm peak keeps growing. It indicates that the specie of the 380 nm peak may be an intermediate to reach a more stable adduct at 320 nm absorbance. The UV-vis spectra of SufS in the presence of DCS and LCS are very different to each other. In contrast, the spectra of free PLP in the presence of DCS and LCS are identical and display maxima at 360 nm[24]. Therefore, it is not simply a PLP-cycloserine aldimine formed in the enzyme. A new specie at 330 nm and a new intermediate at 380 nm are formed in the reaction between the cycloserine and the PLP cofactor of SufS.

L-cysteine can bind to the PLP cofactor to start a transimine reaction, which decreases the internal aldimine at 420 nm and increases the external aldimine at 340 nm (Figure 4.12). If the L-cysteine is excessive then the whole reaction is very fast. To test if L-cysteine can rescue the inhibition of cycloserine to SufS, we incubated SufS and cycloserine for 1 hour before we added L-cysteine. For DCS (Figure 4.13), The absorption peak at 380 nm degrades quickly and the absorptions at both 340 nm and 420 nm increased as the incubation time extends, which indicates that the intermediate at 380 nm formed by SufS and DCS is not stable and SufS can be rescued by L-cysteine. For LCS (Figure 4.14), the absorption peak at 380 nm peak decreases slowly and the absorptions at both 340 nm and 420 nm increased gradually. A shoulder at 320 nm increased with the 340 nm peak. The results indicate that L-cysteine can partially rescue the inhibition from LCS. However, even in the presence of L-cysteine, LCS can shift the reaction towards the production of a more stable adduct at 320 nm.

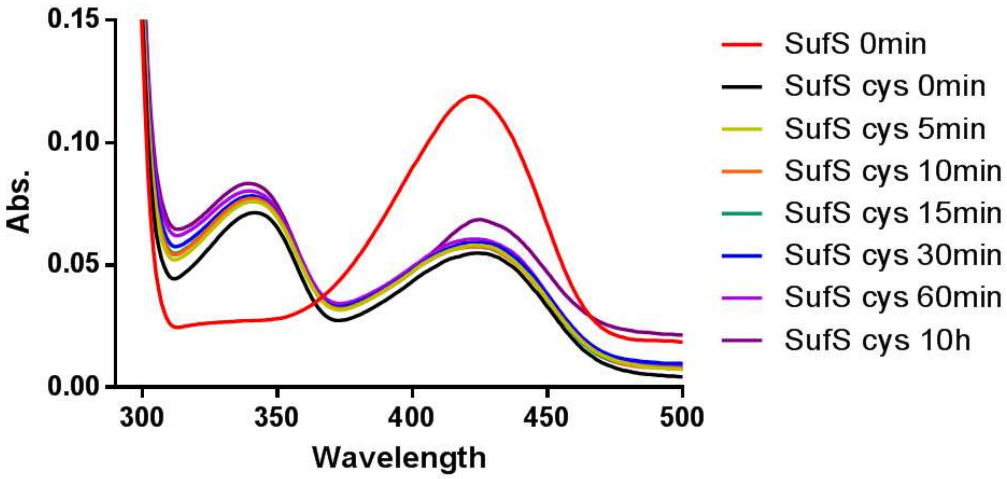

Figure. 4.12. UV-visible spectra of incubation of 25 μM SufS and 5 mM L-cysteine at various time points.

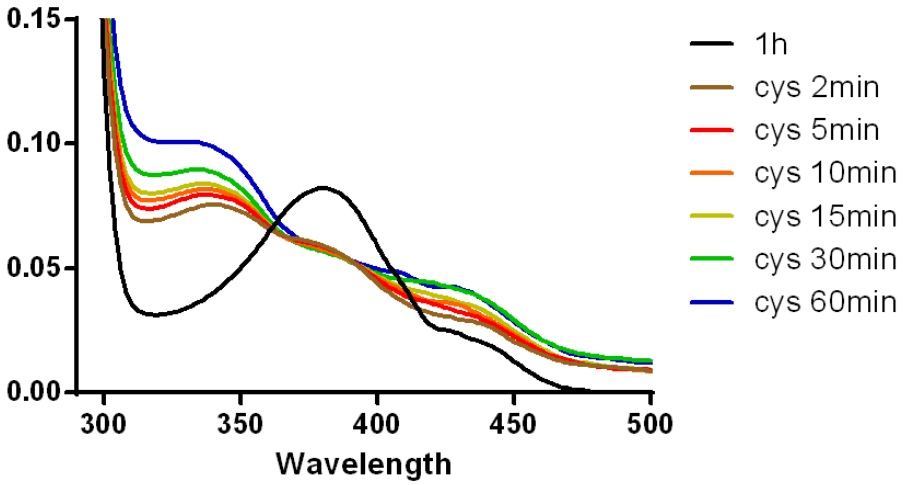

Figure 4.13. Change of UV-visible spectra at various time points after adding L-cysteine to SufS-DCS complex. We incubated 25 μM SufS and 5 mM DCS for 1 hour before we added 5 mM L-cysteine.

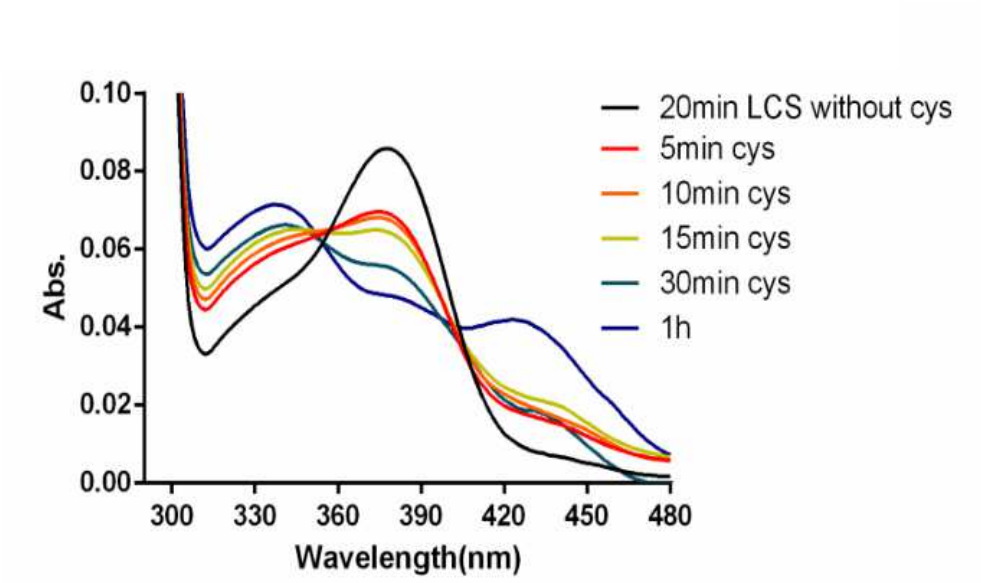

Figure 4.14. Change of UV-visible spectra at various time points after adding L-cysteine to SufS-DCS complex. We incubated 25 μM SufS and 5 mM DCS for 20 min before we added 5 mM L-cysteine.

DISCUSSION

Fe-S clusters are essential for the organism living because they are the key metal cofactors in the electron transfer, catalysis, sensing of reactive oxygen, and genetic regulation[2]. Suf pathway is used for the biosynthesis of Fe-S clusters under oxidative stress and iron limitation status[4]. Suf pathway is a good target for novel antibiotic design due to its necessity and specificity in bacteria[25]. SufS and SufE are the beginning of Suf pathway to extract sulfur from L-cysteine as a sulfur source for the subsequent Fe-S cluster formation. SufS owns a PLP cofactor in its active site which is essential for the cysteine desulfurase reaction[12]. In this study, we applied PLP inhibitor DCS and its enantiomer LCS to the desulfurase reaction of SufS to investigate the inhibitory effects and mechanism of cycloserine on SufS. The results show that both DCS and LCS inhibit the activity of SufS in the presence of SufE and LCS has a better inhibitory effect than DCS. The small-molecular docking study of DCS and LCS into SufS shows LCS exhibits a better orientation towards the Schiff base of the PLP in the rest enzyme, which facilitates the transimination reaction. The UV-vis spectroscopic analysis shows that new species at 380 nm and330 nm are formed after the incubation of DCS/LCS with SufS. The inhibition of SufS by DCS and LCS provides evidence for the possibility of inhibitors targeting the PLP of this important enzyme of Fe-S cluster biosynthesis. The further research on the inhibitory mechanism can be helpful to the design of more potent inhibitors against the PLP of this type of enzymes.

The kinetics of inactivation of DCS and LCS are quite different. DCS inactivates alanine racemase faster than LCS does, which makes it a better antibiotic (seromycine) in the therapy of tuberculosis[14]. In the inhibition of serine palmitoyltransferase, the IC_{50} of

LCS is much lower than that of DCS[24]. Our study shows that LCS is a better inhibitor than DCS in the cysteine desulfurase SufS in *E. coli*. However, in the inhibitory study of pSufS in Plasmodium falciparum, the IC_{50} of DCS to pSufS is 29 μM[16], which is much lower than the IC_{50} of DCS from SufS in *E. coli* (1.98 mM). The chiral symmetry between DCS and LCS may account for the difference of the inactivation kinetics. The orientation of the nitrogen of cycloserine towards the Schiff base of PLP in the resting enzyme determines its inhibitory potential. After cycloserine binds to the active site of the enzyme, if the nitrogen from cycloserine is close enough to the Schiff base of the enzyme PLP for a nucleophilic attack, it is a good orientation for inhibition. Otherwise, the inhibitory effect is poor. We already used small-molecular docking of DCS/LCS into SufS to prove that LCS shows a better orientation towards the Schiff base of the PLP cofactor, which supports this explanation.

As a commonly used PLP inhibitor, a number of mechanisms of the cysloserine inhibition of PLP-dependent enzymes have been proposed[26]. One of a generally accepted mechanism is called “aromatization mechanism”. The incubation of cycloserine and PLP-dependent enzyme results in a transimination reaction that leads to a cycloserine-PLP external aldimine. This external aldimine is not stable. After deprotonation, a stable 3-hydroxyisoxazole-PMP adduct is formed and the cycloserine ring remains intact and covalently linked to the PLP cofactor. This stable adduct contributes to the irreversible inhibition of cycloserine to the PLP-dependent enzyme. This mechanism is called “aromatization mechanism”. In our UV-vis spectra of SufS and DCS/LCS, the specie at 380 nm is formed at first. In the case of DCS, the 380 nm peak is formed slowly after the internal aldimine (420 nm) is degraded and no further shift is observed. However, in the

case of LCS, the 380 nm peak is formed quickly and shift to 320 nm. Based on the UV-vis spectroscopic analysis, an inactivation mechanism of DCS/LCS against SufS is proposed (Figure 4.15). The specie at 380 nm is cycloserine-PLP external aldimine and the specie at 320 nm is 3-hydroxyisoxazole-PMP. The shift from 380 nm to 320 nm is caused by deprotonation. However, we did not observe the 320 nm peak in the DCS within 2 hours. The reason for that may be more time is needed for the formation of the final stable adduct because DCS is not in a good orientation for the transimination reaction. Further mass spec and crystallography are needed to identify the species at 380 nm and 330 nm in order to test this proposed mechanism.

The ultimate goal of the research on the inhibitor against SufS is to develop the design of a new class of antibiotics. The weakness of cycloserine as an inhibitor to the enzyme is its poor specificity. There are a variety of PLP inhibitors based on various mechanisms, some of which are very effective. However, the major challenge for PLP inhibitors is the specificity when they are used in vivo. Because PLP based enzymes are very common in the human body and are principally involved in cellular metabolism, the PLP inhibitor may disrupt the normal human cellular function while inhibiting the activity of SufS. To solve the problem of specificity of the traditional PLP based inhibitors, protein-protein interactions (PPI) are new targets for inhibitor design[27]. This strategy has been used successfully to discover small molecular inhibitors of protein complexes such as Il-2/IL-2 receptor[28], LFA1/ICAM[29], and P53/MDM2[30]. Our future direction is: first, we will observe the growth of *E. coli* in the presence of DCS/LCS to investigate their inhibitory effect in vivo; second, we will investigate the PPI inhibitors that can inhibit SufS specifically.

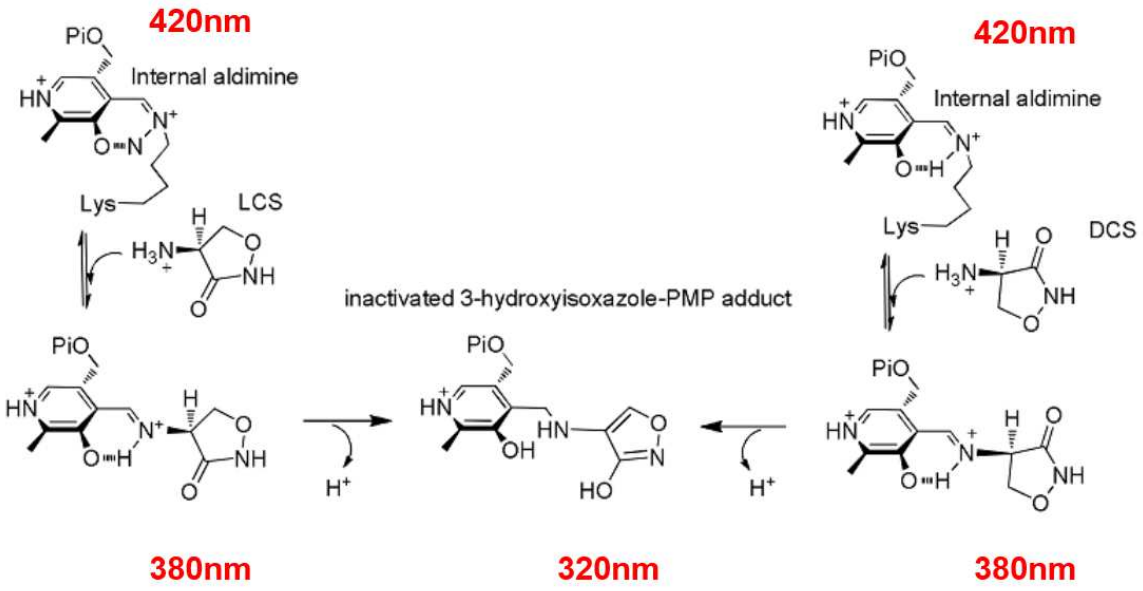

Figure 4.15. Proposed mechanism of inhibition of DCS/LCS against SufS.

The inhibition study reports for the first time that cysloserine DCS/LCS can inhibit the activity of SufS in the presence of SufE. Small-molecular docking study and UV-vis spectroscopic analysis are used to investigate the difference of the inhibitory effects from DCS and LCS. A possible inactivation mechanism is proposed. However, further work will be required to identify the species at 380 nm and 330 nm in order to confirm this mechanism.

REFERENCE

1. Roche B, Aussel L, Ezraty B, Mandin P, Py B, Barras F., Biochim. Biophys. Acta., 2013, 1827 (3), 455-469.

2. Ayala-Castro C, Saini A, Outten FW, Microbiol Mol Biol Rev., 2008, 72 (1), 110-125.

3. Huet G, Daffe M, Saves I, J. Bacteriol., 2005, 187 (17), 6137-6146.

4. F.W. Outten, O. Djaman, G. Storz, Mol. Microbiol., 2004, 52, 861–872.

5. Dai Y, Outten FW, FEBS Lett., 2012 586 (22), 4016-4022.

6. Runyen-Janecky L, Daugherty A, Lloyd B, Wellington C, Eskandarian H, Sagransky M, Infect. Immun., 2008, 76 (3), 1083-92.

7. Layer G, Gaddam SA, Ayala-Castro CN, Ollagnier-de Choudens S, Lascoux D, Fontecave M, Outten FW, J Biol Chem., 2007, 282, 13342-13350.

8. Boyd ES, Thomas KM, Dai Y, Boyd JM, Outten FW, Biochemistry, 2014, 53 (37), 5834-5847.

9. Katherine A. Black, Patricia C. Dos Santos, Biochimica et Biophysica Acta, 2015, 1853, 1470-1480.

10. Fujii, T., Maeda, M., Mihara, H., Kurihara, T., Esaki, N., Hata, Y., Biochemistry, 2000, 39, 1263-1273.

11. Limin Zheng, Robert H. White, Valerie L. Cash, and Dennis R. Dean, Biochemistry, 1994, 33, 4714-4720.

12. Mihara, H., Fujii, T., Kato, S., Kurihara, T., Hata, Y., Esaki, N., J.BIOCHEM.(TOKYO), 2002, 131, 679-685

13. Scoper TS, Manning JM, J Biol Chem., 1981, 10, 256 (9), 4263-4268.

14. Fenn TD, Stamper GF, Morollo AA, Ringe D, Biochemistry, 2003, 42 (19), 5775-5783.

15. Malashkevich VN, Strop P, Keller JW, Jansonius JN, Toney MD, J Mol Biol., 1999, 294 (1), 193-200.

16. Charan M, Singh N, Kumar B, Srivastava K, Siddiqi MI, Habib S, Antimicrob Agents Chemother, 2014, 58 (6): 3389-3398.

17. Marie-Louise Svensson, Sten Gatenbeck, Arch. Microbiol., 1982, 131, 129-131.

18. Di Perri G, Bonora S, J Antimicrob Chemother., 2004, 54 (3), 593-602.

19. Jack L. Strominger, Eiji Ito, Robert H. Threnn, J Am Chem Soc, 1960, 82 (4), 998-999.

20. Sheinin A, Shavit S, Benveniste M, Neuropharmacology, 2001, 41 (2), 151-158.

21. Eliot AC, Kirsch JF, Annu. Rev. Biochem., 2004, 73, 383-415.

22. El-Sayed AS, Shindia AA. 2011. PLP-dependent enzymes: a potent therapeutic approach for cancer and cardiovascular diseases, chapter 7. In YouY(ed), Targets in gene therapy. InTech, Rijeka, Croatia.

23. Lengauer T, Rarey M, 1996, 6 (3), 402–406.

24. Lowther J, Yard BA, Johnson KA, Carter LG, Bhat VT, Raman MC, Clarke DJ, Ramakers B, McMahon SA, Naismith JH, Campopiano DJ, Mol Biosyst., 2010, 6 (9), 1682-1693.

25. Outten FW, Biochim Biophys Acta, 2015, 1853 (6), 1464-1469.

26. Gregory T. Olson, Mengmeng Fu, Sharon Lau, Kenneth L. Rinehart, and Richard B. Silverman, J. Am. Chem. Soc., 1998, 120 (10), 2256-2267.

27. Arkin ME, Wells JA, Nat Rev Drug Discov Sci., 2004, 3:301–317.

28. Emerson SD, Palermo R, Liu CM, Tilley JW, Chen L, Danho W, Madison VS, Greeley DN, Ju G, Fry DC, Protein Sci., 2003, 12, 811–822.

29. Gadek TR, Burdick DJ, McDowell RS, Stanley MS, Marsters JC Jr, Paris KJ, Oare DA, Reynolds ME, Ladner C, Zioncheck KA, Lee WP, Gribling P, Dennis MS, Skelton NJ, Tumas DB, Clark KR, Keating SM, Beresini MH, Tilley JW, Presta LG, Bodary SC, Science, 2002, 295:1086–1089.

30. Vassilev LT, Vu BT, Graves B, Carvajal D, Podlaski F, Filipovic Z, Kong N, Kammlott U, Lukacs C, Klein C, Fotouhi N, Liu EA, Science, 2004, 303, 844–848.

REFERENCE

E. M. Shepard, E. S. Boyd, J. B. Broderick and J. W. Peters, Curr. Opin. Chem. Biol., 2011, 15: 319-327.

Y. Hu and M. W. Ribbe, Angew. Chem. Int. Ed. Engl., 2016, 55, 8216-8226.

Y. Hu and M. W. Ribbe, Annu. Rev. Biochem., 2016, 85, 455-483.

D. H. Flint, J. F. Tuminello and M. H. Emptage, J. Biol. Chem., 1993, 268, 22369-22376.

P. R. Gardner and I. Fridovich, J. Biol. Chem., 1991, 266, 19328-19333.

P. R. Gardner and I. Fridovich, J. Biol. Chem., 1991, 266, 1478-1483.

L. Macomber and J. A. Imlay, Proc. Natl. Acad. Sci. U. S. A., 2009, 106, 8344-8349.

C. Ranquet, S. Ollagnier de Choudens, L. Loiseau, F. Barras and M. Fontecave, J. Biol. Chem., 2007, 282, 30442-30451.

F. F. Xu and J. A. Imlay, Appl. Environ. Microbiol., 2012, 78, 3614-3621.

E. S. Boyd, K. M. Thomas, Y. Dai, J. M. Boyd and F. W. Outten, Biochemistry, 2014, 53, 5834-5847.

Y. Takahashi and U. Tokumoto, J. Biol. Chem., 2002, 277, 28380-28383.

B. Roche, L. Aussel, B. Ezraty, P. Mandin, B. Py and F. Barras, Biochim. Biophys. Acta, 2013, 1827, 455-469.

S. I. Patzer and K. Hantke, J. Bacteriol., 1999, 181, 3307-3309.

M. Zheng, X. Wang, L. J. Templeton, D. R. Smulski, R. A. LaRossa and G. Storz, J. Bacteriol., 2001, 183, 4562-4570.

S. Jang and J. A. Imlay, Mol. Microbiol., 2010, 78, 1448-1467.

J. H. Lee, W. S. Yeo and J. H. Roe, Mol. Microbiol., 2004, 51, 1745-1755.

L. Nachin, M. El Hassouni, L. Loiseau, D. Expert and F. Barras, Mol. Microbiol., 2001, 39, 960-972.

L. Nachin, L. Loiseau, D. Expert and F. Barras, EMBO J., 2003, 22, 427-437.

F. W. Outten, O. Djaman and G. Storz, Mol. Microbiol., 2004, 52, 861-872.

U. Tokumoto, S. Kitamura, K. Fukuyama and Y. Takahashi, J. Biochem., 2004, 136, 199-209.

L. Loiseau, C. Gerez, M. Bekker, S. Ollagnier-de Choudens, B. Py, Y. Sanakis, J. Teixeira de Mattos, M. Fontecave, et al., Proc. Natl. Acad. Sci. U. S. A., 2007, 104, 13626-13631.

K. C. Lee, W. S. Yeo and J. H. Roe, J. Bacteriol., 2008, 190, 8244-8247.

C. J. Schwartz, J. L. Giel, T. Patschkowski, C. Luther, F. J. Ruzicka, H. Beinert and P. J. Kiley, Proc. Natl. Acad. Sci. U. S. A., 2001, 98, 14895-14900.

J. L. Giel, D. Rodionov, M. Liu, F. R. Blattner and P. J. Kiley, Mol. Microbiol., 2006, 60, 1058-1075.

W. S. Yeo, J. H. Lee, K. C. Lee and J. H. Roe, Mol. Microbiol., 2006, 61, 206-218.

A. D. Nesbit, J. L. Giel, J. C. Rose and P. J. Kiley, J. Mol. Biol., 2009, 387, 28-41.

J. L. Giel, A. D. Nesbit, E. L. Mettert, A. S. Fleischhacker, B. T. Wanta and P. J. Kiley, Mol. Microbiol., 2013, 87, 478-492.

S. Rajagopalan, S. J. Teter, P. H. Zwart, R. G. Brennan, K. J. Phillips and P. J. Kiley, Nat. Struct. Mol. Biol., 2013, 20, 740-747.

E. Masse and S. Gottesman, Proc. Natl. Acad. Sci. U. S. A., 2002, 99, 4620-4625.

E. Masse, C. K. Vanderpool and S. Gottesman, J. Bacteriol., 2005, 187, 6962-6971.

G. Desnoyers, A. Morissette, K. Prevost and E. Masse, EMBO J., 2009, 28, 1551-1561.

F. Barras and M. Fontecave, Metallomics, 2011, 3, 1130-1134.

L. Loiseau, S. Ollagnier-de-Choudens, L. Nachin, M. Fontecave and F. Barras, J. Biol. Chem., 2003, 278, 38352-38359.

H. Mihara, M. Maeda, T. Fujii, T. Kurihara, Y. Hata and N. Esaki, J. Biol. Chem., 1999, 274, 14768-14772.

C. J. Schwartz, O. Djaman, J. A. Imlay and P. J. Kiley, Proc. Natl. Acad. Sci. U. S. A., 2000, 97, 9009-9014.

L. Zheng, R. H. White, V. L. Cash and D. R. Dean, Biochemistry, 1994, 33, 4714-4720.

L. Zheng, R. H. White, V. L. Cash, R. F. Jack and D. R. Dean, Proc. Natl. Acad. Sci. U. S. A., 1993, 90, 2754-2758.

H. Mihara and N. Esaki, Appl. Microbiol. Biotechnol., 2002, 60, 12-23.

T. Fujii, M. Maeda, H. Mihara, T. Kurihara, N. Esaki and Y. Hata, Biochemistry, 2000, 39, 1263-1273.

C. D. Lima, J. Mol. Biol., 2002, 315, 1199-1208.

H. Mihara, T. Fujii, S. Kato, T. Kurihara, Y. Hata and N. Esaki, J. Biochem., 2002, 131, 679-685.

J. R. Cupp-Vickery, H. Urbina and L. E. Vickery, J. Mol. Biol., 2003, 330, 1049-1059.

R. Shi, A. Proteau, M. Villarroya, I. Moukadiri, L. Zhang, J. F. Trempe, A. Matte, M. E. Armengod, et al., PLoS Biol., 2010, 8, e1000354.

H. D. Urbina, J. R. Cupp-Vickery and L. E. Vickery, Acta Crystallogr. D Biol. Crystallogr., 2002, 58, 1224-1225.

S. Ollagnier-de-Choudens, D. Lascoux, L. Loiseau, F. Barras, E. Forest and M. Fontecave, FEBS Lett., 2003, 555, 263-267.

F. W. Outten, M. J. Wood, F. M. Munoz and G. Storz, J. Biol. Chem., 2003, 278, 45713-45719.

B. P. Selbach, P. K. Pradhan and P. C. Dos Santos, Biochemistry, 2013, 52, 4089-4096.

Y. Dai, D. Kim, G. Dong, L. S. Busenlehner, P. A. Frantom and F. W. Outten, Biochemistry, 2015, 54, 4824-4833.

S. Goldsmith-Fischman, A. Kuzin, W. C. Edstrom, J. Benach, R. Shastry, R. Xiao, T. B. Acton, B. Honig, et al., J. Mol. Biol., 2004, 344, 549-565.

Y. Dai and F. W. Outten, FEBS Lett., 2012, 586, 4016-4022.

H. Singh, Y. Dai, F. W. Outten and L. S. Busenlehner, J. Biol. Chem., 2013, 288, 36189-36200.

S. Kim and S. Park, J. Biol. Chem., 2013, 288, 27172-27180.

G. Layer, S. A. Gaddam, C. N. Ayala-Castro, S. Ollagnier-de Choudens, D. Lascoux, M. Fontecave and F. W. Outten, J. Biol. Chem., 2007, 282, 13342-13350.

H. K. Chahal, Y. Dai, A. Saini, C. Ayala-Castro and F. W. Outten, Biochemistry, 2009, 48, 10644-10653.

A. Saini, D. T. Mapolelo, H. K. Chahal, M. K. Johnson and F. W. Outten, Biochemistry, 2010, 49, 9402-9412.

S. Wollers, G. Layer, R. Garcia-Serres, L. Signor, M. Clemancey, J. M. Latour, M. Fontecave and S. Ollagnier de Choudens, J. Biol. Chem., 2010, 285, 23331-23341.

J. N. Agar, C. Krebs, J. Frazzon, B. H. Huynh, D. R. Dean and M. K. Johnson, Biochemistry, 2000, 39, 7856-7862.

B. Blanc, M. Clemancey, J. M. Latour, M. Fontecave and S. Ollagnier de Choudens, Biochemistry, 2014, 53, 7867-7869.

K. Rangachari, C. T. Davis, J. F. Eccleston, E. M. Hirst, J. W. Saldanha, M. Strath and R. J. Wilson, FEBS Lett., 2002, 514, 225-228.

S. Watanabe, A. Kita and K. Miki, J. Mol. Biol., 2005, 353, 1043-1054.

S. Kitaoka, K. Wada, Y. Hasegawa, Y. Minami, K. Fukuyama and Y. Takahashi, FEBS Lett., 2006, 580, 137-143.

J. F. Eccleston, A. Petrovic, C. T. Davis, K. Rangachari and R. J. Wilson, J. Biol. Chem., 2006, 281, 8371-8378.

A. Petrovic, C. T. Davis, K. Rangachari, B. Clough, R. J. Wilson and J. F. Eccleston, Protein Sci., 2008, 17, 1264-1274.

K. Wada, N. Sumi, R. Nagai, K. Iwasaki, T. Sato, K. Suzuki, Y. Hasegawa, S. Kitaoka, et al., J. Mol. Biol., 2009, 387, 245-258.

K. Hirabayashi, E. Yuda, N. Tanaka, S. Katayama, K. Iwasaki, T. Matsumoto, G. Kurisu, F. W. Outten, et al., J. Biol. Chem., 2015, 290, 29717-29731.

H. K. Chahal and F. W. Outten, J. Inorg. Biochem., 2012, 116, 126-134.

S. Ollagnier-de Choudens, L. Nachin, Y. Sanakis, L. Loiseau, F. Barras and M. Fontecave, J. Biol. Chem., 2003, 278, 17993-18001.

S. Ollagnier-de-Choudens, Y. Sanakis and M. Fontecave, J. Biol. Inorg. Chem., 2004, 9, 828-838.

K. Wada, Y. Hasegawa, Z. Gong, Y. Minami, K. Fukuyama and Y. Takahashi, FEBS Lett., 2005, 579, 6543-6548.

J. Lu, J. Yang, G. Tan and H. Ding, Biochem. J., 2008, 409, 535-543.

V. Gupta, M. Sendra, S. G. Naik, H. K. Chahal, B. H. Huynh, F. W. Outten, M. Fontecave and S. Ollagnier de Choudens, J. Am. Chem. Soc., 2009, 131, 6149-6153.

G. Tan, J. Lu, J. P. Bitoun, H. Huang and H. Ding, Biochem. J., 2009, 420, 463-472.

D. Vinella, C. Brochier-Armanet, L. Loiseau, E. Talla and F. Barras, Plos Genetics, 2009, 5, e1000497.

D. T. Mapolelo, B. Zhang, S. G. Naik, B. H. Huynh and M. K. Johnson, Biochemistry, 2012, 51, 8071-8084.

B. Ding, E. S. Smith and H. Ding, Biochem. J., 2005, 389, 797-802.

H. Ding and R. J. Clark, Biochem. J., 2004, 379, 433-440.

H. Ding, R. J. Clark and B. Ding, J. Biol. Chem., 2004, 279, 37499-37504.

H. Ding, K. Harrison and J. Lu, J. Biol. Chem., 2005, 280, 30432-30437.

H. Ding, J. Yang, L. C. Coleman and S. Yeung, J. Biol. Chem., 2007, 282, 7997-8004.

D. T. Mapolelo, B. Zhang, S. G. Naik, B. H. Huynh and M. K. Johnson, Biochemistry, 2012, 51, 8056-8070.

J. Yang, G. Tan, T. Zhang, R. H. White, J. Lu and H. Ding, J. Biol. Chem., 2015, 290, 14226-14234.

APPENDIX A – SUPPLEMENTAL EXPERIMENTS AND RESULTS

Oxidative resistance of SufE_D74R in vivo

The interaction of SufS and SufE causes conformational change of the loop containing the active site Cys51 in SufE. It has been proved by our former HDX/MS experiment. According to the crystal structure of CsdA-CsdE complex that is homologue to SufS-SufE, this active site Cys loop may extend from its hydrophobic pocket to the active site loop of SufS. Asp74 of SufE is located close to this loop and forms a hydrogen bond with Gln54, which may stabilize the loop orientation of the active site Cys51 at the resting state. We mutated Asp74 to Arg to break this hydrogen bond. The result shows a better affinity of SufE_D74R to SufS. The interaction of SufS and SufE shows oxidative resistance. To check if SufE_D74R still keeps this ability, we constructed MG1655 Δ*sufE*. The plasmid *pET21a* containing sufE_D74R was transformed into this strain. The final optical density at 600 nm (growth) of MG1655 Δ*sufE* and MG1655 Δ*sufE*/*pET21a_sufD74R* was measured after 20 hours in M9 gluconate minimal media with increasing concentrations of phenazine methosulfate (a generator of oxidative stress) (Figure A1). MG1655 Δ*sufE*/*pET21a_sufE* was added into this experiment as a control. A second control is the MG1655 Δ*sufE* strain containing the empty plasmid *pET21a*. The results show that SufE D74R still keeps the ability of oxidative resistance in vivo.

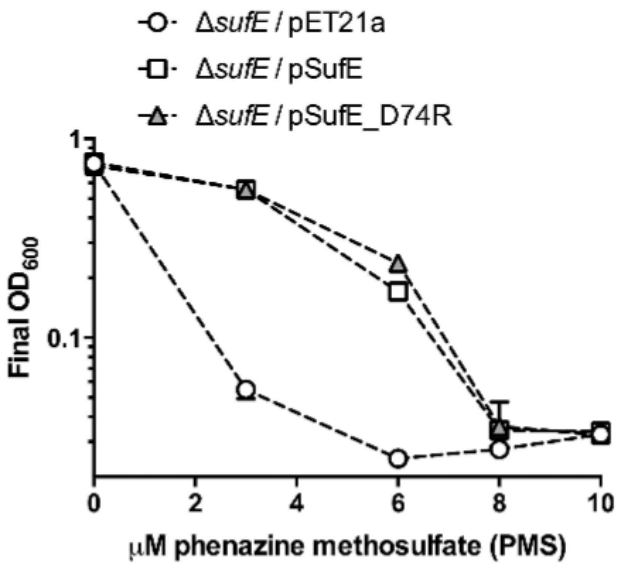

Figure A.1. Growth experiment of MG1655 Δ*sufE*/*pET21a_sufE_D74R* in the presence of oxidative stress.

Sulfur transfer from SufE to SufB

The active site Cys51 of SufE accepts the sulfide from the active site Cys364 of SufE to become a persulfide, which is subsequently transferred to the SufB that is the Fe-S cluster scaffold protein. This transfer of persulfide recycles SufE to participate in another reaction cycle with SufS. So $SufBC_2D$ further enhances the activity of the sulfur mobilization of the SufS-SufE complex. However, the interaction between SufE and SufB is not well characterized at the structural level. To address this question, we alkylated $SufBC_2D$ with iodoacetamide (IAA) to covalently block the solvent accessible free thiols on the surface that may accept persulfide from SufE. After IAA treatment, 13 of the 18 total thiols were alkylated and did not react with DTNB (Figure A2). The alkylated $SufBC_2D$ cannot enhance the activity of SufS and SufE (Figure A3). The alkylated $SufBC_2D$ cannot form Fe-S clusters when it incubated with SufS, SufE, and L-cysteine (Figure A4). When we added Na_2S as the sulfur source, Fe-S clusters were formed (Figure A5).

Among the 13 thiols alkylated by IAA, MS/MS analysis revealed that 9 Cys from SufB, 1 Cys from SufD, and 2 Cys from the SufC dimer. The 5 cys residues protected from the alkylation based on the DTNB analysis and MS/MS are Cys332, Cys405, Cys414 from SufB and Cys295, Cys358 from SufD (Figure A6). We hypothesized that the Cys inside SufB may transfer sulfur from the surface to the location of Fe-S cluster formation. So we mutated both Cys405 and Cys414 to Ala ($SufBC_2D$ C405A/C414A) and checked if the mutant $SufBC_2D$ can still enhance the activity of SufS-SufE (Figure A7). The result shows that this mutant $SufBC_2D$ can still enhance the activity of SufS-SufE. There are two

SufBC$_2$D treatment	Cys detected by DTNB	Total Cys
Unmodified Folded	13.1 ± 0.8	18
Unmodified Denatured	18 ± 0.7	18
Alkylated Folded	0.7 ± 0.2	18
Alkylated Denatured	4.9 ± 0.1	18

Figure A.2. DTNB-detectable thiols in IAA-modified or unmodified SufBC$_2$D measured under native or denaturing conditions. DTNB is a reagent that reacts with thiol group to yield a colored product, providing a reliable method to measure the number of the reductive Cys residues in protein.

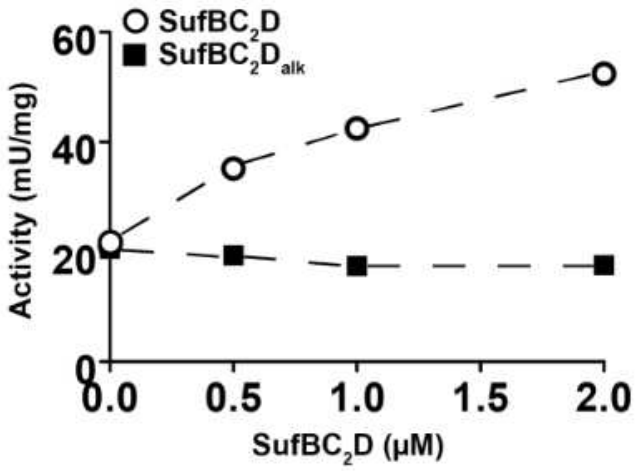

Figure A.3. Enhancement of SufS-SufE cysteine desulfurase activity with $SufBC_2D$ (○) or $SufBC_2D_{alk}$ (■).

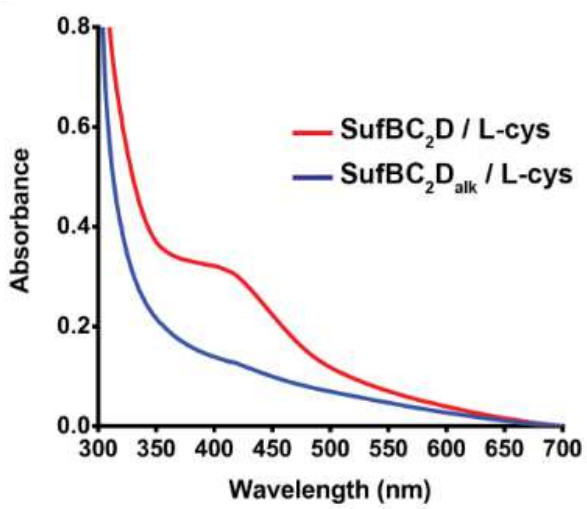

Figure A.4. Fe-S cluster reconstitution on $SufBC_2D$ (**red line**) or $SufBC_2D_{alk}$ (**blue line**) using SufS-SufE-L-cysteine as sulfur source.

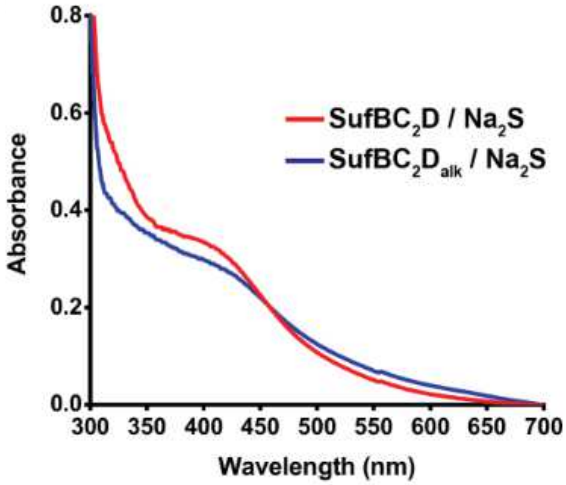

Figure A.5. Fe-S cluster reconstitution on $SufBC_2D$ (**red line**) or $SufBC_2D_{alk}$ (**blue line**) using Na_2S as sulfur donors.

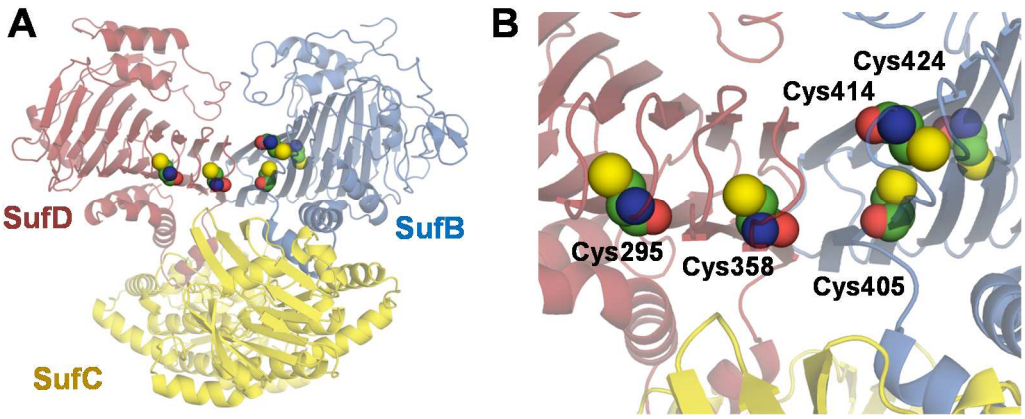

Figure A.6. Unalkylated Cys residues in $SufBC_2D$. (A) Cys residues that were *resistant* to IAA modification identified by MS and MS/MS are mapped on the $SufBC_2D$ structural model in space filling. (B) Close up view of the SufB–SufD interface where several of these protected cysteines are localized.

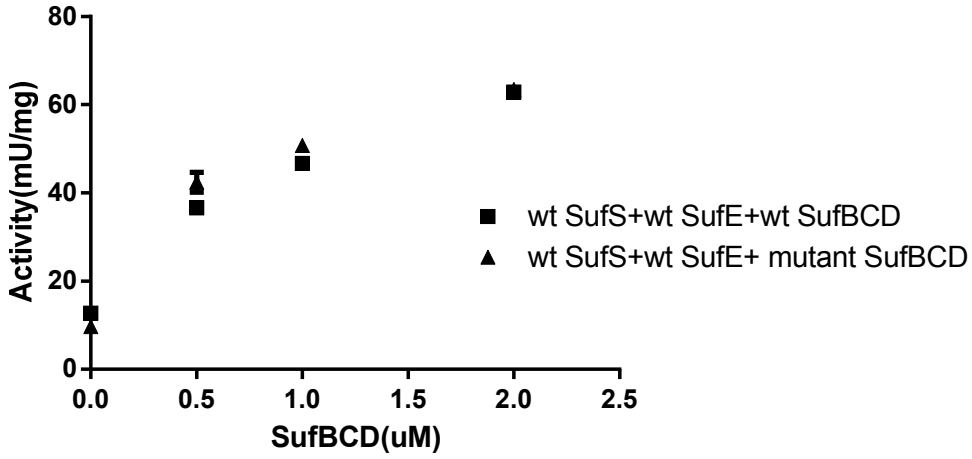

Figure A.7. Desulfurase activity of SufS and SufE in function of $SufBC_2D$. The mutant $SufBC_2D$ is $SufBC_2D$ C405A/C414A.

possible explanations. The first is that Cys405 and Cys414 are not relative to sulfur transfer. The second is that the surface Cys of this mutant SufBC2D still accepts sulfur from SufE, which enhance the desulfurase activity. Further experiments are needed to clarify the role of Cys405 and Cys414 in the formation of Fe-S cluster.

Desulfurase activity of SufS-SufE in low/high activity SufBC$_2$D

We found that SufBC2D can be divided into low activity and high activity according to the difference of its ATPase activity. We incubated SufS, SufE, and either low activity SufBC$_2$D or high activity SufBC$_2$D before we checked the desulfurase activity (Figure A8). The result showed both low and high activity SufBC$_2$D can enhance the desulfurase activity of SufS-SufE. However, the low activity SufBC$_2$D shows better enhancement than that of the high activity SufBC$_2$D. The meaning of low/high ATPase activity of SufBC$_2$D is still under research.

Influence of pH to the desulfurase activity of SufS-SufE

To detect the influence of pH to the desulfurase activity of SufS-SufE, we checked the activity of 0.5 uM SufS and 2uM SufE under various pH of the buffer (Figure A9). The result shows that the activity of SufS-SufE increases following the increasing of pH. The protein collapses under pH 10. In the reaction mechanism, there are two steps that needs deprotonation. The first step is that external aldimine loses a proton to become a quinonoid intermediate. The second step of deprotonation is that the active site Cys364 loses a proton

to accept the sulfide from ketimine. So the increased pH helps the deprotonation process, which enhance the desulfurase reaction.

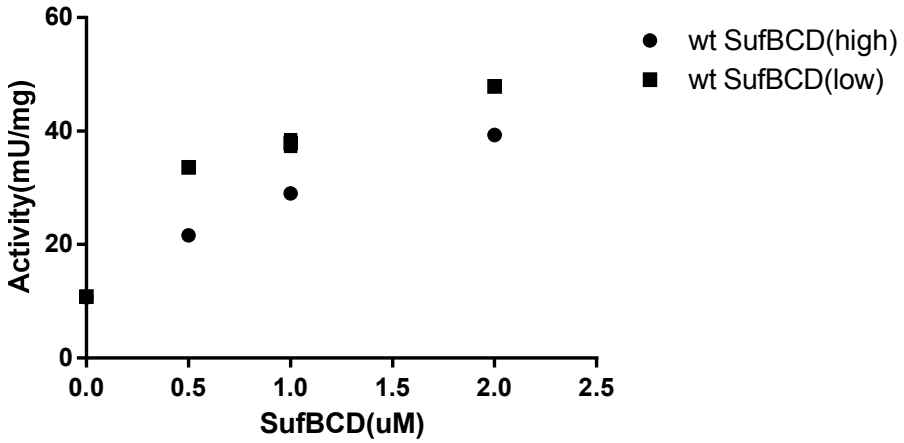

Figure A.8: Desulfurase activity of SufS-SufE in function of high/low activity of $SufBC_2D$.

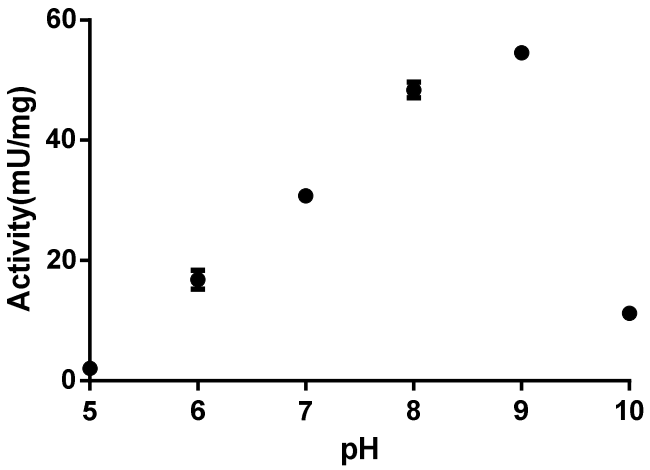

Figure A.9. pH titration of desulfurase activity of SufS and SufE.